Discrimination of artery and bile duct using monopolar bioimpedance measurements

Lars Andreas Pedersen

University of Oslo
Department of Physics
Electronics and Computer Science

Oslo universitetssykehus

Thesis for the degree of Master of Science

February 2014

Acknowledgements

First of all I would like to thank my advisors Jan Olav Høgetveit and Håvard Kalvøy, and also Tormod Martinsen at the medical technology department at Oslo University Hospital for their professional support and assistance throughout this thesis. I would also like to thank the staff of the Institute for Surgical Research at Oslo University Hospital, Professor Ansgar O. Aasen, Tom Erik Ruud, Vivi Bull Stubberud, Claus Danckert Krohn, Yngvar Gundersen, Ola Sveen and Claus Vinter for their ideas, professional assistance and support. Professor Ørjan G. Martinsen and Professor Sverre Grimnes at the Department of Physics, University of Oslo, have also helped me immensely with the basic theory of the bioimpedance field with their book Bioimpedance and Bioelectricity Basics (second edition). Last but not least I would like to thank my fellow student Runar Strand-Amundsen for his thorough support and assistance within almost every aspect of this thesis.

Preface

After finishing up my bachelor degree within electronics engineering at Østfold University College back in 2011 the path was naturally set for me to continue on to a master's degree within a related subject. I applied and got accepted into a masters program within electronics and computer science at the University of Oslo the next semester. I have had a parallel path with Runar Strand-Amundsen through the undergraduate and graduate classes. It was through him I got in touch with Jan Olav for doing a masters thesis on a subject related to bioimpedance.

I have worked part time for a startup company called Dignio AS during the whole master period. This has led to delays in the master schedule overall, but has hopefully not decreased the value of the content in this thesis. My time at the University of Oslo has been a great and rewarding experience, and I would like to thank everyone that has helped me in some way with this thesis. I will not mention everyone here, but hopefully you all know who you are.

Abstract

This thesis explores the use of bioimpedance measurements within the field of electrosurgery. A standard monopolar electrosurgery setup has been utilized in order to discriminate between the characteristic impedance of the proper hepatic artery (PHA) and common bile duct (CBD) in domestic pigs. The end goal is to aid a surgeon performing a cholecystectomy, primarily laparoscopic, in order to avoid dividing or damaging the wrong part of the arteries or ducts in the area surrounding Calot's triangle. It could also be a potential building block for further research into for example smart electrosurgery knives or other tissue discrimination for use within electrosurgery.

The Valleylab E1551X, E1450G and E1475X electrosurgery electrodes has been evaluated. The E1551X blank stainless steel electrosurgery electrode was chosen as the most optimal electrode to use during the experiments. Basic characteristics of this electrode and its sensitivity field have been measured through a series of experiments using a cucumber model.

A total of 9 in vivo pig experiments were performed between March and June 2013 at the Institute for Surgical Research at Oslo University Hospital. Impedance measurement data has been collected from the pig experiments using the Solartron 1260/1294. The measurement locations consists of the common bile duct, proper hepatic artery, gall bladder, right lateral lobe of the liver, hepatic lymph node, splenic artery and spleen. The measurement results for the CBD and PHA has been statistically analyzed.

The proper hepatic artery was found to have overall lower impedance than the common bile duct over almost all frequencies. The results show a statistical significant difference between the CBD and PHA in 6 out of 9 pigs (66%) according to the Mann-Whitney U test. Among these, 5 out of 9 pigs (55%) supported the hypothesis that the phase for the PHA was higher than the phase for the CBD at 630 kHz. 1 out of 9 pigs (11%) were a false positive. The result is based upon what part of the phase data had the most amount of statistically reliable results. The hypothesis is tested with an arithmetic mean test for all of the measurements series combined.

Contents

Acknowledgements 2
Preface 2
Abstract 3
Figures 7
Tables 8
1 Introduction 8
1.1 Hypothesis 9
1.2 Goals 9
1.2.1 Part goals 9
2 Theory 9
2.1 The electrical principles of bioimpedance 9
2.1.1 Resistance and conductance 10
2.1.2 Impedance and admittance 10
2.1.3 Electrolytes 11
2.1.4 Static electric fields 11
2.1.5 Dielectrics 12
2.2 Electrodes 13
2.2.1 Electrodes in a tissue volume 13
2.2.2 CC and PU electrodes 14
2.2.3 Electrode polarization impedance (EPI) 14
2.2.4 The bioelectric dipole 14
2.2.5 The lead vector and reciprocal excitation 15
2.2.6 Sensitivity field 17
2.2.7 Two-electrode system 17
2.2.8 Three-electrode system 19
2.3 Physiological principles 20
2.3.1 Cells and tissue 20
2.3.2 Bile and the biliary system 21
2.3.3 Blood components 23
2.3.4 Arteries 23
2.4 Electrosurgery 24
2.4.1 Monopolar versus bipolar 24
2.4.2 Cut and coagulation 25
2.4.3 Ligasure 25

2.5 Laparoscopic surgery 26
2.6 Laparoscopic cholecystectomy 26
2.6.1 Procedure 26
2.6.2 Bile duct injuries 27
3 Method 28
3.1 Bioimpedance measurement experiment standard 28
3.1.1 Standard equipment 28
3.1.2 Standard initiating procedure and settings 28
3.2 Preliminary testing 29
3.2.1 Coated vs. non-coated electrodes 29
3.2.2 Electrosurgery pen and wire 30
3.3 Blade electrode sensitivity field 30
3.3.1 The cucumber model 30
3.3.2 Experiment A – Initial cucumber measurements 31
3.3.3 Experiment B – Cucumber in deionized water 31
3.3.4 Equipment for cucumber experiments 32
3.4 Pig experiments 32
3.4.1 Equipment 33
3.4.2 Measurement locations 33
3.4.3 Procedure 34
3.4.4 Statistics and data analysis 35
4 Results 35
4.1 Preliminary testing 35
4.1.1 Coated vs. non-coated 35
4.1.2 Electrosurgery pen and wire 36
4.2 Blade electrode sensitivity field 37
4.2.1 Experiment A – Initial cucumber model measurements 37
4.2.2 Experiment B – Cucumber model in deionized water 37
4.3 Pig experiments 38
4.3.1 Arithmetic mean analysis 38
4.3.2 Frequency distribution 41
4.3.3 Statistics assuming normal distribution 42
4.3.4 Mann-Whitney U test (any distribution) 45
4.3.5 Mean vs. Mann-Whitney U vs. unpaired t-test 48
4.3.6 Spleen and splenic artery reference measurements 49
5 Discussion 50

5.1 Preliminary tests 50
5.2 Blade electrode sensitivity field 50
5.2.1 Data reliability and sources of error 50
5.3 Pig experiments 50
5.3.1 Sources of error 50
5.3.2 Time restrictions 53
5.3.3 Choice of locations 53
5.3.4 Discussion of data 54
5.3.5 Future improvements 55
6 Conclusion 56
6.1.1 Continuation 56
7 Literature 56
Appendix A – Application for animal models 58
Appendix B – Response from "Forsøksdyrutvalget" 62
Appendix C – Protocol for bioimpedance measurements on pigs – Spring 2013 63
1 Experiment overview 63
1.1 Discrimination of ischemic small intenstine 63
1.1.1 Measurement details 63
1.2 Discrimination of tissue 63
1.2.1 Measurement details 63
Appendix D – Graphs for impedance vs. frequency and phase vs. frequency for pig experiments 67
Operation 1 68
Operation 2 69
Operation 3 70
Operation 4 71
Operation 5 72
Operation 6 73
Operation 7 74
Operation 8 75
Operation 9 76
Appendix E – Distribution graph for common bile duct and proper hepatic artery measurements 77
Appendix F – True/False table for the Wilcoxon signed-rank test on CBD vs. PHA data 79
Appendix G – Impedance and phase graphs for spleen and splenic artery measurements 81
Operation 4 81

Operation 5 82
Operation 6 83
Operation 7 84
Operation 8 85

Figures

Figure 1 – Two ideal dipoles far apart (large r) in an infinite homogeneous medium. $\boldsymbol{L}cc$ and $\boldsymbol{L}pu$ represent the current carrying dipole and the pick-up dipole respectively. (Grimnes & Martinsen, 2008) 15
Figure 2 – The reciprocal lead field in a finite and inhomogeneous medium where **m** is the current source dipole moment. (Grimnes & Martinsen, 2008) 16
Figure 3 – Equation (23) (blue) vs. (24) (red, function of r), where $I = 10A$ and the electrode radius is 1m. Please note that eqation (23) is constant (not a function). (Grimnes & Martinsen, 2008) 19
Figure 4 – Sensitivity plot for a three-electrode system using spherical electrodes in an infinite homogeneous medium. The sensitivity is the highest in the red area, and slowly decreases down the color scale as shown. (Kalvøy, 2010) 20
Figure 5 – The abdomen of a domestic pig showing leaked bile fluid (**A**) and the severed common bile duct (**B**). The CBD continues through the right side of circle **C** and splits off into the cystic and hepatic duct (not visible). The neck of the gall bladder is shown to the very left inside circle **C**. 21
Figure 6 – Anatomy of the extrahepatic biliary tree. This figure is used with permission from Ewen Harrison at DataSurg.net. (DataSurg.net, 2013) 22
Figure 7 – Stewart-Way classification of laparoscopic bile duct injuries. (Lygia Stewart et al., 2007) 28
Figure 8 – A blade electrode covered with insulating black tape around the edge of the blade is held down into a 0.9% saline electrolyte solution. The neutral electrode is held in place and at the same time connected to the impedance analyzer using crocodile clips. 29
Figure 9 – Experiment A. Initial testing of the cucumber model using a non-coated electrosurgery electrode (E1551X) and an aluminium plate as the neutral electrode. 32
Figure 10 – Experiment B. The cucumber in deionized water model. The same electrode and setup as in the initial testing. 32
Figure 11 - Impedance vs. frequency at 200 mV amplitude for two coated (red, blue) and one non-coated (black) blade electrode. 36
Figure 12 – Phase vs. frequency at 200 mV amplitude for two coated (red, blue) and one non-coated (black) blade electrode. See Figure 11 for details. 36
Figure 13 – Impedance vs. frequency for electrode with pen (red) and without (black). 36
Figure 14 – Phase vs. frequency for electrode with pen (red) and without (black). 37
Figure 15 – Impedance vs. frequency for E1551X non-coated blade electrode on a cucumber. 37
Figure 16 – Phase vs. frequency for E1551X non-coated blade electrode on a cucumber. 37
Figure 17 – Impedance vs. frequency for a blade electrode in a bath of deionized water using the cucumber model at various distances. 38

Figure 18 – Phase vs. frequency for a blade electrode in a bath of deionized water using the cucumber model at various distances. 38
Figure 19 – Frequency distribution of standard deviations for all CBD and PHA impedance measurement results combined. 41

Tables

Table 1 – Sex and weight for each individual pig across all surgeries. 33
Table 2 – True/False table f or arithmetic impedance mean across all CBD and PHA measurements for all operations. 39
Table 3 – True/False table f or arithmetic phase mean across all CBD and PHA measurements for all operations. 40
Table 4 – Unpaired t-test on all CBD vs. PHA impedance measurements for each frequency. 43
Table 5 – Unpaired t-test on all CBD vs. PHA phase measurements for each frequency. 44
Table 6 – Mann-Whitney U test for all CBD vs. PHA impedance measurements for each frequency, with a 5% critical value. 46
Table 7 – Mann-Whitney U test for all CBD vs. PHA phase measurements for each frequency, with a 5% critical value. 47
Table 8 – Mean, unpaired t-test and Mann-Whitney U test overview for 2 kHz impedance measurements. 48
Table 9 – Mean, unpaired t-test and Mann-Whitney U test overview for 630 kHz phase measurements. 48
Table 10 – Summary of arithmetic mean vs. Mann-Whitney U test. 49
Table 11 – Summary of arithmetic mean vs. unpaired t-test. 49

1 Introduction

In cholecystectomy, both open and laparoscopic, the cystic duct and artery are divided in order to remove the gallbladder from the abdominal cavity. To achieve this, the surgeon must first visually distinguish between the arteries, bile ducts and other tissue surrounding the gallbladder. If the surgeon somehow misreads the anatomic landmarks, the common or hepatic bile duct may be wrongfully identified as the cystic duct and thereafter partially or fully divided. Although uncommon, misreadings like this may lead to serious complications for the patient. If the surgeon had an extra tool to aid in the identification of the various structures around Calot's triangle, the risk for serious complications will likely decrease as a result.

Electrosurgery is a widely used tool during surgeries, and can be used for both cutting and coagulating. Since it uses electricity as a tool to perform its tasks it has a natural electrode setup that can be used to perform bioimpedance measurements. It can be very useful to know the characteristics of this setup for various reasons. This could for example potentially be used to automatically prevent a surgeon from cutting into the wrong tissue.

1.1 Hypothesis

The electrical characteristics of the common bile duct (CBD) and proper hepatic artery (PHA) can be discriminated between using common electrosurgery electrodes in a monopolar electrosurgery setup.

1.2 Goals

The main goal of this thesis is to figure out if a standard electrosurgery electrode and setup can be used to reliably measure electrical characteristics of tissue. It should be able to discriminate between at least two structures in close proximity with each other. The end goal from this is to aid a surgeon performing a cholecystectomy so that he or she has an additional point of reference while identifying the anatomic structures adjoining and surrounding Calot's triangle.

1.2.1 Part goals

- Document theory relevant for the most important aspects of this thesis. (section 2)
- Create and get approval for a protocol in order to perform pig trials. (Appendix A, B and C)
- Identify common electrosurgery equipment and figure out what is the best suited for reaching the main goal of this thesis. (section 3.2 and 3.3)
- Perform pig experiments to gather data for the electrosurgery electrode(s) and equipment. (section 3.4)
- Analyze the data from the pig trials and figure out whether or not it supports your hypothesis. (section 4 and 5)

2 Theory

Most of the theory discussed in this chapter is not very in-depth, but it's meant such that the reader can get a basic understanding of the underlying laws and principles of the physics behind the various aspects of bioimpedance. Some subjects might be more in-depth than others; either because they might be harder to comprehend, or because they are more relevant to the theme of this paper. For further information regarding the different subjects, I would suggest looking up the literature in the references.

2.1 The electrical principles of bioimpedance

To measure bioimpedance is to measure the electrical response of living tissue while an external current is being applied. This is essentially a combination of several fields within physics, the main ones being biology and electronics - hence the name bioimpedance (bioelectrical impedance). In order to measure bioimpedance some electronic circuitry is required. The Solartron 1260/1294 has been utilized throughout this thesis, but in general any properly calibrated impedance analyzer can be used for this. Since the charge carriers in living tissue are almost exclusively ions, electrodes are needed to convert between the electrons of the electronics and the ions of the tissue. The impedance analyzer is attached to the electrodes through wiring, and the electrodes are in turn galvanically attached to the tissue. This theory section will not focus on circuitry problems as this is not a big part of this

thesis. Circuitry and wiring is however a very important factor in getting good results from bioimpedance measurements, so it is not to be taking lightly.

Bioimpedance is not to be confused with the related field bioelectricity, which deals with the tissues own ability to generate electricity (e.g. ECG), and also how to control tissue using electric current. Though keep in mind that these fields are so closely related that they may overlap in certain aspects. (Grimnes & Martinsen, 2008)

2.1.1 Resistance and conductance

The flow of electric charge through an electrical conductor is known as an electric current. Electrical resistance describes the opposition to the passage of this current. Electrical conductance is the inverse of this quantity, and thus describes the electrical conductors ability to conduct (and not resist) electric current. They can both be defined using Ohm's law,

$$\mathrm{R} = \frac{\mathrm{V}}{\mathrm{I}}, \mathrm{G} = \frac{1}{\mathrm{R}} = \frac{\mathrm{I}}{\mathrm{V}} \tag{1}$$

where the resistance (R) are defined as the ratio between the voltage (V) and the current (I). The conductance (G) is simply the inverse ratio. (Britannica, 2013c)

2.1.2 Impedance and admittance

The concept of electrical resistance only describes direct current (DC) circuits. When describing alternating current (AC) circuits, there is more than just the resistance to hinder the flow of current. Impedance introduces a reactance in addition to the normal resistance, making it a complex number,

$$\mathrm{Z} = \mathrm{R} + \mathrm{jX} \tag{2}$$

where the real part is the resistance (R) and the imaginary part is the reactance (X). Thus impedance also introduces a phase describing the phase shift by which the current is ahead of the voltage. Admittance is, like conductance is to resistance, the inverse of impedance. It is shown in a similar fashion through $\mathrm{Y} = \mathrm{G} + \mathrm{jB}$, where the real part is the conductance (G) and the imaginary part is the susceptance (B). Bode invented the expression *immittance* in order to describe a system of both impedance and admittance. Though immittance does not have a unit in itself, it may be better suited to describe an overall system. The reactance of impedance can be divided into two sub-parts: Inductance and capacitance.

2.1.2.1 Inductance

Faraday's Law of induction states that a time-varying magnetic field will create, or induce, a voltage in a nearby electrical conductor. This is essentially setting up an electric field, which is discussed later in this chapter. At the same time will an electrical current in a conductor create a magnetic field around that conductor (Oersted's law). These observations considered, one can see that by sending an alternating current through a conductor, you also create an alternating magnetic field around that conductor. This time-varying magnetic field will in turn induce a voltage proportional to the current back into the conductor, essentially opposing it's own change in current (Lenz's law). A conductor's ability to oppose it's own change in current is defined as the *inductance* of a conductor.

2.1.2.2 Capacitance

Capacitance is a body's ability to store electrical charge. Any matter that has the ability to be electrically charged has a capacitance. The capacitance is an important factor within dielectrics, which is discussed later in this chapter. (Grimnes & Martinsen, 2008)

2.1.3 Electrolytes

In electronic DC conductors such as metal or semi-conductors, electric current flows through the material as electrons. In electrolytic conductors however, current instead flows through the substance as free moving ions. Electrolytes are essential within bioimpedance as almost all living tissue consists of it. Both intracellular and extracellular fluids can be considered electrolytic conductors. The expression 'electrolyte' is generally referring to a material that ionizes when dissolved in a proper solvent. It can however also refer to the complete electrolyte solution, depending on the context. For example, the human body contains a lot of water which is a very common solvent for electrolytes. Two of the main electrolytes of the body are the ions sodium (Na^{+}) and chloride (Cl^{-}). The combination of these ions is known as sodium chloride (NaCl), or common table salt. When the solid material NaCl is dissolved in water, it is split into the ions that make up the salt, thereby making an electrolyte solution:

$$\mathrm{NaCl}_{(s)} \rightarrow \mathrm{Na}^{+}_{(aq)} + \mathrm{Cl}^{-}_{(aq)} \tag{3}$$

This is one of the most important electrolyte solutions in the human body. Due to its significance, characteristics and availability it's very common to perform experiments with this electrolyte. The electric conductive characteristics for 0.9% NaCl in water ($\frac{9\mathrm{g}}{1000\mathrm{g}} = \frac{9\mathrm{g}}{\mathrm{L}}$) is very well documented, making it an excellent substance for finding the electric characteristics for electrodes. It is also often just referred to as saline instead of its chemical compounds.

2.1.3.1 Weak and non-electrolytes

Where saline is considered a strong electrolyte because of its high electric conductance, other electrolytic solutions that are still able to conduct current but with a greater resistance is referred to as weak electrolytes. These are solutions where the electrolytic substance does not dissociate all the way, hence there aren't as many free moving ions left to conduct the current.

Non-electrolytes are distinct from electrolyte solutions in that they have no free-moving ions to conduct electric current. Deionized (distilled) water is a solution that has had all free ions removed, which essentially make it act as an electric insulator. Though this is true with perfect circumstances, deionized water used for experimentation is often not completely free of ions. This is often due to impurities derived from the distillation process, immediate environment or other various causes. Therefore, instead of having a resistance $R \rightarrow \infty$ it simply has a very large resistance comparable to that of a weak electrolyte. (Zumdahl & DeCoste, 2011)

2.1.4 Static electric fields

In order to understand what an electric field is, you must first understand the concept behind the force that drives it. Two particles that have an electric charge exert a force on each other based on the property of their electric charge. This force is known as the electrostatic force.

Particles can either be negatively(-) or positively(+) charged. Two particles with opposite signs will attract each other, while two particles with the same sign will repulse each other. This electrostatic force F can be calculated using Coulomb's law (SI system):

$$F = \frac{q_1 q_2}{4\pi r^2 \varepsilon_s} \tag{4}$$

q_1 and q_2 are two charges at a distance r from each other, and ε_s is the static permittivity of the material surrounding the charges. In the case of two particles in a vacuum, ε_s would be equal to ε_0, also known as the electric constant.

If a point charge q is influenced by an electric force F that is proportional to the charge, there is by definition an electric field present:

$$E(x, y, z) = \frac{F(x, y, z)}{q} \tag{5}$$

The magnitude of the electric field E can be measured in Newton's/Coulombs (N/C) or Volts/meter (V/m). (Kovacs, 2001)

2.1.5 Dielectrics

A dielectric has traditionally been described as an electric polarizable and insulating material. This is however not always the case, particularly in the case of living tissue. An electrolyte may have the ability to store energy capacitively, and thus it also acts as a dielectric. For materials in general this definition is frequency dependent; a material may act as an electrolytic conductor at lower frequencies, yet have dielectric properties at higher frequencies.

Within dielectrics, electric charge does not flow through the material like it does in an electrical conductor, but rather displace the positive and negative charges to cause *dielectric polarization*. This displacement of charges is done in the presence of an electric field. The positive charges are displaced in the same direction as the electric field while the negative charges are displaced towards it, causing a reduction of the electric field within the dielectric. Because of the purely local movement within a dielectric, there is no DC conductance; current can only pass through a dielectric as an AC using capacitive displacement. (Britannica, 2013a)

2.1.5.1 Permittivity and susceptibility

In order to describe how an electric field affects and is affected by a dielectric, you want to know a dielectrics *permittivity*. In other words, the permittivity of a material describes how well that material "permits" an electric field. A dielectrics polarization and permittivity are closely linked together; if a dielectric is highly polarized it also has a high permittivity.

Permittivity is directly related to electric *susceptibility*, which says how easily a material polarizes. *Relative permittivity* ε_r, that is the permittivity of a material relative to that of vacuum, is related to a materials susceptibility χ through

$$\chi = \varepsilon_r - 1 \tag{6}$$

which means that in the case of vacuum $\varepsilon_r = 1$ and thus $\chi = 0$ (no susceptibility). Note that both relative permittivity and susceptibility are dimensionless numbers. The a*bsolute*

permittivity ε of a material can thus be found by multiplying the permittivity of vacuum (ε_0, the electric constant) with the relative permittivity:

$$\varepsilon = \varepsilon_r \varepsilon_0 = (1 + \chi)\varepsilon_0 \quad (7)$$

2.1.5.2 Relaxation

Whenever an electric field is exerted onto a dielectric material, there will be a change in the polarization of that material according to the charge of the electric field. The change however will not be instantaneous. The charges in the material need some time to change their actual positions in order to make up the new polarization charge in the material. This can be described as the relaxation time of the material. The concept of relaxation describes how a step function can be used to find the relaxation time.

An important thing to keep in mind here is that the relaxation time of a material is strictly tied up to the dipole moment (section 2.2.4) of the charge that is to be polarized. The electronic dipole has a very small dipole moment, hence the time it take for it to displace is also very small. The polarization of a larger molecule or cell however can take quite some time longer.

2.1.5.3 Dispersion

In order to analyze relaxation properly from bioimpedance measurements you want to bring it into the frequency domain. Dispersion is simply a measure of a materials permittivity as a function of frequency. If a dipole is not given enough time to polarize fully, the materials permittivity will naturally decrease as a consequence. This means that for lower frequencies the polarization will be to the dielectrics maximum potential, while on the higher frequencies it will decrease. In other words, at lower frequencies the dielectric will have one permittivity level, while at the higher frequencies it will have another lower level. There will also be a field in between these levels describing the characteristic relaxation time for the target material. (Grimnes & Martinsen, 2008)

2.2 Electrodes

The electrode is a crucial part of any bioimpedance system. Every single property of an electrode matters for the measurement results, including their size, shape and material. There is generally no electrode that is fit for all purposes, but rather the right electrode for the right job. An electrode is never used alone, but rather in a specific electrode configuration. Like the electrodes themselves there is no “perfect” electrode configuration, but rather the right setup for the right job. The task at hand often limits the choices of electrodes or what electrode setup one can use. Knowledge about electrodes and electrode configurations weakness, sources of error and strong points are therefore very important for success.

2.2.1 Electrodes in a tissue volume

An electrode placed in an electrolyte acts as a converter between electrons and ions; the ionic current of the electrolyte are transformed at the electrode to an electronic current of the electronic conductor and vice versa. An electrode can thereby act as either a source or a sink for ions and electrons. In a tissue volume, if the electrode is smaller than the dimensions of the volume, the ionic current will spread out into the volume relative to the distance from the electrode. The current density will therefore be the highest adjacent to the electrode

surface, and lower as the distance increases. Since the path that the ionic current takes through the medium defines what the measured impedance will be, the measurement results will usually be dominated by the location where the current density is the highest (see section 2.2.5).

2.2.2 CC and PU electrodes

In any electrode system it is important to distinguish between current carrying (CC) and pick-up (PU) electrodes. The CC electrodes provide current to the system, and they are polarized for that reason. A CC electrode can be classified as neutral or dispersive, meaning that the current density of the electrode is so low that the result of the current flow is insignificant. An example for such an electrode would be the dispersive electrode for monopolar electrosurgery (see section 2.4).

The PU electrodes are measuring, or "picking up", electric potential difference in the system. These electrodes are not polarized because they are not providing any current. A PU electrode can also be classified as neutral, again depending on the current density (mainly the electrode area), but also it's positioning relative to the current source.

2.2.3 Electrode polarization impedance (EPI)

If an electrode is solid (e.g. metal) and the electrolytic solvent is a polar fluid such as water, the surface charges of the solid medium will tend to attract the counterions of the water. This will result in the formation of an *electric double layer* at the interface between the electrode and the electrolyte. Due to the irregular distribution of charges across the interface, the electric double layer will have an electric potential across it. This is known as the *polarization impedance* of an electrode. The EPI is in series with the impedance of the electrolyte solution and the electrode. This means that, in electrode systems where the PU electrodes are the same as the CC electrodes (e.g. two-electrode systems), the EPI will be added onto the measured impedance of the target medium. This makes it a common problem for this kind of electrode setups in low frequency measurements, and it's particularly distinct while measuring on materials with low resistance.

2.2.4 The bioelectric dipole

2.2.4.1 Ideal CC dipole

An electric dipole consists of two adjacent electric point charges with opposite polarity. The point charges can either be located on top of each or closely together. A dipole is defined by its dipole moment $\boldsymbol{p}$:

$$\boldsymbol{p} = q\boldsymbol{d} \tag{8}$$

where $\boldsymbol{d}$ is a displacement vector pointing from the position of the negative point charge to the positive. This can be mathematically considered an ideal current carrying dipole in an infinite homogenous medium where $q \to \infty$ and $\boldsymbol{d} \to 0$. A bioelectric dipole is however better defined within engineering mathematics, where spheres can be used instead of point charges. The current carrying dipole moment $\boldsymbol{m}$ of a dipole with two current carrying spheres of radius *a*, is defined by the equation:

$$\boldsymbol{m} = I\boldsymbol{L}_{cc} \tag{9}$$

where $\mathrm{L_{cc}}$ is a displacement vector pointing from the negative charged sphere to the positive (center to center). Within physics and engineering mathematics, the current carrying dipole is still ideal in a finite homogeneous medium with dimensions much larger than $\boldsymbol{L}_{\mathrm{cc}}$ where $a > 0$, if $\boldsymbol{L}_{\mathrm{cc}} \gg \mathrm{a}$ and $I \to \infty$.

If the superposition theorem is valid the electric field potential Φ at any position can be calculated based on the distance from the dipole:

$$\Phi = \frac{I\rho}{4\pi}\left(\frac{1}{r_1} - \frac{1}{r_2}\right) \tag{10}$$

where $\mathrm{r_1}$ and $\mathrm{r_2}$ are the distance from the center of the positive and negative dipole spheres. If you include the dipole moment you can describe the directional sensitivity of the field as a dot product:

$$\Phi = \frac{\rho}{4\pi}\boldsymbol{m} \cdot \frac{\vec{r}}{r^2} \tag{11}$$

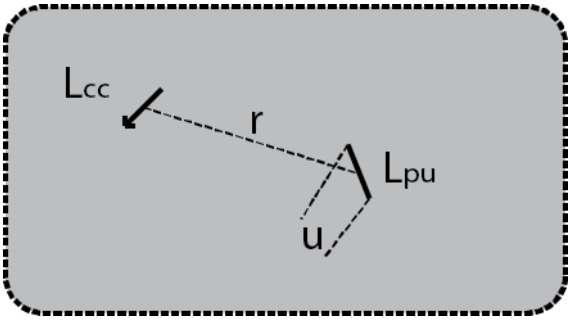

Figure 1 – Two ideal dipoles far apart (large r) in an infinite homogeneous medium. $\boldsymbol{L}_{cc}$ and $\boldsymbol{L}_{pu}$ represent the current carrying dipole and the pick-up dipole respectively. (Grimnes & Martinsen, 2008)

2.2.4.2 Ideal PU dipole

A PU dipole can record the potential difference between two points in an electric field. An ideal PU dipole is not current carrying, and the radius of the spheres $a \to 0$. Also, unlike the ideal CC dipole, the distance between the positive and negative points of the ideal PU dipole should not approach 0. If this distance $\boldsymbol{L}_{\mathrm{pu}} = 0$ the position of the dipole points and their potential would be equal, and naturally there would be no potential difference. Instead an ideal PU dipole has a finite $\boldsymbol{L}_{\mathrm{pu}}$. If the distance r between a PU dipole and a CC dipole is large and $\boldsymbol{L}_{\mathrm{pu}}$ is small, the potential difference $\Delta\Phi$ can be calculated with:

$$\Delta\Phi = \frac{\rho}{4\pi r^3}\boldsymbol{m} \cdot \boldsymbol{L}_{pu} \tag{12}$$

Note the similarities between the single PU position used in equation (10) and (11) vs. (12). The potential difference for a dipolar setup falls more quickly with distance than with the monopolar case. (Grimnes & Martinsen, 2008)

2.2.5 The lead vector and reciprocal excitation

The lead vector is a transfer factor which determines how much of the signal from the current source that can be picked up at a location. It is defined by the part of the previous equation

that has to do with the PU dipole. Hence, if we remove the dipole moment $\boldsymbol{m}$ from equation (12) we get the lead vector $\boldsymbol{H}$:

$$\boldsymbol{H} = \frac{\rho}{4\pi r^3}\boldsymbol{L}_{pu} \tag{13}$$

The equation for potential difference can therefore be rewritten as:

$$\Delta\Phi = u = \boldsymbol{H} \cdot \boldsymbol{m} \tag{14}$$

where u is the recorded voltage at the PU dipole (Figure 1). By using Ohm's law you can find the transfer impedance Z_t at the same dipole:

$$Z_t = \frac{\rho}{4\pi r^3}\boldsymbol{L}_{pu} \cdot \boldsymbol{L}_{cc} \tag{15}$$

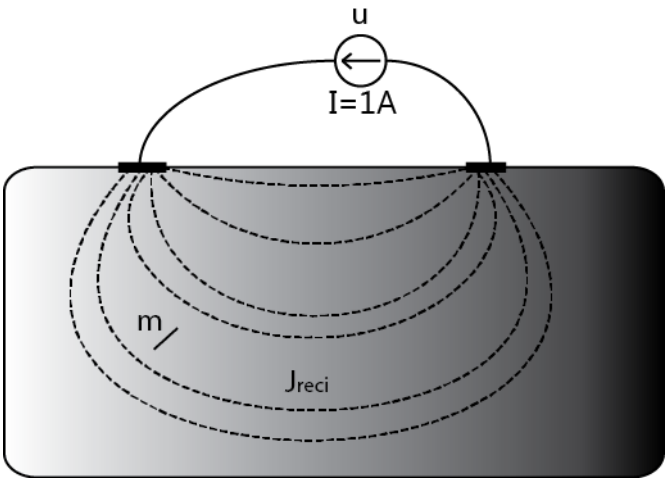

Figure 2 – The reciprocal lead field in a finite and inhomogeneous medium where $\boldsymbol{m}$ *is the current source dipole moment. (Grimnes & Martinsen, 2008)*

These equations demonstrate the principle of the lead vector very well, but it's not necessarily as good for non-ideal substances. In order to find the lead vector in a finite and inhomogeneous medium, the concept of *reciprocal excitation* can be used. This assumes that the PU electrodes are current carrying with a current of 1 A, which creates a current density field $\boldsymbol{J}'_{reci}$ (Figure 2). This is known as the reciprocal lead field. The voltage u measured is equal to:

$$u = \iiint \rho \boldsymbol{J}_{cc} \cdot \boldsymbol{J}'_{reci} dv \tag{16}$$

which means that the transfer impedance is:

$$Z_t = \iiint \rho \boldsymbol{J}'_{cc} \cdot \boldsymbol{J}'_{reci} dv \tag{17}$$

2.2.6 Sensitivity field

In order to help describe the local resistivity of a medium that is measured in various electrode setups, the sensitivity parameter S is introduced. The transfer impedance Z_t for a 4-electrode setup with two CC and two PU electrodes is defined in equation (17). From this equation we can describe the sensitivity parameter S as:

$$S = \boldsymbol{J}'_{cc} \cdot \boldsymbol{J}'_{reci} \tag{18}$$

The sensitivity for the PU electrodes is directly related to the current density of the current source in the medium. The angle of the current source density field $\boldsymbol{J}'_{cc}$ with respect to the reciprocal density field $\boldsymbol{J}'_{reci}$ is critical as the dot product between these defines the sensitivity. If the fields are perpendicular on each other the dot product will be 0, and thus there will be no measured impedance at the PU electrodes. In other words, the location of the PU electrodes relative to the CC electrodes in a 4-electrode system is very significant. In general the location should be so that the sensitivity field is the highest at the location in the tissue you wish to measure. This rule of thumb accounts for all electrode setups.

2.2.7 Two-electrode system

In order to have a flow of electric current, you need at least one source and one sink for electric charges. The two-electrode system is therefore the least amount of electrodes practically usable in a bioimpedance system. As there are only two electrodes in this configuration, the PU electrodes must be the same as the CC electrodes, which means that the electrode polarization impedance becomes a part of the measured impedance. This is a very important source of error for two-electrode systems. The EPI will change with respect to both current density and frequency. It's shown to be dependent on almost all physical properties of an electrode including its material, radius and shape. It's also shown to be affected by the properties of the target material. All of these factors make it very hard to remove the EPI from the impedance of the target tissue.

2.2.7.1 Sensitivity field

The sensitivity field for a two-electrode setup is based on the same principles as the 4-electrode setup. Since the CC and PU electrodes are the same, the fields $\boldsymbol{J}'_{cc}$ and $\boldsymbol{J}'_{reci}$ are parallel to each other. Based on equation (18) the sensitivity field can therefore be described as:

$$S = |J'|^2 \tag{19}$$

A two-electrode system can thus be described simply by using the current density; there is no angle between the CC and PU electrodes.

2.2.7.2 Monopolar configuration

A two-electrode system can be set up in a couple of different configurations: Monopolar and dipolar (Greek definition). A dipolar setup makes use of two electrodes of the same size in a symmetrical setup. A monopolar configuration makes use of two electrodes of different sizes. The size difference should be enough to make the current density for one of the electrodes significantly higher than the other electrode. In other words you will have one "active" electrode that will dominate the results, and one "neutral" electrode that will be indifferent.

Consider an ideal sphere shaped electrode with no resistance half-submerged in a homogenous medium, with a concentric neutral electrode located in the same medium infinitely far away. The resistance R of the hemisphere this electrode makes in the medium is defined by:

$$R = \frac{\rho}{2\,\pi a} \tag{20}$$

where *a* is the radius of the electrode, and ρ is electrical resistivity of the medium. From this you can see that the resistance is inversely proportional to the radius of the electrode. The EPI is however based upon the surface area of the electrode, and is therefore inversely proportional to a^2. Hence by making an electrode larger you also make the EPI exponentially less significant relative to the actual resistance of the medium. The precision for the measurement results can also be calculated based on where the current density is the highest. The contribution to resistance in a half-infinite medium is:

$$R = \frac{\rho}{2\pi}\left(\frac{1}{a} - \frac{1}{r}\right), r \geq a \tag{21}$$

where r is the radius for the contributing hemisphere in the medium. The resistance contribution from within a sphere of radius 10 times the radius of the electrode will then be:

$$\left(\frac{1}{a} - \frac{1}{10a}\right) = \left(\frac{1}{1} - \frac{1}{10}\right) = 0.9 = 90\%$$

Likewise, a sphere with 100 times the radius will account for:

$$\left(\frac{1}{a} - \frac{1}{100a}\right) = \left(\frac{1}{1} - \frac{1}{100}\right) = 0.99 = 99\%$$

This kind of electrode may therefore be fairly precise in terms of what part of the volume you wish to measure.

An electrode shaped like a disc might however be a more common shape for an electrode. A disc can be considered a flat sphere, and may therefore be approached much in the same manner as a spherical electrode. The resistance of a disc electrode with radius a is:

$$R = \frac{\rho}{4a} \tag{22}$$

If you compare this to the equivalent formula for the spherical electrode, you find that this is simply $\frac{2}{\pi}$ times the resistance. Despite this being so similar, the current density for a disc is vastly different to that of a sphere. The current density J for a spherical electrode is uniform across its surface, and is defined by the formula:

$$J = \frac{I}{2\pi r^2} \tag{23}$$

where r is the radius for the current hemisphere. The current density for a disc electrode with radius a and hemisphere r is:

$$J = \frac{I}{2\pi a\sqrt{a^2 - r^2}} \tag{24}$$

By comparing these two types of electrodes of the same radius, with the latter as a function of r, we find that the current density of a spherical electrode equals the current density of a disc electrode only at the center (see Figure 3). The current density then rises exponentially towards the edge of the disc electrode, peaking at the very edge.

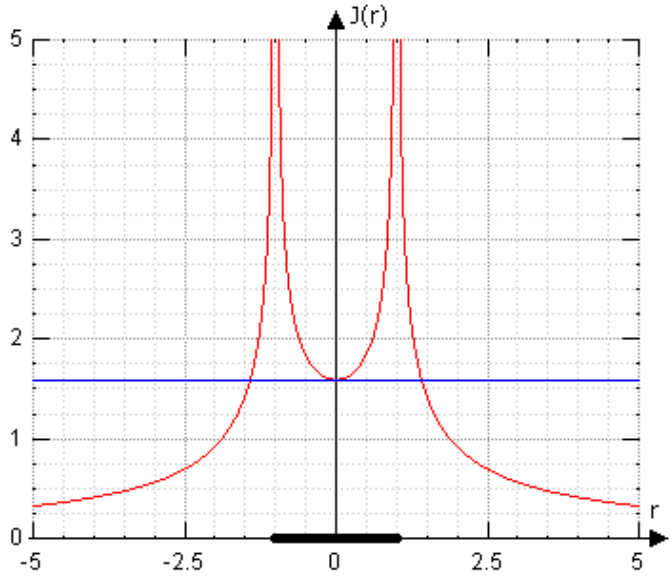

Figure 3 – Equation (23) (blue) vs. (24) (red, function of r), where $I = 10A$ and the electrode radius is 1m. Please note that eqation (23) is constant (not a function). (Grimnes & Martinsen, 2008)

These facts are important to remember when choosing the right electrode for an application. A smaller electrode will result in a higher precision, but at a cost of more EPI. If the medium is small you naturally also require smaller electrodes, but in general you'd want the electrode to be as large as possible without sacrificing spatial precision. (Grimnes & Martinsen, 2008)

2.2.8 Three-electrode system

In section 0 it's described how a 4-electrode system can be set up using separate CC and PU electrodes. The three-electrode system can be looked at like a hybrid between a pure separation of these electrodes and a combination like in the two-electrode system. The three-electrode setup is in principle a 4-electrode system with only one CC and PU electrode merged together. This electrode is known as the M electrode (the measuring electrode). The separate PU and CC electrodes are known as the R (reference) and C (common) electrodes respectively.

2.2.8.1 Sensitivity field

The sensitivity field for such an electrode setup is a bit peculiar compared to the two counterpart configurations. The M electrode is current carrying and will therefore have a polarization impedance in series with the recorded impedance of the tissue. The M electrode otherwise acts as an almost regular recording electrode (e.g. sphere or disc), and the characteristics of the tissue volume around it will affect the results accordingly. In addition to this there is a negative sensitivity zone in the tissue volume between the R and C electrodes.

Figure 4 shows that the spatial selectivity of a three-electrode setup is mainly narrowed down to the area between the R and M electrodes, and in particular adjacent to the M electrode. The negative sensitivity field between the R and C electrodes is not visible, so

the C electrode can be described as a neutral or dispersive electrode. This figure also shows how a typical three-electrode system can be set up using an operation amplifier (op amp). (Grimnes & Martinsen, 2008)

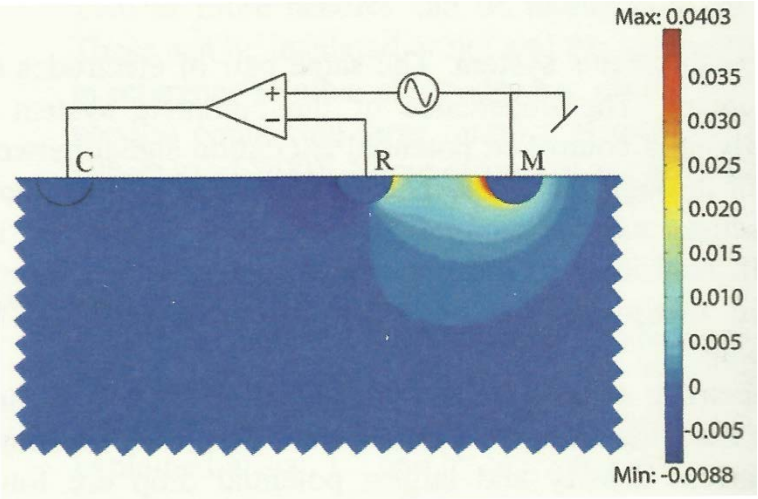

Figure 4 – Sensitivity plot for a three-electrode system using spherical electrodes in an infinite homogeneous medium. The sensitivity is the highest in the red area, and slowly decreases down the color scale as shown. (Kalvøy, 2010)

2.3 Physiological principles

Although the boundaries between the electrical and physiological principles of bioimpedance may be a bit vague in certain aspects, bioimpedance is still very much based upon electronics. The physiological part of this thesis describes the theory behind the parts not necessarily directly related to all aspects of bioimpedance, yet still connected through this thesis.

2.3.1 Cells and tissue

While performing bioimpedance measurements on tissue it is important to know the theory behind the principles of how exactly tissue in general reacts while exposed to an alternating electric current. Different tissue may respond in different ways, and it can be helpful to try and generalize the basic concepts.

First and foremost, tissue consists of a lot of different cells doing various jobs. For this reason it must be considered a heterogeneous material. This means that current may not flow through tissue in perfectly predictable ways, which again can affect any predicted measurement results. A very important factor to consider here is the electrical response of the cells themselves. Cell membranes consist of phospholipids that make up a so called bilayer lipid membrane (BLM). These membranes do not in general let any ions pass freely through them, and is therefore considered to have a very low conductivity. They are however very thin (around 7 nm), and the dielectric breakdown potential isn't very high. Because of the dielectric property of the cells, lower frequency current often choose to pass around the cells in the interstitial fluid instead of through them, essentially changing the current path and in turn the resulting impedance. Higher frequency current on the other hand may pass straight through the cells, spreading it out more homogeneously in the tissue. The cell membrane will also break down at voltage differences exceeding 150 mV. (Grimnes & Martinsen, 2008)

2.3.2 Bile and the biliary system

Bile, or gall, is a greenish yellow fluid that aids the body in the digestion of fats (Figure 5 – **A**). It contains a lot of water with different organic and inorganic substances. This includes electrolytes like sodium (Na^+), potassium (K^+), calcium (Ca^{2+}) and bicarbonate (HCO_3^-).[1] Bile also contains bile acids, cholesterol, phospholipids and bilirubin, all of which makes it slightly acidic with a ph of about 5 to 6.

Bile exist in the body as a part of the biliary system, which consist of organs and ducts that produce, store, transport and release the bile into the digestive system. Bile is secreted by hepatocyte cells in the liver, and it's collected by a series of ducts called bile canaliculus. These ducts merge into bile ductules which eventually forms the left and right hepatic ducts. Note that the bile ducts that are inside the liver are called intrahepatic and the ducts which are outside of the liver are called extrahepatic. The hepatic ducts merge into the common hepatic duct, which again merges with the cystic duct to form the common bile duct (Figure 5 – **C**, far right). The cystic duct is what connects the gallbladder to the biliary tree. The common bile duct is connected to the duodenum, thus making up the final part of the biliary tree.

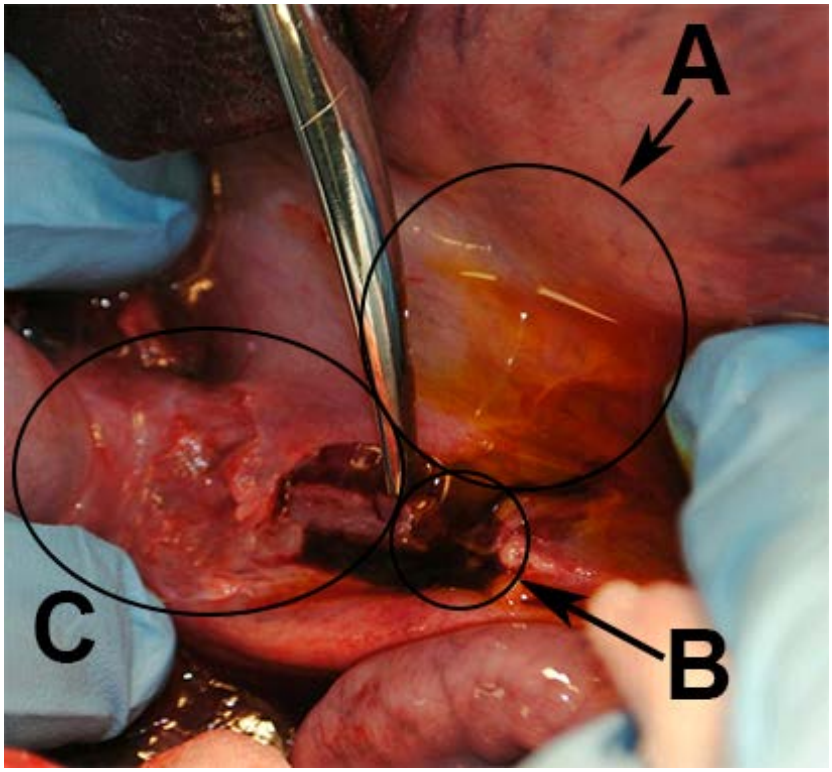

*Figure 5 – The abdomen of a domestic pig showing leaked bile fluid (**A**) and the severed common bile duct (**B**). The CBD continues through the right side of circle **C** and splits off into the cystic and hepatic duct (not visible). The neck of the gall bladder is shown to the very left inside circle **C**.*

The common bile duct primarily consists of connective tissue with a high collagen count. Unlike artery walls it only contains a very small amount of smooth muscle cells which makes it quite passive and unable to control the flow of bile by itself. The flow of bile is instead controlled by the contractions of the smooth muscle cells in gallbladder and the sphincter of Oddi in the duodenum.[2]

[1] (Esteller, 2008)
[2] (Duch, Andersen, & Gregersen, 2004)

About half of the bile that is produced by the liver is stored in the gallbladder before it's sent through to the duodenum.[3] The bile is concentrated within the gallbladder from about 5 times to as high as 18 times its original density. This is largely due to the reabsorption of water, chloride and bicarbonate. The common bile duct therefore contains a much more concentrated bile fluid than the bile ducts from the liver. The amount of bile produced by an average adult human each day may range from 400 to 800 ml. (Bowen, 2001) The total bile acid pool at any one time may however only be about 3 grams, with most of that being stored in the gallbladder. (William Sircus, 2013)

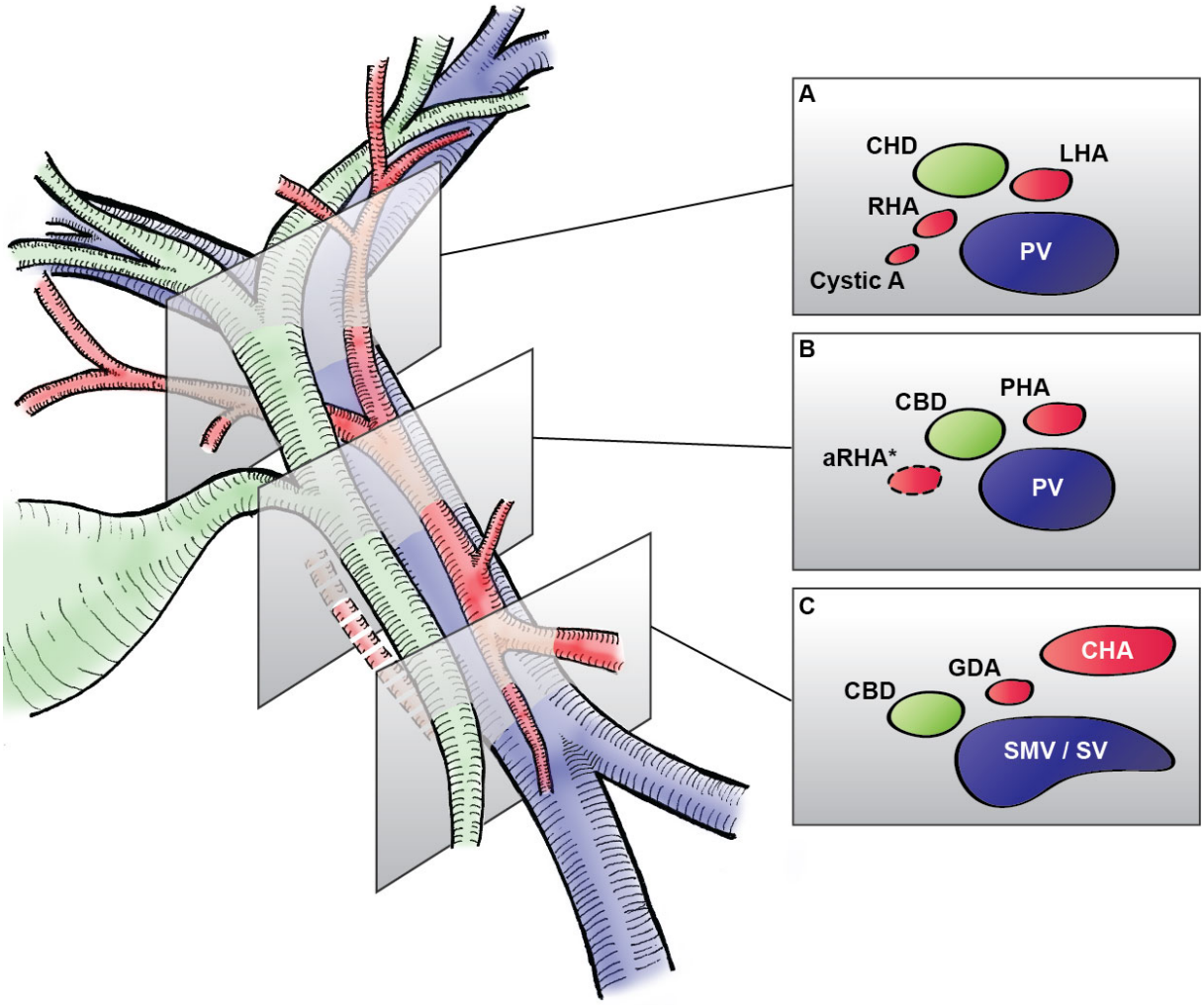

Figure 6 – Anatomy of the extrahepatic biliary tree. This figure is used with permission from Ewen Harrison at DataSurg.net. (DataSurg.net, 2013)

Figure 6 shows the locations of various arteries, bile ducts and veins surrounding the extrahepatic biliary tree. The bile ducts include the common hepatic duct (CHD) and the common bile duct (CBD), with the cystic duct and gallbladder being shown in-between plane A and B. The arteries include the left and right hepatic arteries (LHA, RHA), the cystic artery (Cystic A), proper hepatic artery (PHA), gastroduodenal artery (GDA) and the common hepatic artery (CHA). An accessory right hepatic artery (aRHA) is present in 15% of patients. The portal vein (PV) splits off into the superior mesenteric and splenic vein (SMV/SV). (DataSurg.net, 2013)

[3] ("Liver, Biliary, and Pancreatic Disorders," 2014)

2.3.2.1 The cystic duct

The part of the biliary tree that connects the gallbladder to the common bile duct and common hepatic duct is called the cystic duct. The cystic duct is distinct from the other bile ducts in that it contains spiral shaped concentric folds within the duct. This is known as the spiral valves of Heister. Despite being called valves they are really mucosal folds from the mucosa of the cystic duct.[4] The dimensions of the cystic duct may range from 2 to 5 mm in diameter, and 1 to 6 cm in length. The number of folds of the spiral valves may range from 2 to 14. (Ooi, Luo, Chin, Johnson, & Bird, 2004)

2.3.3 Blood components

Whole blood has two main components: blood plasma and formed elements. Blood plasma is a clear watery liquid that takes up 55% of normal blood content. It contains about 91.5% water and 8.5% solutes. The solutes mainly consist of proteins (7%), but also electrolytes, nutrients, gases, regulatory substances (vitamins, enzymes and hormones) and waste products. Formed elements take up the remaining 45% of the whole blood content, and consist primarily of red blood cells (RBCs). The other components of the formed elements, white blood cells (WBCs) and platelets, take up less than 1% of the contents. (Tortora & Derrickson, 2011)

2.3.4 Arteries

Arteries are vessels in which blood is transported from the heart to the rest of the body. They connect the ventricles of the heart to capillaries inside all organs and all tissue. Because of high pressure inside the arteries the artery walls can be quite thick, the thickest being the aorta with a wall thickness of around 2-3 mm. The internal diameter of the aorta is usually around 1-3 cm. The smallest of arteries are called arterioles and might be as small as 25-100 µm, with a wall thickness of around 20-30 µm. (Bronzino, 2000)

Properties like thickness, diameter and biochemical properties strongly depend on the location of the artery in the body. In general, the further away the artery is from the heart, the smaller the artery is, though the wall thickness vs. artery diameter is larger.

2.3.4.1 Artery wall components

An artery wall consists of four main components.

Smooth muscle cells (SMCs) is what makes arteries able to expand and contract. The amount of SMCs in the artery walls depends on their distance from the heart; smaller arteries are less able to change its geometry and elastic modulus.

The scleroproteins elastin and collagen are both synthesized by the SMCs. The molecules bond to form respective networks of thin fibers in the artery walls. In general it could be said that elastin is what makes the arteries more elastic, while collagen is what gives them their strength. Note also that collagen fibers are much thinner than elastin fibers. The ratio of collagen vs. elastin also change with respect to the distance from the heart, making arteries closer to the heart more elastic than the more remote ones.

Both the proteins and muscle cells are embedded in a sort of connective tissue called ground substance. This amorphous gel-like substance is made up by the non-fibrous components of the extracellular matrix.

[4] (Stocksley, 2001)

2.3.4.2 Tunicae

The artery wall can be divided into three layers of so called tunicae: Intima, Media and Adventitia.

Tunica intima is the innermost and thinnest layer of the artery wall. It consists of a single layer of endothelial cells (ECs) resting on a thin membrane called basal lamina, which in turn is secreted by the ECs. The tunica intima also consists of a subendothelial layer of ground substance containing SMCs and protein fibers.

Tunica media is the intermediate and thickest layer in the artery wall. In smaller muscular arteries this consist a thick homogeneous layer of SMCs, while in more elastic arteries this is instead a layer of lamellar units. Lamellar units are concentric rings of elastin surrounded by SMCs. Tunica media is sandwiched in between two thin layers of elastin, which separates the three layers of the artery wall from each other. These separating layers are called the internal and external elastic lamina, and count as the most inner and outer lamellar units respectively.

Tunica adventitia is the outmost layer and mainly consists of ground substance. The nerves that control the SMCs of the inner layers are embedded in this layer, together with some elastin, collagen fibres and fibroblasts. These however do not make up a lot of this layer. (Tortora & Derrickson, 2011)

2.4 Electrosurgery

Electrosurgery, also sometimes referred to as diathermy, is a surgical technique which uses a high-frequency electric current to cut or coagulate tissue. An electrosurgery unit (ESU) provides the current via electrodes which interacts with the target tissue. When an electric current is sent through the tissue between the electrodes, the resistance of the tissue converts the electric energy into thermal energy (heat). This is known as Joule heating. (Britannica, 2013b) Electrosurgery is based on this very principle.

Electrosurgery is distinct from electrocautery which is another way of cutting or coagulating tissue. Electrocautery uses a probe which itself is heated using electric current, much like a soldering iron. The heat is then transferred from the probe to the tissue (while adjacent) using heat conduction.

2.4.1 Monopolar versus bipolar

There are two main electrode configurations used for electrosurgery: Monopolar and bipolar.

Monopolar surgery uses one large and one relatively small electrode. By using a setup like this, only the small electrode will have sufficient current density to heat up the surrounding tissue. This electrode is known as the active electrode, and it is the working tool for the surgeon. At the other larger electrode, located at a relative distance from where the active electrode is working, the current will be spread out so much across the electrode that it hardly produces any heat at all in the tissue. In other words, the large electrode has a very low current density relative to the small electrode. This is known as a dispersive electrode pad, or simply the return electrode.

Bipolar surgery does not use a large dispersive electrode pad, but instead uses two small electrodes both attached to the surgical instrument. The instrument can for instance be a pair of scissors or graspers with each blade being an electrode. In this case the current density will be equally high for each electrode, and thus both electrodes can essentially be seen as an active electrode. There is also no current going through the patient’s body other than in the immediate proximity of the electrodes.

2.4.2 Cut and coagulation

By altering the output current waveform of the ESU, you achieve different reactions in the target tissue. The two main output modes on a typical ESU is cut and coagulate.

When the device is set to cut, the output current will be a low-voltage, high-energy current set to a continuous fixed frequency. This causes a very rapid heating of both the intracellular and extracellular fluids in close proximity of the active electrode, making them boil almost instantaneously. As the intracellular fluid boils, the pressure within the cells rises causing them to explode. This process is known as vaporization.[5] When the active electrode is moved through the target tissue, this process will in turn cause an incision directly in front of the electrode, essentially cutting the tissue. The electrode should (in theory) never be in direct contact with the tissue, making the instrument have very little mechanical resistance and thus feel very sharp.

When the ESU is set to coagulation, the output current will be a high-voltage, modulated frequency current. The high voltage makes it reach deeper into the tissue, resulting in an overall lower current density compared to that of cutting. The modulation technique have some resemblance to pulse-width modulation (PWM), in that the current is on and then off for a variable time period. The configuration can for instance be so that the current is on only 6% of the time.[6] The long pauses in between the pulses allows the intracellular fluids to slightly cool, resulting in a dehydration rather than a vaporization. This dehydration process is ideal for sealing blood vessels, but it doesn't feel as sharp while cutting tissue.

If the surgeon feels that a pure cut mode is too sharp and without adequate control, it is possible to mix variable amounts of coagulation together with the cutting current. This mode is called "blend". Keep in mind that there is always a degree of coagulation, even if the ESU is set to a pure cut mode. The coagulation that occurs might however not always be strong enough to completely seal the blood vessels. (Grimnes & Martinsen, 2010)

2.4.3 Ligasure

Ligasure (LigaSure™) is a bipolar electrosurgery technique used for sealing blood vessels. This makes use of a custom plier-like tool, with two electrodes located on the working end. This is a particularly interesting tool within the field of bioimpedance as it makes use of continuous impedance measurements in order to seal the blood vessels. While the blood vessel is held under constant pressure from the pliers, a high-current and low-voltage signal is applied by the ESU through the electrodes. As the protein in the tissue heats up, the electrolyte fluids are driven out of the tissue resulting in increased impedance. After a short while (typically 2-4 seconds) the collagen and elastin of the vessel walls will deform in such a way that they fuse together the walls on the opposite side. This is however no normal process of desiccation; It essentially creates a new and whole structure without completely destroying the tissue. This new seal is proven to withstand up to three times normal systolic pressure, and it's efficient for blood vessels as large as 4-7 mm. (Grimnes & Martinsen, 2010)

[5] (Wu, Ou, Chen, Yen, & Rowbotham, 2000)
[6] (Jon Ivar Einarsson & Jon Gould, 2013)

2.5 Laparoscopic surgery

Laparoscopic surgery, also known as minimally invasive surgery or keyhole surgery, is a method of performing surgery in the abdomen with small incisions. This is distinct from laparotomy, or open surgery, which instead requires large incisions.

The minimally invasive approach has some distinct advantages compared to those of laparotomy. Since no large incisions are required, there is less hemorrhage, and also less pain for the patient. The patient is at the same time less likely to have an infection. Recovery time is shortened post-operation which again leads to a shorter stay at the hospital. The small initial incisions also mean less visible scarring.

All these advantages however come at a price. In traditional open surgery the surgeon can usually rely on direct visual feedback from the operating field. The surgeon can also use his hands and fingers to directly manipulate organs and tissue. This is not possible during a minimally invasive procedure. In laparoscopic surgery the surgeon is relying on video from a laparoscope (camera) projected onto a monitor for visual feedback. This gives bad depth perception and a limited view of the anatomy. The surgeon is also using tools that pivot at the location of the incision, making for an extra challenge. Regular tools also have less tactile feedback than your actual hands and fingers.

2.6 Laparoscopic cholecystectomy

Laparoscopic cholecystectomy (LC) is the minimally invasive surgical procedure for removing the gallbladder. Cholecystectomy is a very common surgical procedure with approximately 750,000 patients undergoing the procedure during 2008 in the United States, 90% of which were done laparoscopically. It is known as a very safe procedure with an extremely low mortality rate (0.22-0.4%)[7] [8], and a 5% rate for major morbidity.[9] Cholecystectomy has been one of the major reasons for early laparoscopic development, and the procedure itself has benefited immensely from it.

2.6.1 Procedure

After initial preparations of the patient, a small incision is made at the umbilicus for the initial entry into the abdominal cavity. An 11 mm blunt Hasson trocar is inserted in order to provide CO_2 insufflation of the abdomen and an entrance for the laparoscope itself. After vision has been established, an incision is made below the xiphoid process and a 11 mm trocar is advanced through the abdominal wall into the abdominal cavity. The entry should be just to the right of the falciform ligament. The operating table is then placed at an angle so that the small bowel and colon fall away from the operative field. Following this a 5 mm grasper is inserted through the subxiphoid port. The gallbladder can now be manipulated in order to get a better overview of the bladder itself and the surrounding tissue. Based on this information, two more skin incisions are made for two 2.5 mm lateral trocars which go into the peritoneal cavity. Two 5 mm graspers with locking mechanisms are inserted into each of these ports. The graspers will aid in manipulating the gallbladder so that the cystic duct is straightened and put at a 90° angle relative to the common bile duct (CBD). It is very important that the cystic duct is not in line with the CBD, as this can cause inadvertent injury.[10] Any adhesions

[7] (Steiner, Bass, Talamini, Pitt, & Steinberg, 1994)
[8] (Csikesz, Ricciardi, Tseng, & Shah, 2008)
[9] (Giger et al., 2006)
[10] (Samira Y Khera, David A Kostyal, & Narayan Deshmukh, 1999)

that might be encountered are to be dissected using careful hook cautery or similar techniques.

Misidentification of the biliary structures is the most common cause of serious biliary injury. For this reason, visually identifying the cystic duct and the cystic artery are pivotal for success. In order to achieve this, the entire subhepatic area is to be carefully dissected and exposed so that only two structures are seen entering the gallbladder. This is known as the "critical view of safety".[11] The critical view must be obtained before dividing the cystic artery or duct.[12] Once the critical view has been established, an endoscopic clip applier is used to apply clips to both the artery and duct. This is to prevent bile leakage and hemorrhage. The artery and duct are then transected in between the clips using endoshears.

The gallbladder can now be dissected from the liver bed. This can be done using regular hook electrocautery. Once the gallbladder is completely separated from its bed it can be removed from the abdominal cavity using an endocatch bag through the umbilical trocar. The laparoscope is then sent through the subxiphoid port. Lastly, a final inspection and washout are performed, and the trocars are removed. (Danny A Sherwinter et al., 2013)

2.6.2 Bile duct injuries

Complications of laparoscopic cholecystectomy are rare in general. Serious complications occurred in as many as 2.6% in a study involving 8856 patients.[13] Bile duct injuries are one of the more common complications of LC (0.26% - 0.6%).[14] [15] The reason for bile duct injury is more often than not the result of the surgeon performing an incorrect action in good faith, e.g. wrongfully identifying the common bile duct as the cystic duct and thereafter dividing it. As such the operation may be completed without the surgeon knowing he or she made a mistake. This is known as an active type of injury. The surgeon can also make a passive injury, e.g. inadvertently damaging part of a bile duct by working on a nearby structure.

2.6.2.1 Stewart-Way classification

Bile duct injuries during LC can be classified using Stewart-Way classification of bile duct injury (Figure 7). This method divides the various injuries into 4 different classes. Class I injuries are an active type injury where the surgeon mistakes the common bile duct for the cystic duct, but notices his mistake before completely dividing the duct. Class II is a passive type injury where the common hepatic duct is damaged either by clips or by working too close to it using electrocautery. In Class III injuries the surgeon makes the same active mistake as in Class I injuries, but does not notice the mistake before completely dividing the CBD. This is the most common type of injury. Class IV can involve both active and passive injuries. The surgeon either mistakes the right hepatic duct for the cystic duct and divides it (active), or passively damages it during dissection. (Lygia Stewart, Lawrence W. Way, & Cynthia O. Dominguez, 2007)

[11] (Steven M Strasberg & L Michael Brunt, 2010)
[12] (Strasberg, 2005)
[13] (Nezam H Afdhal & Charles M Vollmer, 2014)
[14] (Hobbs, Mai, Knuiman, Fletcher, & Ridout, 2006)
[15] (Thurley & Dhingsa, 2008)

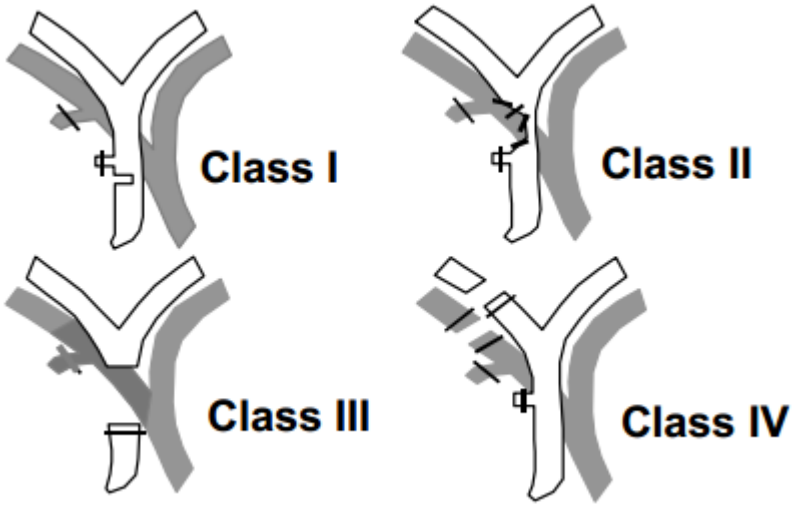

Figure 7 – Stewart-Way classification of laparoscopic bile duct injuries. (Lygia Stewart et al., 2007)

There are several reasons for why Class III type injuries occur so often relative to the other classes of injuries. First of all you have the general limitations of laparoscopic surgery (section 0). Other than that you have inexperience, faulty dissection techniques and failure of clips on the cystic duct as prominent sources of error. (Palanivelu, 2008)

3 Method

This section describes what experiments, tests and trials that took place in order to reach the goals of this thesis.

3.1 Bioimpedance measurement experiment standard

All experiments described in this section followed a set of standard routines for the bioimpedance measurements. The standard routines include some equipment, measurement settings for the impedance analyzer and some initiating procedures. Any deviations from the standard are noted in the experiment description.

3.1.1 Standard equipment

- Solartron 1260/1294 impedance analyzer
- Computer with ZView/ZPlot software for Solartron
- Black test box for impedance analyzer check
- Banana cables with both insulated and non-insulated crocodile clips

3.1.2 Standard initiating procedure and settings

First the Solartron 1260/1294 is turned on, and the ZView/ZPlot software started on the connected computer. The impedance analyzer settings in ZPlot are now validated. For regular experiments it should be set to a logarithmic declining sweep from 1 MHz to 10 Hz, using the average of 10 sine-waves at each frequency with a fixed voltage. The voltage levels may vary depending on the experiment. Lastly the functionality of the Solartron and the connected cables is validated using the black impedance test box.

3.2 Preliminary testing

Before the main pig experiments took place, a series of preliminary tests were performed in order to evaluate what electrodes and equipment would be the best suited for the trials. A set of blade electrodes were evaluated (section 3.2.1) and whether or not to use more of the standard electrosurgery equipment (section 3.2.2).

3.2.1 Coated vs. non-coated electrodes

Within electrosurgery, so called “non-stick” blade electrodes are often used instead of the plain stainless steel electrode. A layer of PTFE (polytetrafluoroethylene/Teflon) or silicon is added onto the steel covering almost the entire blade of the electrode except a small gap along the edge of the blade. This should in theory account for a lot of unwanted EPI due to the small surface area of the coated electrodes, but could also potentially provide better spatial precision. Since all electrodes were frequently used at Oslo University Hospital, a small test was setup in order to determine what effect the coating would have on the impedance measurement results.

3.2.1.1 Procedure

Two coated and one non-coated stainless steel blade electrode were tested and compared in a 0.9% saline solution. Insulating black plastic tape was wrapped around the blade of the electrodes, exposing only 0.6 cm of the lower part of the blade to the electrolyte solution. The electrodes were connected to the impedance analyzer in a monopolar configuration with the blade electrode acting as the active electrode, and a 9x9 cm aluminium, copper and brass plate as the neutral/dispersive electrodes. The plates were fastened using a crocodile clip exposing 8x9 cm of the plates to the saline solution. The blade electrodes were held in place using insulated crocodile clips at a set distance from the plate. (Figure 8)

The standard initiating procedure (section 3.1.2) was performed at the beginning of the experiment. Two different voltage levels were tested for each of the blade electrodes: 50 mV and 200 mV.

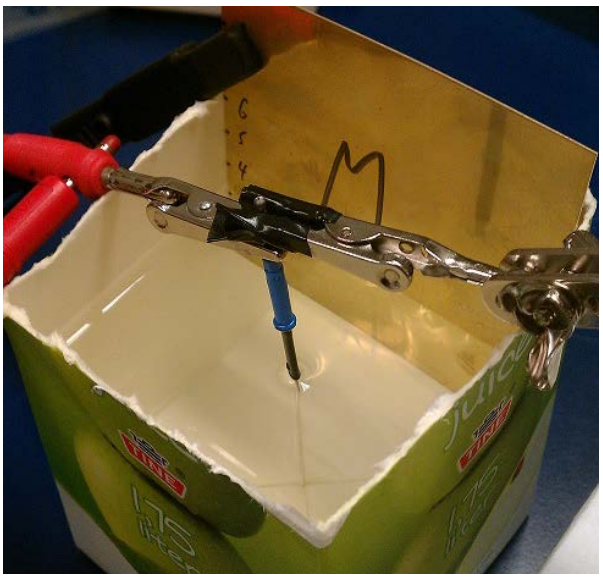

Figure 8 – A blade electrode covered with insulating black tape around the edge of the blade is held down into a 0.9% saline electrolyte solution. The neutral electrode is held in place and at the same time connected to the impedance analyzer using crocodile clips.

3.2.1.2 Equipment

Stainless steel electrosurgery blade electrodes:

- Valleylab E1450G – Silicon Coated
- Valleylab E1475X – Silicon Coated
- Valleylab E1551X – Non-coated

Other equipment:

- Standard equipment (section 3.1.1)
- Black plastic insulating tape, “electrical tape”
- Container with a 0.9% saline solution
- 9x9 cm aluminium, brass and copper plate electrodes

3.2.2 Electrosurgery pen and wire

Since the electrosurgery unit (ESU) is not necessarily within the immediate vicinity of the operating field, the electrosurgery pens are usually equipped with a fairly long wire connecting the electrode to the ESU. A standard Valleylab electrosurgery pen with an approximated 5 meter wire was connected to an E1551X blade electrode and tested with the same procedure as described in section 3.2.1.1.

3.3 Blade electrode sensitivity field

It is very useful to know the sensitivity field for any electrode used for bioimpedance measurements. It can however be very difficult to figure out exact numbers for this depending on the physical aspects and attributes of the electrode and the specific problem at hand. The most important fact for the sensitivity field in this particular monopolar configuration is to figure out how deep into the tissue the electrode is actually measuring. If the sensitivity field is too large it can result in an insufficient spatial precision.

3.3.1 The cucumber model

In order to get an estimation of the sensitivity field, a model using a cucumber in deionized water were proposed. The cucumber contains a lot of water (~95%) and electrolytes like potassium and sodium,[16] making it highly conductive. Previous testing had also shown a tendency for a single clear dispersion within the target frequency range of the pig trials (100 Hz – 1 MHz).

Experiment **A** was first setup to find the characteristic impedance for the cucumber in a monopolar electrode setup. This should be getting the data on the cucumber in an isolated environment. After getting data on any dispersion, experiment **B** was setup using the cucumber model in deionized water in order to test the sensitivity field. The choice of the neutral and active electrode for both experiments was derived from the preliminary testing of the electrosurgery blade electrodes (section 3.2.1 and 4.1.1).

[16] ("Full Report (All Nutrients): 11205, Cucumber, with peel, raw," 2014)

3.3.2 Experiment A – Initial cucumber measurements

A stainless steel electrosurgery blade electrode was setup in a monopolar electrode configuration using an aluminium plate as the dispersive electrode. Figure 9 shows the main part of the initial cucumber experiment setup. The cucumber was laterally sliced half way through the center using the aluminium plate. This was done to get as large surface area as possible in contact with the electrode, and also for it to properly stay in place during the measurements. The active electrode was sliced vertically about 1 mm into the front of the cucumber, and held in place using insulated crocodile clamps. 6 mm of the lower exposed part of the blade electrode edge was in direct contact with the cucumber.

3.3.2.1 Procedure

Three bioimpedance measurements were performed consecutively on three different voltage levels: 50 mV, 200 mV and 500 mV. Measurements otherwise followed this thesis standard routines for bioimpedance measurements (section 3.1.2).

3.3.3 Experiment B – Cucumber in deionized water

Figure 10 shows the basic setup of this experiment. A cylindrical waterproof steel container with an electric insulating acrylic glass bottom were thoroughly cleaned and dried. The steel container was connected in a monopolar electrode setup as the dispersive electrode. A 6 cm piece of a cucumber divided at the center was fastened to the bottom using black plastic tape. The container was then filled with deionized water. The active electrode was fastened using crocodile clamps, which in turn were held in place by clamps and an aluminium rod for overhead support.

3.3.3.1 Procedure

A short ruler was held down into the water next to the active electrode blade, supporting itself on the cucumber. The vertical position of the active electrode was then adjusted so that the measuring distance was correct. Measurements were performed at the distances 1.5 cm, 1.0 cm, 0.5 cm, 0.2 cm, 0.1 cm, 0.0 cm (blade edge adjacent to the cucumber) and -0.6 cm (blade edge inside the cucumber). Distances were measured as approximations from the flat edge of the cucumber to the very lower edge of the electrode blade. The ruler was removed from the deionized water bath while any measurements took place. All measurements were performed at 100 mV amplitude. The experiment followed the standard initiating procedures and setup for this thesis (section 3.1.2).

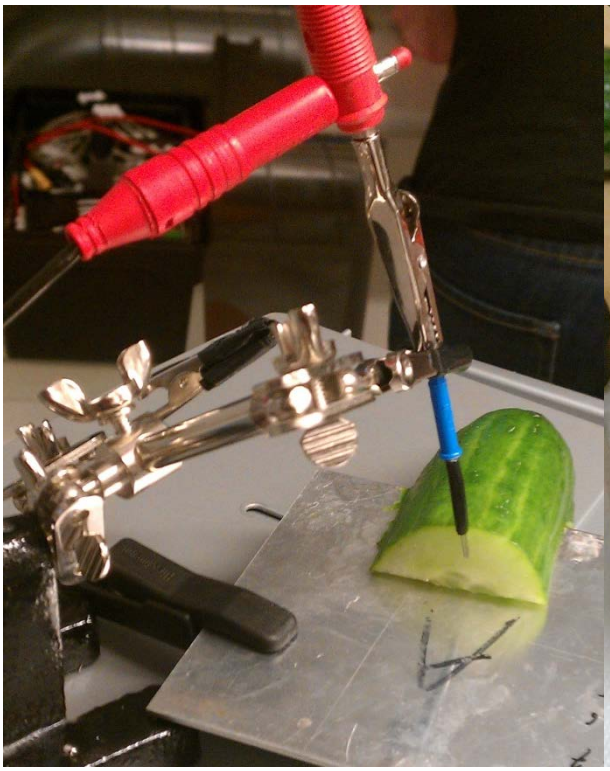

Figure 9 – Experiment A. Initial testing of the cucumber model using a non-coated electrosurgery electrode (E1551X) and an aluminium plate as the neutral electrode.

Figure 10 – Experiment B. The cucumber in deionized water model. The same electrode and setup as in the initial testing.

3.3.4 Equipment for cucumber experiments

The following items were used for both experiments **A** and **B**:

- Standard equipment (section 3.1.1)
- Plastic insulating tape
- Valleylab E1551X blade electrode – Non-coated
- Fresh cucumber (Cucumis sativus) bought at a local grocery store
- Clamps, fasteners, various supporting equipment

Additional items used in experiment **A**:

- 9x9 cm aluminium plate

Additional items used in experiment **B**:

- Cylindrical steel container fastened to a square piece of acrylic glass
- 30 cm metallic ruler
- Aluminium rod and clamps, div. equipment for structural support

3.4 Pig experiments

A total of 9 surgeries/experiments were conducted on male and female Norwegian domestic pigs (sus scrofa domesticus) between the 7th of March and the 6th of June 2013. The

experiments consisted of 5 male and 4 female pigs between 24.5 kg and 30 kg (Table 1). The surgeries were performed at the Institute for Surgical Research at Oslo University Hospital. Bioimpedance measurements were performed at predefined anatomic locations during the operations. A minimum of 5 unique measurements were recorded on each individual location for each surgery. The 9th surgery was cut somewhat short due to time restrictions, but the main measurements were recorded nonetheless.

OP #	Date	Sex	Weight (kg)
1	07.03.2013	male	26.5
2	14.03.2013	female	27.5
3	04.04.2013	female	28
4	11.04.2013	male	24.5
5	18.04.2013	male	29
6	02.05.2013	male	29
7	02.05.2013	female	30
8	06.06.2013	male	26.5
9	06.06.2013	female	27.5

Table 1 – Sex and weight for each individual pig across all surgeries.

3.4.1 Equipment

The following equipment was used as a main part of the bioimpedance measurements. Please keep in mind that this list of equipment does not include the general operating theater equipment otherwise used during the operation.

- Standard equipment (section 3.1.1)
- Valleylab E1551X – Non-coated stainless steel electrosurgery blade electrode
- 3M™ 9130 Universal Electrosurgical Pad
- Custom made dispersive electrode pad to banana connector adapter
- Custom made USB foot pedal with electronics
- Plastic insulating tape

3.4.2 Measurement locations

A set of anatomic locations were decided upon prior to the experiment launch. The locations can be divided into primary and reference measurement locations:

- **Primary** **-** Proper hepatic artery *(PHA, Figure 6 – Plane B)*
- **Primary** **-** Common bile duct *(CBD, Figure 6 – Plane B)*
- **Reference** **-** Body of Gallbladder
- **Reference** **-** Anterior portion of the right lateral lobe of the liver
- **Reference** **-** Hepatic lymph node*

**Not recorded on the 9th surgery*

During operations 4-8 two additional reference points were recorded in addition to the ones mentioned above:

- **Reference** **-** Medial anterior portion of the spleen
- **Reference** **-** Splenic artery

3.4.3 Procedure

First the pig is sedated and initially prepared. During preparation the monopolar dispersive electrosurgery electrode is placed by the surgical nurse in a standard location according to hospital guidelines. The location is usually at the femoral, and generally towards the posterior dorsal portion of the pig. In order to get the best grip and surface area for the electrode the location is shaven using an electric razor before the electrode is placed. The standard initiating procedure is performed as described in section 3.1.2 during the preparation of the surgery.

3.4.3.1 Initiating surgery

A large incision is made to the medial, superior part of the abdomen using regular electrosurgery. Due to the experiments running in parallel this incision was large enough to expose most of the small intestine, but this would not be necessary for this experiment alone. The liver and gallbladder can now be clearly identified, and the extrahepatic bile ducts and arteries exposed. See Figure 6 (section 0), mainly the structures in between transverse plane A and B. Any connective tissue surrounding the common bile duct and proper hepatic artery are carefully dissected in order to expose the vessel walls directly for the blade electrode. All identified locations were confirmed by the surgeon at the beginning of the experiment before any of the measurements were initiated.

3.4.3.2 Measurement cycle

Measurements were performed with reference to the surgery protocol (Appendix C). Another experiment running in parallel required a series of measurements on the small intestine every 15 minutes. As such, measurements for this thesis were to be performed for approximately 5-7 minutes every 15 minutes. A measurement cycle consists of the following steps:

1. Connect the blade electrode cable and the dispersive electrosurgery pad to the impedance analyzer.
2. Open the abdomen and locate the current anatomic measurement location.
3. Perform measurements.
4. Close the abdominal cavity if there is any time to spare in-between measurements.
5. Disconnect blade electrode cable and dispersive electrosurgery pad from the impedance analyzer.

The measurement itself was performed by holding the flat edge of the blade electrode onto the target tissue, covering at least 60% of the 0.6 cm stripped edge of the electrode.

3.4.3.3 End of experiment

After the pig has been euthanized the Solartron is shut down and all equipment disconnected. The blade electrode, cables, crocodile clips and any other item that has been in contact with the pig is carefully washed using alcohol and soap, and then dried.

3.4.4 Statistics and data analysis

Basic statistics and data analysis has been applied to the various data generated by the pig surgeries. The data sets for the common bile duct and proper hepatic artery have been analyzed using the following methods:

- Arithmetic mean test
- Normality test by frequency distribution
- Student's t-Test (unpaired)
- Wilcoxon Signed-Rank Test (aka. Mann-Whitney U test) for normal distribution and any distribution

All statistical analysis has been performed using Microsoft Excel 2010 v14.0.7106.5003 (32-bit), included as a part of Microsoft Office Professional Plus 2010. Some simple VBA scripts have been utilized to simplify some of the visual statistics generation.

4 Results

This section shows the measurement results from the experiments and trials performed in order to reach the goals of this thesis. The results are shown in the same order as the experiments are presented in section 3.

4.1 Preliminary testing

4.1.1 Coated vs. non-coated

The three different neutral electrodes with brass, copper and aluminium did not show any significant differences between them while using the E1551X electrode, so only the aluminium plate was used to test the remaining electrodes E1450G and E1475X. Figure 11 shows the impedance measurement results of all three blade electrodes at 200 mV amplitude. Since all electrodes showed the same basic trends at both 50 mV and 200 mV, only the 200 mV results are included.

The E1450G electrode starts off at around 100 Ω on the highest frequency (1 MHz) and moves upwards linearly towards the lower frequencies, ending at around 40 kΩ (10 Hz). In other words, the EPI is so large it completely takes over the resulting impedance, and is therefore not very suitable in this monopolar electrode configuration. The E1551X stays at around 40 Ω for almost the entire frequency spectrum until the EPI takes over at around 200 Hz. The EPI for E1475X is not as obvious, but is still somewhat present along parts of the frequency spectrum. The E1475X also have a larger overall resistance than the plain E1551X. From these results the E1551X non-coated blade electrode were chosen as the most optimal choice in terms of low EPI and other influences.

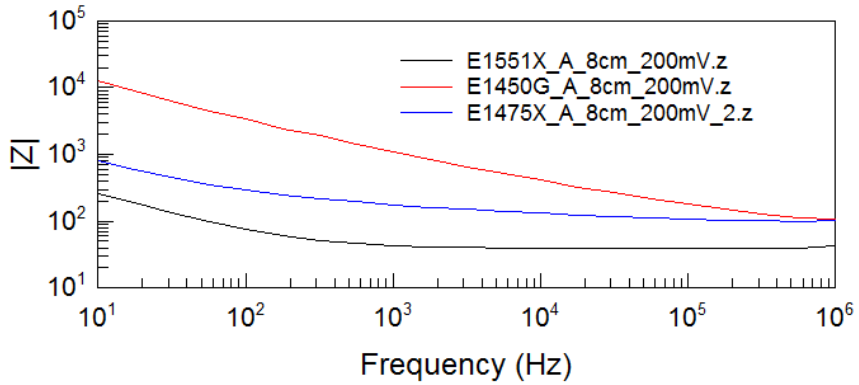

Figure 11 - Impedance vs. frequency at 200 mV amplitude for two coated (red, blue) and one non-coated (black) blade electrode.

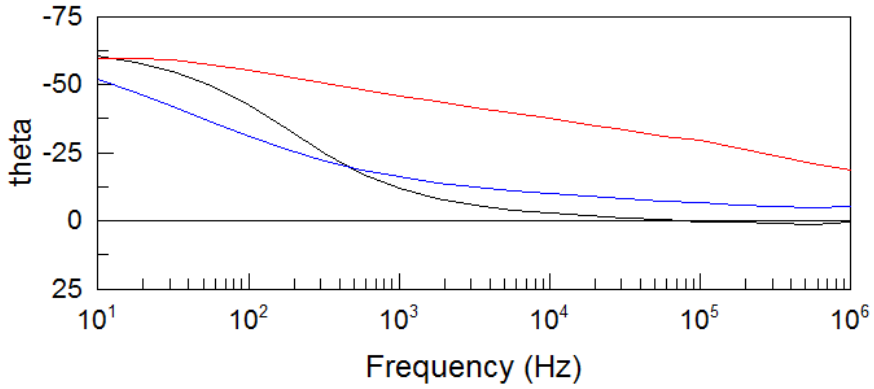

Figure 12 – Phase vs. frequency at 200 mV amplitude for two coated (red, blue) and one non-coated (black) blade electrode. See Figure 11 for details.

4.1.2 Electrosurgery pen and wire

The phase plot at Figure 14 tells us that there is significant noise from around 100 kHz and upwards as a result of the inductive coupling in between the wires. The impedance at Figure 13 clearly reflects the changes shown in the phase plot. From these results it was concluded that the electrode pen and wire should not be used as a part of the further trials.

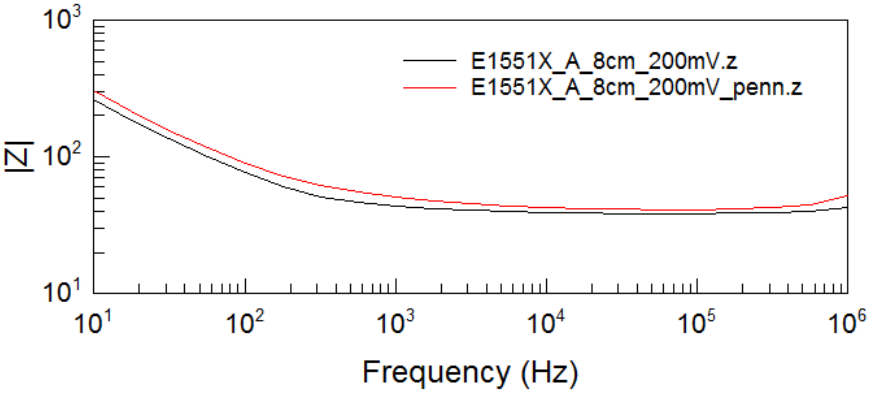

Figure 13 – Impedance vs. frequency for electrode with pen (red) and without (black).

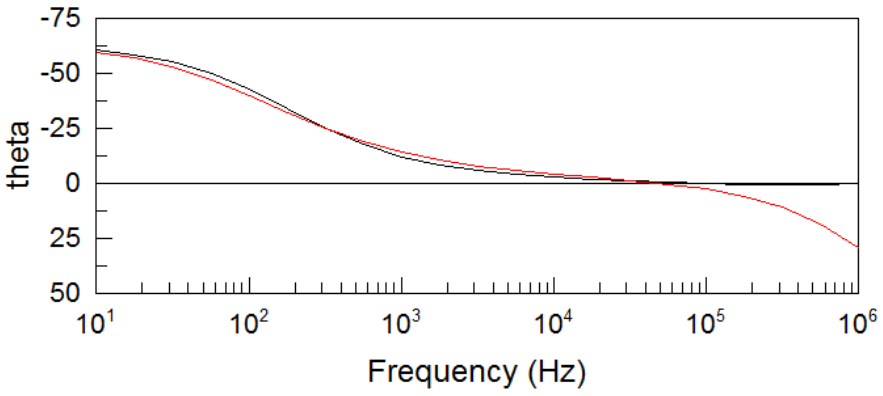

Figure 14 – Phase vs. frequency for electrode with pen (red) and without (black).

4.2 Blade electrode sensitivity field

4.2.1 Experiment A – Initial cucumber model measurements

Figure 15 and Figure 16 represent the measurement of the first cucumber model at 50 mV. A clear dispersion can be seen with a peak in the phase at around 50 kHz. Repeated measurements on different voltage levels, 200 mV and 600 mV, showed no significant change in the measurement results.

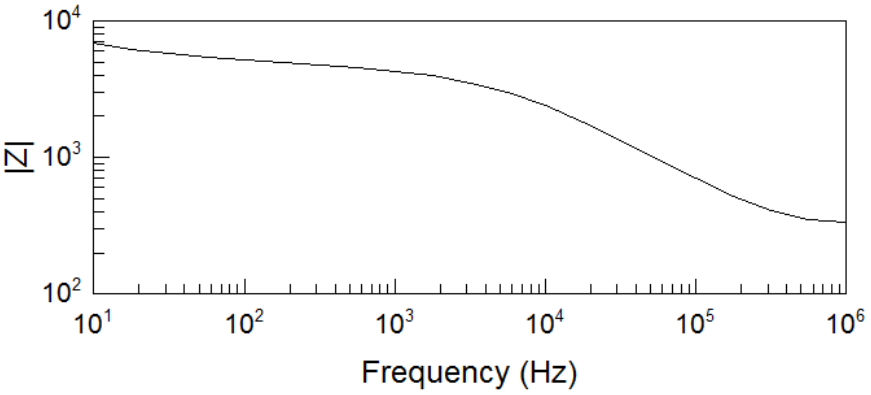

Figure 15 – Impedance vs. frequency for E1551X non-coated blade electrode on a cucumber.

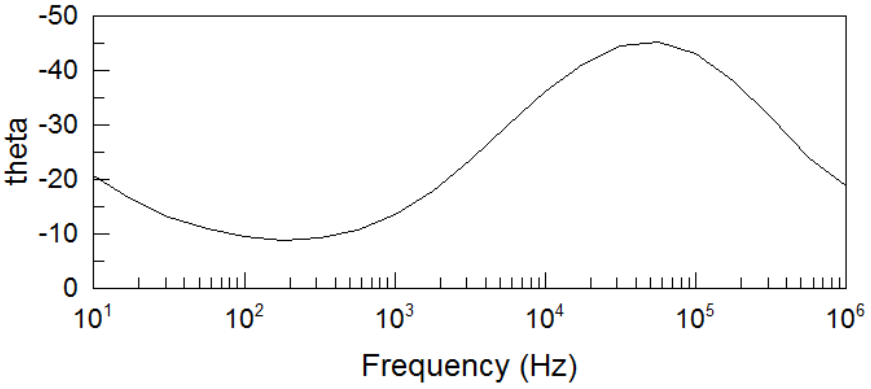

Figure 16 – Phase vs. frequency for E1551X non-coated blade electrode on a cucumber.

4.2.2 Experiment B – Cucumber model in deionized water

Figure 17 and Figure 18 represent the measurement results from the cucumber model in experiment B. At the distances 1.5 cm through 0.2 cm no significant cucumber dispersion can be seen at 50 kHz. At a distance of 0.1 cm a small dispersion can be seen. At 0.0 cm (adjacent) and -0.6 cm (inside the cucumber) a large dispersion can clearly be identified at

50 kHz corresponding with the result from Experiment A. In other words, the blade electrode shows no significant contribution from the characteristic impedance of the cucumber at distances 0.2 cm and greater. It does however show tendencies for the 50 kHz dispersion of the cucumber at 0.1 cm and closer.

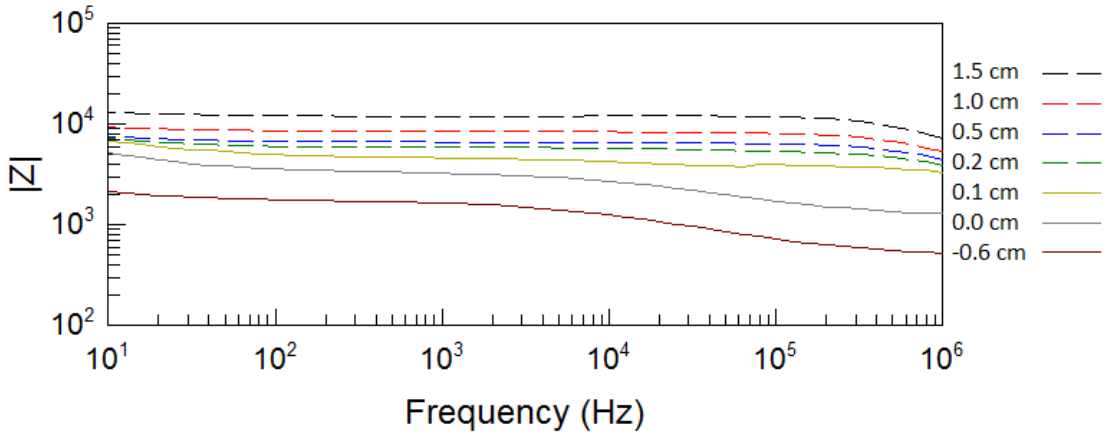

Figure 17 – Impedance vs. frequency for a blade electrode in a bath of deionized water using the cucumber model at various distances.

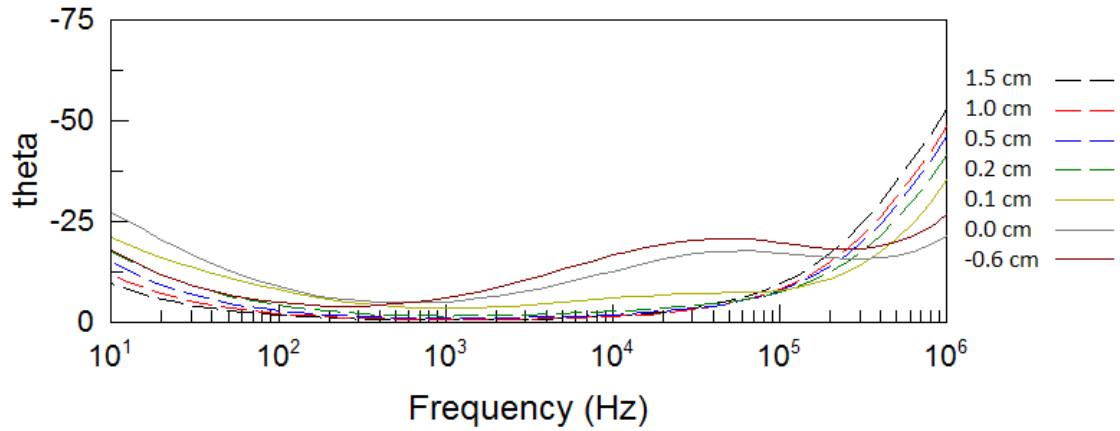

Figure 18 – Phase vs. frequency for a blade electrode in a bath of deionized water using the cucumber model at various distances.

4.3 Pig experiments

Appendix D contains impedance vs. frequency and phase vs. frequency graphs for all common bile duct (CBD) and proper hepatic artery (PHA) measurements across all pig surgeries. These graphs also plot the mean impedance and mean phase based on the same measurements.

4.3.1 Arithmetic mean analysis

Table 2 and Table 3 are True/False tables generated based on the mean data of all CBD and PHA measurements. Each column in the table represents an operation (OP1-OP9), and each row represents a specific frequency. The TRUE/FALSE statements are based upon whether or not the hypothesis for the table is true or false for that particular operation on that particular frequency.

Combined, the tables show the most true hypotheses (14) between the frequencies 316 kHz and 631 kHz, and the least amount (9) on the very lowest frequency (100 Hz).

Hypothesis for Table 2: $\bar{Z}_{CBD} > \bar{Z}_{PHA}$

Frequency	OP1	OP2	OP3	OP4	OP5	OP6	OP7	OP8	OP9
1.00E+06	TRUE	TRUE	TRUE	FALSE	TRUE	TRUE	TRUE	FALSE	FALSE
7.94E+05	TRUE	TRUE	FALSE	TRUE	TRUE	TRUE	TRUE	FALSE	FALSE
6.31E+05	TRUE	TRUE	TRUE	FALSE	TRUE	TRUE	TRUE	FALSE	FALSE
5.01E+05	TRUE	TRUE	TRUE	TRUE	TRUE	TRUE	TRUE	FALSE	FALSE
3.98E+05	TRUE	TRUE	TRUE	TRUE	TRUE	TRUE	TRUE	FALSE	FALSE
3.16E+05	TRUE	TRUE	TRUE	TRUE	TRUE	TRUE	TRUE	FALSE	FALSE
2.51E+05	TRUE	TRUE	TRUE	TRUE	TRUE	TRUE	TRUE	FALSE	FALSE
2.00E+05	TRUE	TRUE	TRUE	TRUE	TRUE	TRUE	TRUE	FALSE	FALSE
1.58E+05	TRUE	TRUE	TRUE	TRUE	TRUE	TRUE	TRUE	FALSE	FALSE
1.26E+05	TRUE	TRUE	TRUE	TRUE	TRUE	TRUE	TRUE	FALSE	FALSE
1.00E+05	TRUE	TRUE	TRUE	FALSE	TRUE	TRUE	TRUE	FALSE	FALSE
7.94E+04	TRUE	TRUE	TRUE	FALSE	TRUE	TRUE	TRUE	FALSE	FALSE
6.31E+04	TRUE	TRUE	TRUE	FALSE	TRUE	TRUE	TRUE	FALSE	FALSE
5.01E+04	TRUE	TRUE	TRUE	FALSE	TRUE	TRUE	TRUE	FALSE	FALSE
3.98E+04	TRUE	TRUE	TRUE	TRUE	TRUE	TRUE	TRUE	FALSE	FALSE
3.16E+04	TRUE	TRUE	TRUE	TRUE	TRUE	TRUE	TRUE	FALSE	FALSE
2.51E+04	TRUE	TRUE	TRUE	FALSE	TRUE	TRUE	TRUE	FALSE	FALSE
2.00E+04	TRUE	TRUE	TRUE	FALSE	TRUE	TRUE	TRUE	FALSE	FALSE
1.58E+04	TRUE	TRUE	TRUE	TRUE	TRUE	TRUE	TRUE	FALSE	FALSE
1.26E+04	TRUE	TRUE	TRUE	FALSE	TRUE	TRUE	TRUE	FALSE	FALSE
1.00E+04	TRUE	TRUE	TRUE	FALSE	TRUE	TRUE	TRUE	FALSE	FALSE
7.94E+03	TRUE	TRUE	TRUE	FALSE	TRUE	TRUE	TRUE	FALSE	FALSE
6.31E+03	TRUE	TRUE	TRUE	FALSE	TRUE	TRUE	TRUE	FALSE	FALSE
5.01E+03	TRUE	TRUE	TRUE	FALSE	TRUE	TRUE	TRUE	FALSE	FALSE
3.98E+03	TRUE	TRUE	TRUE	FALSE	TRUE	TRUE	TRUE	FALSE	FALSE
3.16E+03	TRUE	TRUE	TRUE	TRUE	TRUE	TRUE	TRUE	TRUE	FALSE
2.51E+03	TRUE	TRUE	TRUE	TRUE	TRUE	TRUE	TRUE	TRUE	FALSE
2.00E+03	TRUE	TRUE	TRUE	TRUE	TRUE	TRUE	TRUE	TRUE	FALSE
1.58E+03	TRUE	TRUE	TRUE	TRUE	TRUE	TRUE	TRUE	TRUE	FALSE
1.26E+03	TRUE	TRUE	TRUE	TRUE	TRUE	TRUE	TRUE	TRUE	FALSE
1.00E+03	TRUE	TRUE	TRUE	TRUE	TRUE	TRUE	TRUE	TRUE	FALSE
7.94E+02	TRUE	TRUE	TRUE	TRUE	TRUE	TRUE	TRUE	TRUE	FALSE
6.31E+02	TRUE	TRUE	TRUE	TRUE	TRUE	TRUE	TRUE	TRUE	FALSE
5.01E+02	TRUE	TRUE	TRUE	TRUE	TRUE	TRUE	TRUE	TRUE	FALSE
3.98E+02	TRUE	TRUE	TRUE	TRUE	TRUE	TRUE	TRUE	TRUE	FALSE
3.16E+02	TRUE	TRUE	TRUE	TRUE	TRUE	TRUE	TRUE	TRUE	FALSE
2.51E+02	TRUE	TRUE	TRUE	TRUE	TRUE	TRUE	TRUE	TRUE	FALSE
2.00E+02	TRUE	TRUE	TRUE	TRUE	TRUE	TRUE	TRUE	TRUE	FALSE
1.58E+02	TRUE	TRUE	TRUE	TRUE	TRUE	TRUE	TRUE	TRUE	FALSE
1.26E+02	TRUE	TRUE	TRUE	TRUE	TRUE	TRUE	TRUE	TRUE	FALSE
1.00E+02	TRUE	TRUE	TRUE	TRUE	FALSE	FALSE	TRUE	TRUE	FALSE

Table 2 – True/False table f or arithmetic impedance mean across all CBD and PHA measurements for all operations.

Hypothesis for Table 3: $\bar{\theta}_{CBD} < \bar{\theta}_{PHA}$

Frequency	OP1	OP2	OP3	OP4	OP5	OP6	OP7	OP8	OP9
1.00E+06	TRUE	TRUE	TRUE	TRUE	TRUE	TRUE	TRUE	FALSE	FALSE
7.94E+05	TRUE	TRUE	FALSE	TRUE	TRUE	TRUE	TRUE	FALSE	FALSE
6.31E+05	TRUE	TRUE	TRUE	TRUE	TRUE	TRUE	TRUE	FALSE	FALSE
5.01E+05	TRUE	TRUE	TRUE	TRUE	TRUE	TRUE	TRUE	FALSE	FALSE
3.98E+05	TRUE	TRUE	TRUE	TRUE	TRUE	TRUE	TRUE	FALSE	FALSE
3.16E+05	TRUE	TRUE	TRUE	TRUE	TRUE	TRUE	TRUE	FALSE	FALSE
2.51E+05	TRUE	FALSE	TRUE	TRUE	TRUE	TRUE	FALSE	FALSE	FALSE
2.00E+05	TRUE	FALSE	TRUE	TRUE	TRUE	TRUE	FALSE	FALSE	FALSE
1.58E+05	TRUE	FALSE	TRUE	TRUE	TRUE	FALSE	FALSE	TRUE	FALSE
1.26E+05	TRUE	FALSE	TRUE	TRUE	TRUE	FALSE	FALSE	TRUE	FALSE
1.00E+05	TRUE	FALSE	TRUE	TRUE	TRUE	FALSE	FALSE	TRUE	FALSE
7.94E+04	TRUE	FALSE	TRUE	FALSE	TRUE	FALSE	FALSE	TRUE	FALSE
6.31E+04	TRUE	FALSE	TRUE	TRUE	TRUE	FALSE	FALSE	TRUE	FALSE
5.01E+04	TRUE	FALSE	TRUE	TRUE	FALSE	FALSE	FALSE	TRUE	FALSE
3.98E+04	TRUE	FALSE	TRUE	TRUE	FALSE	FALSE	FALSE	TRUE	FALSE
3.16E+04	TRUE	FALSE	TRUE	TRUE	FALSE	FALSE	FALSE	TRUE	FALSE
2.51E+04	TRUE	FALSE	TRUE	TRUE	TRUE	FALSE	FALSE	TRUE	FALSE
2.00E+04	TRUE	FALSE	TRUE	TRUE	FALSE	FALSE	FALSE	TRUE	FALSE
1.58E+04	TRUE	FALSE	TRUE	TRUE	FALSE	FALSE	FALSE	TRUE	FALSE
1.26E+04	TRUE	FALSE	TRUE	TRUE	FALSE	FALSE	FALSE	TRUE	FALSE
1.00E+04	TRUE	FALSE	TRUE	TRUE	FALSE	FALSE	FALSE	TRUE	FALSE
7.94E+03	TRUE	FALSE	TRUE	TRUE	FALSE	FALSE	FALSE	TRUE	FALSE
6.31E+03	TRUE	FALSE	TRUE	TRUE	FALSE	FALSE	FALSE	TRUE	FALSE
5.01E+03	TRUE	FALSE	TRUE	TRUE	FALSE	FALSE	FALSE	TRUE	FALSE
3.98E+03	TRUE	FALSE	TRUE	TRUE	FALSE	FALSE	FALSE	TRUE	FALSE
3.16E+03	TRUE	FALSE	FALSE	TRUE	FALSE	FALSE	FALSE	TRUE	FALSE
2.51E+03	TRUE	FALSE	FALSE	TRUE	FALSE	FALSE	FALSE	TRUE	FALSE
2.00E+03	TRUE	FALSE	FALSE	TRUE	FALSE	FALSE	FALSE	TRUE	FALSE
1.58E+03	TRUE	FALSE	FALSE	TRUE	FALSE	FALSE	FALSE	TRUE	FALSE
1.26E+03	TRUE	FALSE	FALSE	TRUE	FALSE	FALSE	FALSE	TRUE	FALSE
1.00E+03	TRUE	FALSE	FALSE	TRUE	FALSE	FALSE	FALSE	TRUE	FALSE
7.94E+02	TRUE	FALSE	FALSE	TRUE	FALSE	FALSE	FALSE	TRUE	FALSE
6.31E+02	TRUE	FALSE	FALSE	TRUE	FALSE	FALSE	FALSE	FALSE	FALSE
5.01E+02	TRUE	FALSE	FALSE	FALSE	FALSE	FALSE	FALSE	FALSE	TRUE
3.98E+02	TRUE	FALSE	FALSE	FALSE	FALSE	FALSE	FALSE	FALSE	TRUE
3.16E+02	TRUE	FALSE	FALSE	FALSE	FALSE	FALSE	FALSE	FALSE	TRUE
2.51E+02	TRUE	FALSE	FALSE	FALSE	FALSE	FALSE	FALSE	FALSE	TRUE
2.00E+02	TRUE	FALSE	FALSE	FALSE	FALSE	FALSE	FALSE	FALSE	TRUE
1.58E+02	TRUE	FALSE	FALSE	FALSE	FALSE	FALSE	FALSE	FALSE	TRUE
1.26E+02	TRUE	FALSE	FALSE	FALSE	FALSE	FALSE	FALSE	FALSE	TRUE
1.00E+02	TRUE	FALSE	FALSE	FALSE	FALSE	FALSE	FALSE	TRUE	TRUE

Table 3 – True/False table f or arithmetic phase mean across all CBD and PHA measurements for all operations.

4.3.2 Frequency distribution

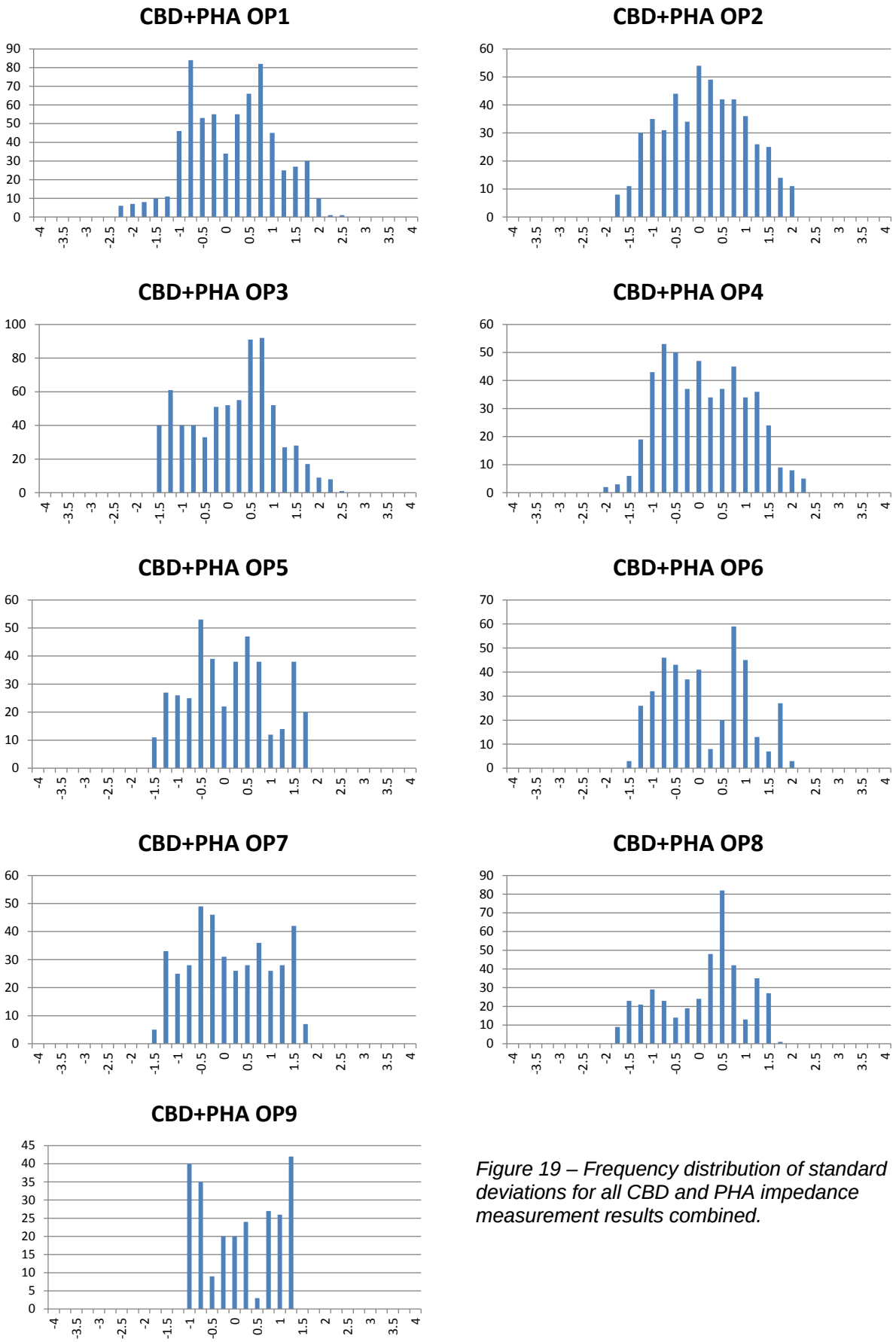

Figure 19 – Frequency distribution of standard deviations for all CBD and PHA impedance measurement results combined.

Figure 19 shows the frequency distribution of standard deviations for the combined value of all impedance measurements on the CBD and PHA. Appendix E contains the graphs for the frequency distribution of the impedance standard deviation values separately for CBD and PHA measurements.

4.3.2.1 Normal distribution

The graph that most closely represents a bell shaped normal distribution is OP2. The other frequency distributions do not seem to be normally distributed across all frequencies.

Keep in mind that this is indeed a representation across all frequencies. There were not enough data to check for any normal distribution across each individual frequency for each of the measurement series (CBD and PHA). Distributions for different frequency windows were also plotted and checked for normality. The windows 100 Hz – 1 kHz, 1 kHz – 10 kHz, 10 kHz – 100 kHz and 100 kHz – 1 MHz all showed the same tendency as the combined result for all frequencies.

4.3.3 Statistics assuming normal distribution

Too few measurements were recorded in order to determine whether or not the measurement results for each individual frequency are normally distributed. An unpaired t-test and a Wilcoxon signed-rank test were still performed on the CBD vs. PHA measurement data in the case this data are shown to be normally distributed at a later time.

4.3.3.1 Student's t-Test (unpaired)

Assuming a normal distribution across each individual frequency, an unpaired t-test was applied to each series of CBD vs. PHA measurements. Table 4 and Table 5 shows the probabilities from the results of this test for impedance and phase measurement data respectively. The t-test used a two-tailed model with unequal variance for each data series.

Both tables use a gradient color scheme between red and green to color the result based on the probability score. As such one can easily identify visually where the scores are the lowest and highest. The frequency with the lowest overall probability score is at 1.26 kHz for the impedance data and 794 kHz for the phase data.

Frequency	OP1	OP2	OP3	OP4	OP5	OP6	OP7	OP8	OP9
1.00E+06	15.14 %	0.24 %	3.33 %	45.74 %	6.69 %	79.05 %	0.48 %	8.00 %	29.93 %
7.94E+05	44.15 %	0.19 %	5.61 %	46.88 %	8.73 %	70.70 %	0.20 %	10.60 %	29.14 %
6.31E+05	9.45 %	0.01 %	48.97 %	84.39 %	2.59 %	66.24 %	0.18 %	8.67 %	34.17 %
5.01E+05	6.14 %	0.10 %	25.23 %	86.50 %	11.45 %	57.51 %	0.08 %	9.86 %	31.77 %
3.98E+05	7.54 %	0.05 %	48.63 %	16.12 %	2.72 %	38.11 %	0.05 %	9.08 %	28.18 %
3.16E+05	8.14 %	1.61 %	18.33 %	46.51 %	1.54 %	44.01 %	0.04 %	8.77 %	28.26 %
2.51E+05	12.58 %	0.21 %	15.71 %	28.26 %	1.25 %	45.31 %	0.07 %	8.96 %	27.67 %
2.00E+05	14.21 %	0.11 %	14.45 %	76.09 %	1.30 %	45.08 %	0.04 %	7.03 %	36.50 %
1.58E+05	14.41 %	0.17 %	18.99 %	63.68 %	8.32 %	50.08 %	0.02 %	6.78 %	39.00 %
1.26E+05	21.98 %	0.05 %	20.76 %	90.09 %	1.40 %	38.03 %	0.01 %	10.54 %	40.43 %
1.00E+05	25.34 %	4.19 %	15.21 %	77.01 %	1.63 %	37.69 %	0.01 %	8.80 %	35.77 %
7.94E+04	16.71 %	0.10 %	14.42 %	81.18 %	10.76 %	38.08 %	0.01 %	8.71 %	24.71 %
6.31E+04	19.53 %	0.03 %	10.88 %	44.26 %	7.52 %	19.32 %	0.02 %	17.93 %	35.54 %
5.01E+04	43.11 %	0.48 %	15.98 %	61.21 %	1.84 %	13.84 %	0.03 %	21.82 %	34.81 %
3.98E+04	51.15 %	1.14 %	10.19 %	93.90 %	1.66 %	17.17 %	0.00 %	26.63 %	32.60 %
3.16E+04	66.99 %	0.58 %	11.29 %	94.88 %	1.78 %	21.95 %	0.00 %	29.97 %	25.16 %
2.51E+04	41.69 %	0.18 %	13.50 %	66.96 %	11.76 %	24.17 %	0.00 %	38.10 %	23.55 %
2.00E+04	56.50 %	0.11 %	14.66 %	59.96 %	2.55 %	25.75 %	0.00 %	35.67 %	29.24 %
1.58E+04	40.12 %	0.31 %	7.42 %	79.80 %	2.64 %	35.26 %	0.00 %	30.85 %	26.78 %
1.26E+04	21.34 %	0.09 %	5.61 %	54.20 %	3.48 %	29.88 %	0.00 %	32.52 %	24.51 %
1.00E+04	29.76 %	1.04 %	6.00 %	85.49 %	6.50 %	31.65 %	0.00 %	44.73 %	22.82 %
7.94E+03	26.69 %	0.30 %	2.86 %	95.24 %	11.26 %	32.27 %	0.01 %	46.28 %	24.29 %
6.31E+03	11.77 %	0.22 %	2.19 %	91.86 %	4.59 %	30.64 %	0.01 %	42.64 %	22.28 %
5.01E+03	3.33 %	0.31 %	7.31 %	75.81 %	6.02 %	30.85 %	0.01 %	67.16 %	21.46 %
3.98E+03	2.40 %	0.89 %	3.77 %	63.79 %	9.45 %	30.89 %	0.03 %	84.76 %	22.37 %
3.16E+03	2.37 %	1.43 %	1.03 %	95.49 %	25.16 %	25.45 %	0.06 %	90.79 %	21.50 %
2.51E+03	0.46 %	1.79 %	1.54 %	50.03 %	18.34 %	22.56 %	0.08 %	50.95 %	20.93 %
2.00E+03	0.24 %	0.07 %	1.93 %	45.71 %	13.40 %	20.76 %	0.06 %	43.41 %	20.64 %
1.58E+03	0.42 %	0.23 %	1.81 %	30.30 %	13.50 %	18.33 %	0.09 %	46.40 %	21.01 %
1.26E+03	0.07 %	0.06 %	3.81 %	31.51 %	13.79 %	15.86 %	0.13 %	31.67 %	21.81 %
1.00E+03	0.04 %	1.62 %	5.12 %	9.17 %	16.59 %	12.89 %	0.25 %	17.43 %	22.09 %
7.94E+02	0.03 %	0.80 %	15.24 %	24.45 %	3.29 %	11.02 %	0.42 %	36.46 %	21.93 %
6.31E+02	0.04 %	2.47 %	21.75 %	5.65 %	5.54 %	11.95 %	0.53 %	45.88 %	21.92 %
5.01E+02	0.04 %	3.63 %	24.19 %	11.11 %	5.67 %	11.36 %	0.78 %	31.88 %	22.40 %
3.98E+02	0.04 %	17.47 %	31.24 %	9.13 %	13.42 %	12.71 %	1.66 %	42.69 %	23.01 %
3.16E+02	0.05 %	15.82 %	38.80 %	22.70 %	6.85 %	16.12 %	3.36 %	59.30 %	24.12 %
2.51E+02	0.05 %	28.39 %	45.55 %	40.56 %	36.96 %	25.95 %	4.60 %	69.32 %	25.45 %
2.00E+02	0.07 %	27.07 %	43.35 %	9.72 %	24.79 %	7.21 %	7.73 %	57.50 %	27.12 %
1.58E+02	0.06 %	39.46 %	50.47 %	29.64 %	49.99 %	52.46 %	9.84 %	62.87 %	28.93 %
1.26E+02	0.06 %	47.70 %	53.38 %	42.45 %	38.39 %	61.58 %	13.02 %	86.61 %	30.73 %
1.00E+02	0.06 %	45.56 %	49.23 %	14.69 %	73.42 %	31.65 %	14.93 %	85.01 %	31.72 %

Table 4 – Unpaired t-test on all CBD vs. PHA impedance measurements for each frequency.

Frequency	OP1	OP2	OP3	OP4	OP5	OP6	OP7	OP8	OP9
1.00E+06	2.43 %	0.00 %	23.94 %	0.06 %	3.95 %	25.64 %	0.19 %	5.34 %	12.98 %
7.94E+05	0.17 %	0.00 %	0.01 %	0.02 %	3.84 %	19.34 %	0.03 %	4.58 %	13.91 %
6.31E+05	0.26 %	0.01 %	0.00 %	0.46 %	3.09 %	21.92 %	0.05 %	4.39 %	11.57 %
5.01E+05	0.55 %	0.04 %	0.46 %	0.63 %	5.98 %	20.86 %	1.24 %	3.65 %	9.96 %
3.98E+05	0.84 %	1.86 %	2.60 %	0.55 %	8.85 %	21.92 %	15.36 %	5.09 %	9.53 %
3.16E+05	0.66 %	44.10 %	3.28 %	1.86 %	16.67 %	26.76 %	46.53 %	5.93 %	8.80 %
2.51E+05	0.70 %	12.81 %	5.36 %	5.70 %	26.26 %	33.35 %	32.70 %	9.27 %	13.28 %
2.00E+05	0.81 %	3.66 %	7.94 %	14.12 %	39.08 %	36.59 %	18.93 %	20.83 %	13.35 %
1.58E+05	0.99 %	0.90 %	7.03 %	34.40 %	31.96 %	43.29 %	11.21 %	10.22 %	14.79 %
1.26E+05	0.80 %	0.29 %	6.48 %	38.80 %	33.40 %	48.47 %	12.20 %	4.14 %	14.57 %
1.00E+05	0.12 %	0.83 %	10.50 %	37.23 %	23.07 %	49.66 %	11.90 %	1.36 %	17.50 %
7.94E+04	0.14 %	0.31 %	14.45 %	48.06 %	16.38 %	33.54 %	7.71 %	0.66 %	16.75 %
6.31E+04	0.20 %	0.22 %	12.15 %	38.83 %	23.45 %	12.47 %	5.83 %	0.72 %	15.28 %
5.01E+04	0.07 %	0.17 %	7.71 %	44.49 %	45.19 %	25.84 %	6.02 %	0.56 %	13.52 %
3.98E+04	0.06 %	0.14 %	9.87 %	26.57 %	43.82 %	17.43 %	3.35 %	0.48 %	12.95 %
3.16E+04	0.07 %	0.29 %	9.86 %	30.10 %	38.36 %	25.40 %	1.60 %	0.54 %	13.36 %
2.51E+04	0.16 %	0.12 %	11.45 %	18.54 %	35.21 %	8.99 %	0.56 %	0.43 %	14.17 %
2.00E+04	0.10 %	0.10 %	13.25 %	11.35 %	28.75 %	10.63 %	0.44 %	0.28 %	14.04 %
1.58E+04	0.13 %	0.07 %	21.48 %	30.13 %	11.07 %	22.59 %	0.36 %	0.23 %	13.19 %
1.26E+04	0.28 %	0.09 %	22.94 %	5.23 %	8.42 %	23.58 %	0.35 %	0.40 %	13.84 %
1.00E+04	0.35 %	0.52 %	25.32 %	10.09 %	20.33 %	27.56 %	0.57 %	0.20 %	14.31 %
7.94E+03	0.19 %	0.58 %	30.34 %	14.43 %	30.64 %	29.38 %	0.52 %	0.20 %	13.18 %
6.31E+03	0.24 %	0.36 %	35.03 %	16.06 %	4.83 %	31.33 %	0.49 %	0.17 %	14.13 %
5.01E+03	0.45 %	1.74 %	36.76 %	8.60 %	8.20 %	32.83 %	0.27 %	0.17 %	14.88 %
3.98E+03	0.63 %	2.80 %	42.63 %	6.48 %	10.14 %	33.43 %	0.17 %	0.29 %	14.68 %
3.16E+03	0.80 %	2.75 %	48.48 %	10.22 %	36.02 %	28.64 %	0.16 %	0.50 %	14.27 %
2.51E+03	0.91 %	2.44 %	42.51 %	32.84 %	23.71 %	25.14 %	0.20 %	1.72 %	14.32 %
2.00E+03	1.33 %	4.85 %	39.98 %	22.04 %	16.86 %	22.98 %	0.05 %	3.92 %	14.64 %
1.58E+03	1.34 %	4.84 %	33.55 %	29.00 %	20.88 %	18.57 %	0.03 %	6.30 %	15.59 %
1.26E+03	1.87 %	1.22 %	28.48 %	26.50 %	23.96 %	16.11 %	0.05 %	18.90 %	16.20 %
1.00E+03	6.19 %	2.35 %	23.80 %	42.69 %	23.99 %	12.23 %	0.04 %	39.08 %	19.15 %
7.94E+02	8.55 %	3.46 %	24.02 %	30.93 %	7.19 %	8.65 %	0.02 %	46.70 %	27.68 %
6.31E+02	7.15 %	2.72 %	22.03 %	45.59 %	6.47 %	7.55 %	0.01 %	41.96 %	48.91 %
5.01E+02	7.11 %	0.82 %	17.83 %	48.35 %	9.89 %	7.56 %	0.06 %	29.98 %	24.00 %
3.98E+02	10.37 %	1.54 %	15.70 %	43.99 %	11.51 %	7.30 %	0.06 %	27.30 %	5.01 %
3.16E+02	16.73 %	0.66 %	16.12 %	48.88 %	5.07 %	7.63 %	0.01 %	25.17 %	0.69 %
2.51E+02	22.07 %	0.58 %	16.44 %	48.82 %	10.17 %	6.32 %	0.03 %	26.65 %	0.35 %
2.00E+02	18.27 %	0.13 %	14.30 %	33.33 %	11.54 %	31.63 %	0.01 %	23.39 %	0.51 %
1.58E+02	20.66 %	0.03 %	16.11 %	37.28 %	10.62 %	12.59 %	0.02 %	28.41 %	0.21 %
1.26E+02	26.01 %	0.02 %	17.56 %	40.32 %	7.15 %	10.04 %	0.02 %	33.93 %	0.12 %
1.00E+02	40.77 %	0.46 %	21.22 %	35.08 %	22.06 %	9.83 %	0.02 %	29.05 %	0.25 %

Table 5 – Unpaired t-test on all CBD vs. PHA phase measurements for each frequency.

4.3.3.2 Wilcoxon signed-rank test

Appendix F shows the True/False tables for the result of the Wilcoxon signed-rank test. This test was performed on the impedance and phase of the CBD vs. PHA measurement data. It was tested with a two-tailed test and an $\alpha = 0.05, Z = 1.96$. A result of TRUE means that the H_0 hypothesis has been rejected, or in other words that there is a difference between the two data sets. Note that this is a paired test, and as such some of the datasets has been ruled out of the test.

The frequency with the largest amount of H_0 rejects is again at the higher frequencies (794 kHz), corresponding with the results from the unpaired t-test.

4.3.4 Mann-Whitney U test (any distribution)

Table 6 and Table 7 shows the True/False tables for the result of the Mann-Whitney U test for any distribution. This test was performed on the CBD vs. PHA impedance and phase measurement data. The test used a critical value $\alpha = 0.05$. A value of TRUE represents a rejected H_0 hypothesis, which means that there is a statistical difference between the two measurement groups. Note that this test simply checks if there a significant difference between the data series. It does not evaluate any additional hypothesis regarding the goals of this thesis.

The frequency with the most amount of rejected H_0 across both phase and impedance is at 631 kHz. The impedance data shows an overall higher amount of rejects at the lower frequencies (1.58 kHz – 5 kHz), while the phase seem to work better at the higher frequencies. This again corresponds on average to the overall results from the previous unpaired t-test.

Frequency	OP1	OP2	OP3	OP4	OP5	OP6	OP7	OP8	OP9
1.00E+06	FALSE	TRUE	FALSE	FALSE	FALSE	FALSE	TRUE	FALSE	TRUE
7.94E+05	FALSE	TRUE	FALSE	FALSE	FALSE	FALSE	TRUE	FALSE	TRUE
6.31E+05	FALSE	TRUE	FALSE	FALSE	TRUE	FALSE	TRUE	FALSE	TRUE
5.01E+05	FALSE	TRUE	FALSE	FALSE	FALSE	FALSE	TRUE	FALSE	TRUE
3.98E+05	TRUE	TRUE	FALSE	FALSE	TRUE	FALSE	TRUE	FALSE	TRUE
3.16E+05	FALSE	TRUE	FALSE	FALSE	TRUE	FALSE	TRUE	FALSE	TRUE
2.51E+05	FALSE	TRUE	FALSE	FALSE	TRUE	FALSE	TRUE	FALSE	TRUE
2.00E+05	FALSE	TRUE	FALSE	FALSE	TRUE	FALSE	TRUE	FALSE	TRUE
1.58E+05	FALSE	TRUE	FALSE	FALSE	FALSE	FALSE	TRUE	FALSE	TRUE
1.26E+05	FALSE	TRUE	FALSE	FALSE	TRUE	FALSE	TRUE	FALSE	TRUE
1.00E+05	FALSE	TRUE	FALSE	FALSE	TRUE	FALSE	TRUE	FALSE	TRUE
7.94E+04	FALSE	TRUE	FALSE	FALSE	FALSE	FALSE	TRUE	FALSE	TRUE
6.31E+04	FALSE	TRUE	FALSE	FALSE	FALSE	FALSE	TRUE	FALSE	TRUE
5.01E+04	FALSE	TRUE	FALSE	FALSE	TRUE	FALSE	TRUE	FALSE	TRUE
3.98E+04	FALSE	TRUE	FALSE	FALSE	TRUE	FALSE	TRUE	FALSE	TRUE
3.16E+04	FALSE	TRUE	FALSE	FALSE	TRUE	FALSE	TRUE	FALSE	TRUE
2.51E+04	FALSE	TRUE	FALSE	FALSE	FALSE	FALSE	TRUE	FALSE	TRUE
2.00E+04	FALSE	TRUE	FALSE	FALSE	TRUE	FALSE	TRUE	FALSE	TRUE
1.58E+04	FALSE	TRUE	FALSE	FALSE	TRUE	FALSE	TRUE	FALSE	TRUE
1.26E+04	FALSE	TRUE	FALSE	FALSE	FALSE	FALSE	TRUE	FALSE	TRUE
1.00E+04	FALSE	TRUE	FALSE	FALSE	FALSE	FALSE	TRUE	FALSE	TRUE
7.94E+03	FALSE	TRUE	TRUE	FALSE	FALSE	FALSE	TRUE	FALSE	TRUE
6.31E+03	FALSE	TRUE	TRUE	FALSE	FALSE	FALSE	TRUE	FALSE	TRUE
5.01E+03	TRUE	TRUE	TRUE	FALSE	FALSE	FALSE	TRUE	FALSE	TRUE
3.98E+03	TRUE	TRUE	TRUE	FALSE	FALSE	FALSE	TRUE	FALSE	TRUE
3.16E+03	FALSE	TRUE	TRUE	FALSE	FALSE	FALSE	TRUE	FALSE	TRUE
2.51E+03	TRUE	TRUE	TRUE	FALSE	FALSE	FALSE	TRUE	FALSE	TRUE
2.00E+03	TRUE	TRUE	TRUE	FALSE	FALSE	FALSE	TRUE	FALSE	TRUE
1.58E+03	TRUE	TRUE	TRUE	FALSE	FALSE	FALSE	TRUE	FALSE	TRUE
1.26E+03	TRUE	TRUE	FALSE	FALSE	FALSE	FALSE	TRUE	FALSE	TRUE
1.00E+03	TRUE	TRUE	FALSE	FALSE	FALSE	FALSE	TRUE	FALSE	TRUE
7.94E+02	TRUE	TRUE	FALSE	FALSE	FALSE	FALSE	TRUE	FALSE	TRUE
6.31E+02	TRUE	TRUE	FALSE	FALSE	FALSE	FALSE	TRUE	FALSE	TRUE
5.01E+02	TRUE	FALSE	FALSE	FALSE	FALSE	FALSE	TRUE	FALSE	TRUE
3.98E+02	TRUE	FALSE	FALSE	FALSE	FALSE	FALSE	TRUE	FALSE	TRUE
3.16E+02	TRUE	FALSE	FALSE	FALSE	FALSE	FALSE	TRUE	FALSE	TRUE
2.51E+02	TRUE	FALSE	FALSE	FALSE	FALSE	FALSE	FALSE	FALSE	TRUE
2.00E+02	TRUE	FALSE	FALSE	FALSE	FALSE	FALSE	FALSE	FALSE	TRUE
1.58E+02	TRUE	FALSE	FALSE	FALSE	FALSE	FALSE	FALSE	FALSE	TRUE
1.26E+02	TRUE	FALSE	FALSE	FALSE	FALSE	FALSE	FALSE	FALSE	TRUE
1.00E+02	TRUE	FALSE	FALSE	FALSE	FALSE	FALSE	FALSE	FALSE	TRUE

Table 6 – Mann-Whitney U test for all CBD vs. PHA impedance measurements for each frequency, with a 5% critical value.

Frequency	OP1	OP2	OP3	OP4	OP5	OP6	OP7	OP8	OP9
1.00E+06	FALSE	TRUE	FALSE	TRUE	TRUE	FALSE	TRUE	FALSE	TRUE
7.94E+05	TRUE	TRUE	TRUE	TRUE	FALSE	FALSE	TRUE	FALSE	TRUE
6.31E+05	TRUE	TRUE	TRUE	TRUE	FALSE	FALSE	TRUE	FALSE	TRUE
5.01E+05	TRUE	TRUE	TRUE	TRUE	FALSE	FALSE	FALSE	FALSE	TRUE
3.98E+05	TRUE	FALSE	FALSE	TRUE	FALSE	FALSE	FALSE	FALSE	TRUE
3.16E+05	TRUE	FALSE	FALSE	TRUE	FALSE	FALSE	FALSE	FALSE	TRUE
2.51E+05	TRUE	FALSE	FALSE	FALSE	FALSE	FALSE	FALSE	FALSE	TRUE
2.00E+05	TRUE	FALSE	FALSE	FALSE	FALSE	FALSE	FALSE	FALSE	TRUE
1.58E+05	TRUE	TRUE	FALSE	FALSE	FALSE	FALSE	FALSE	FALSE	TRUE
1.26E+05	TRUE	TRUE	FALSE	FALSE	FALSE	FALSE	FALSE	FALSE	TRUE
1.00E+05	TRUE	TRUE	FALSE	FALSE	FALSE	FALSE	FALSE	TRUE	TRUE
7.94E+04	TRUE	TRUE	FALSE	FALSE	FALSE	FALSE	FALSE	TRUE	TRUE
6.31E+04	TRUE	TRUE	FALSE	FALSE	FALSE	FALSE	FALSE	TRUE	TRUE
5.01E+04	TRUE	TRUE	FALSE	FALSE	FALSE	FALSE	FALSE	TRUE	TRUE
3.98E+04	TRUE	TRUE	FALSE	FALSE	FALSE	FALSE	FALSE	TRUE	TRUE
3.16E+04	TRUE	TRUE	FALSE	FALSE	FALSE	FALSE	TRUE	TRUE	TRUE
2.51E+04	TRUE	TRUE	FALSE	FALSE	FALSE	FALSE	TRUE	TRUE	TRUE
2.00E+04	TRUE	TRUE	FALSE	FALSE	FALSE	FALSE	TRUE	TRUE	TRUE
1.58E+04	TRUE	TRUE	FALSE	FALSE	FALSE	FALSE	TRUE	TRUE	TRUE
1.26E+04	TRUE	TRUE	FALSE	FALSE	FALSE	FALSE	TRUE	TRUE	TRUE
1.00E+04	TRUE	TRUE	FALSE	FALSE	FALSE	FALSE	TRUE	TRUE	TRUE
7.94E+03	TRUE	TRUE	FALSE	FALSE	FALSE	FALSE	TRUE	TRUE	TRUE
6.31E+03	TRUE	TRUE	FALSE	FALSE	FALSE	FALSE	TRUE	TRUE	TRUE
5.01E+03	TRUE	TRUE	FALSE	FALSE	FALSE	FALSE	TRUE	TRUE	TRUE
3.98E+03	TRUE	TRUE	FALSE	FALSE	FALSE	FALSE	TRUE	TRUE	TRUE
3.16E+03	TRUE	TRUE	FALSE	FALSE	FALSE	FALSE	TRUE	TRUE	TRUE
2.51E+03	TRUE	FALSE	FALSE	FALSE	FALSE	FALSE	TRUE	TRUE	TRUE
2.00E+03	TRUE	FALSE	FALSE	FALSE	FALSE	FALSE	TRUE	FALSE	TRUE
1.58E+03	TRUE	FALSE	FALSE	FALSE	FALSE	FALSE	TRUE	FALSE	TRUE
1.26E+03	TRUE	TRUE	FALSE	FALSE	FALSE	FALSE	TRUE	FALSE	TRUE
1.00E+03	TRUE	TRUE	FALSE	FALSE	FALSE	FALSE	TRUE	FALSE	TRUE
7.94E+02	FALSE	FALSE	FALSE	FALSE	FALSE	FALSE	TRUE	FALSE	TRUE
6.31E+02	FALSE	FALSE	FALSE	FALSE	FALSE	FALSE	TRUE	FALSE	TRUE
5.01E+02	FALSE	TRUE	FALSE	FALSE	FALSE	FALSE	TRUE	FALSE	TRUE
3.98E+02	FALSE	TRUE	FALSE	FALSE	FALSE	FALSE	TRUE	FALSE	TRUE
3.16E+02	FALSE	TRUE	FALSE	FALSE	FALSE	FALSE	TRUE	FALSE	TRUE
2.51E+02	FALSE	TRUE	FALSE	FALSE	FALSE	FALSE	TRUE	FALSE	TRUE
2.00E+02	FALSE	TRUE	FALSE	FALSE	FALSE	FALSE	TRUE	FALSE	TRUE
1.58E+02	FALSE	TRUE	FALSE	FALSE	FALSE	FALSE	TRUE	FALSE	TRUE
1.26E+02	FALSE	TRUE	FALSE	FALSE	FALSE	FALSE	TRUE	FALSE	TRUE
1.00E+02	FALSE	TRUE	FALSE	FALSE	FALSE	FALSE	TRUE	FALSE	TRUE

Table 7 – Mann-Whitney U test for all CBD vs. PHA phase measurements for each frequency, with a 5% critical value.

4.3.5 Mean vs. Mann-Whitney U vs. unpaired t-test

Table 8 shows the frequency with the statistically best test results for the impedance measurement data when combining the mean test, unpaired t-test and Mann-Whitney U test (for any distribution). Likewise, Table 9 shows the same overview for the phase measurement data.

Impedance (Ω)									
Frequency	1995.3	Hz							
OP	1	2	3	4	5	6	7	8	9
CBD mean	375.4078	281.2783	574.5967	693.3475	659.086	649.302	605.054	305.326	375.1567
PHA mean	280.9971	260.0317	483.2645	677.7625	605.12	607.882	482.132	294.496	592
Mean test	TRUE	TRUE	TRUE	TRUE	TRUE	TRUE	TRUE	TRUE	FALSE
t-test p-value	0.24 %	0.07 %	1.93 %	45.71 %	13.40 %	20.76 %	0.06 %	43.41 %	20.64 %
Mann-Whitney U	TRUE	TRUE	TRUE	FALSE	FALSE	FALSE	TRUE	FALSE	TRUE

Table 8 – Mean, unpaired t-test and Mann-Whitney U test overview for 2 kHz impedance measurements.

A frequency of 2 kHz was selected as the best overall statistical result for the impedance measurement data. Looking at Table 8 for the mean test one can see a single false positive across the span of all operations. The Mann-Whitney U test shows there is a significant difference between the CBD and PHA measurements in 5 out of 9 operations. 4 out of 9 operations are undefined. The t-test agrees with the Mann-Whitney U test for all except on operation 9 with a critical p-value of 5%.

Phase (°)									
Frequency	630960	Hz							
OP	1	2	3	4	5	6	7	8	9
CBD mean	6.8394	2.34575	0.811635	-0.31621	-2.22946	-4.97948	-5.82574	7.0214	3.457233
PHA mean	10.79446	4.957817	3.25192	2.0744	-1.27703	-4.24126	-3.44768	5.24644	1.744147
Mean test	TRUE	TRUE	TRUE	TRUE	TRUE	TRUE	TRUE	FALSE	FALSE
t-test p-value	0.26 %	0.01 %	0.00 %	0.46 %	3.09 %	21.92 %	0.05 %	4.39 %	11.57 %
Mann-Whitney U	TRUE	TRUE	TRUE	TRUE	FALSE	FALSE	TRUE	FALSE	TRUE

Table 9 – Mean, unpaired t-test and Mann-Whitney U test overview for 630 kHz phase measurements.

A frequency of 630 kHz was selected for the best overall statistical results in phase data. Looking at Table 9 for the mean test one can see two false positives across all operations, one of which is not statistically significant as a result. The Mann-Whitney U test shows a significant difference of the phase measurements in 6 out of 9 operations, with 3 left undefined. With a critical p-value of 5% the t-test disagrees with the Mann-Whitney U test in 3 operations.

4.3.5.1 Mean vs. Mann-Whitney U summary

Table 10 represents the summary of the data from Table 8 and Table 9 using only the data from the arithmetic mean and Mann-Whitney U tests. If the Mann-Whitney U test did not reject H_0, the operation result is assumed undefined.

$\boldsymbol{\alpha = 0.05}$	**Impedance**	**Phase**
True positive	4 (44%)	5 (55%)
False positive	1 (11%)	1 (11%)
Undefined	4 (44%)	3 (33%)

Table 10 – Summary of arithmetic mean vs. Mann-Whitney U test.

4.3.5.2 Mean vs. unpaired t-test summary

Table 11 represents the summary of the data from Table 8 and Table 9 using only the data from the arithmetic mean and unpaired t-test. Note that this assumes all measurements are normally distributed across these frequencies. If the t-test test did not reject H_0, the operation result is assumed undefined.

Note that the false positive in this setting is on the phase in operation 8. By lowering the critical value $\boldsymbol{\alpha = 0.01}$ the false positive disappears, but there is less true positives in total.

$\boldsymbol{\alpha = 0.05}$	**Impedance**	**Phase**
True positive	4 (44%)	6 (66%)
False positive	0 (0%)	1 (11%)
Undefined	5 (55%)	2 (22%)

Table 11 – Summary of arithmetic mean vs. unpaired t-test.

4.3.6 Spleen and splenic artery reference measurements

The impedance and phase measurement data from the spleen and splenic artery can be found in Appendix G. All of the data displayed in the graphs shows a clear discrimination between the spleen and the splenic artery for all operations.

5 Discussion

This section discusses the results derived from section 4. The experiments are discussed individually in the same order as they are presented in section 3 and 4.

5.1 Preliminary tests

The preliminary tests are fairly straight forward experiments of bioimpedance measurement. The general thought process was to remove as many variables as possible while not compromising accuracy or precision of the measurement results. It was done early on in the thesis, and it was necessary in order to avoid gathering too much data during the pig experiments. There might not has been a huge difference between one of the silicon coated blade electrode and the plain stainless steel one, but the choice fell on the latter simply because it provided the most pure results.

5.2 Blade electrode sensitivity field

Similar to the preliminary tests, this test was a standard bioimpedance measurement test with only a few human variables to take into account in the measurement results. The basic point was to try and estimate the electrode sensitivity field as accurately as possible. This can be extremely helpful to know, but the experiments are often hard to setup and run properly.

5.2.1 Data reliability and sources of error

There are some important sources of errors to grasp in order to understand the accuracy of this test. First of all you have the human aspect. Preferably you would like no human interaction whenever possible, but there was simply no time to construct more advanced automatic tests to estimate the sensitivity field. The human aspect revolves around how accurate the placement of the blade electrode was relative to the cucumber. This estimation was done manually by visually looking down on a ruler through the refraction of deionized water.

An important part of the results of this test was a noticeable drift in the impedance during larger distances. This might be due to impurities landing in the deionized water in-between or during the measurements, making it gradually more conductive. Even though this should not affect the dispersion itself, it might still color the sensitivity field for the blade electrode. Because of these uncertainties the result of this test should only be regarded as an approximation.

5.3 Pig experiments

5.3.1 Sources of error

There are many sources of error that can obscure or disfigure the measurement results. This is an attempt at breaking down every source of error that might have had an impact on the results in any way.

5.3.1.1 The human factor

First and foremost, a large source of error in all measurements is the human factor. The electrosurgery blade electrode had to be pinpointed on a specific anatomic location of a particular organ or tissue. Due to the large frequency range of the trial, a single measurement can take upwards to one minute to complete. The person measuring on the tissue must keep the blade electrode in the same anatomic location during the whole duration of the measurement. The pig might move around for various reasons during this time. One of the most common and significant physical movement is due to its normal respiratory rate. This especially affects measurement locations close to the diaphragm and lungs, like the liver and the extrahepatic bile ducts and arteries. If the pig is stressed the heart and respiratory rate might increase even further, making this an even greater challenge. The one thing that can be done decrease this factor as much as possible is to make sure the pig is properly sedated under the anesthetics at all times. The temperature in the operating theater must be kept at a constant high to keep the internal temperature of the pig warm enough to prevent shivering.

The second problem when it comes to the human factor is accessibility. This problem can be seen as a mix between the human factor and the anatomy of the pig. The small intestine is usually located so that it covers up the area around the hepatobiliary triangle (Calot's Triangle). As such, the location of the common bile duct and proper hepatic artery might be very difficult to reach. Another person might not always be nearby to assist in keeping the small intestine away from the measurement area, and even with another person to help this might still be a challenge. In order to improve upon this an electronic foot pedal was created and connected to the PC and impedance analyzer software through USB. This made it so that a measurement could be started using the foot instead of the hand, essentially freeing up one hand to aid in reaching the location of the measurements.

A third related human factor is inexperience within medicine/anatomy and lack of visibility or visual confusion. The common bile duct and proper hepatic artery might be difficult to locate visually, even after the surgeon has confirmed the location. Since the surgeon cannot always be present for confirmation of the various locations, the choice of measurement locations might not always be optimal. As previously mentioned it is also in a hard to reach spot, which might act as an additional visual obstruction.

5.3.1.2 Variations in anatomy between pigs

The anatomy of each individual pig might vary a lot depending on its age, size, weight and gender. The size of the proper hepatic artery and common bile duct usually reflects these factors. Based on the sensitivity field of the blade electrode and general electrode theory, any changes in in the size of the target tissue will have an impact on the measurement results. For example, if the electrode is larger than the organ or part of tissue that is to be measured, a significant part of the measurement result could be from adjacent tissue instead. A very large artery will cover up the blade electrode edge completely, whereas a small artery might not contribute as much to the total measurement result. To get some sort of grasp on the extent of this problem the splenic artery were added to the list of measurement locations starting from operation 4.

5.3.1.3 Extracellular fluid

A very big factor during the surgeries was the constant presence of extracellular fluids. These fluids contain a lot of electrolytes, and as such acts as a good electrolytic conductor.[17] When measuring, you usually have to put some amount of tactile pressure on the electrode in order for it to better stay in place and also have proper contact with the target tissue. This naturally creates a tiny dent in the tissue, which often quickly fills up with extracellular fluids. This may have a significant impact on the electrode sensitivity field. In addition, since the dent is at the very place where you are measuring, you also measure the extracellular fluid. The general anatomy of the pig is also often such that extracellular fluids pools up around the measurement location, sometimes drowning the blade electrode completely.

In order to minimize the effect of the extracellular fluids, regular white towels/sheets and occasionally suction machines were used to dry off the measurement location before measuring. If there was a particular large amount of fluids, an assistant would dry the location off during measurements whenever possible.

5.3.1.4 Electrical noise

Electrical noise is one factor that should never be ruled out during any kind of experiment of involving electronics. The electrode used for measurement is an electric conductor of stainless steel. The wires connected directly to the Solartron 1260/1294 are very well shielded. However, the wires which in turn are connected to these wires are not. Both the electrode and the wires are very susceptible for local electromagnetic interference (EMI). The operating theater and nearby labs contains a lot of various electronics and tools used for a lot of different purposes, all of which could have a potential of interfering with the measurement data.

5.3.1.5 Change in resistance of the dispersive electrode pad over time

The resistance of a dispersive electrode pad relative to the body of the pig might change or drift over the course of the operation. The electrode pad is fastened to the pig at the beginning of the operation, but it didn't always stick perfectly to the pig. For various reasons the area below the dispersive electrode might be wet or dirty, which in theory should increase the total resistance in the system. Unlike humans however pigs do not have sweat glands, but blood or other substances might still be a problem.[18] The best thing to try and prevent any problems with this is to make sure the electrode is properly fastened at the beginning of the operation, and if a lot of trouble is had potentially choose a different location on the pig to place the electrode. There is less risk for measurement errors as long as the electrode stays in the same location for the whole experiment.

5.3.1.6 Pulsation of blood through arteries

The heart rate creates a natural change in the mechanical flow of blood through the arteries. Since the proper hepatic artery is a relatively large artery close to the heart, the mechanical change in blood flow cannot be ruled out as a possible source of error.

5.3.1.7 Accuracy of sensitivity field

Even though the sensitivity field for the blade electrode used has been estimated using a simple experiment in section 3.3 and 4.2, the actual sensitivity field for the electrode might

[17] section 2.1.3 of this thesis and (Tortora & Derrickson, 2011)
[18] ("Pigs," 2002)

not be entirely accurate. If the sensitivity field is larger than expected it might end up measuring a lot of unwanted tissue.

5.3.2 Time restrictions

The measurements were preferably performed in order according to the protocol whenever there was time to measure. However, the CBD and PHA measurements were difficult to execute as described in section 0, and could sometimes only be done when there was assistant present. Because of the experiments running in parallel requiring the use of the impedance analyzer every 15 minutes, there were very specific time restrictions set in place for all of the measurements in this thesis. In addition to this, due to the general difficulty of the measurements, a lot of time was often lost trying to either locate or confirm an anatomic location, or trying to make it through a measurement without it failing (e.g. the electrode slipping off the target). In other words, because of the constant pressure of time restrictions, a lot of additional time would often go lost. Any bad or unreliable measurements that were recorded as a result of this had to be thrown away, which in turn meant fewer overall data points for the end result and analysis.

A large problem with all of this was the fact that the protocol times were not adhered to. If the time was about to run out and there was confusion about any anatomic location, the well known locations like the liver, gallbladder or other reference points would get measured instead.

5.3.3 Choice of locations

A possible practical use of the experiments in this thesis was to aid a surgeon performing a cholecystectomy (primarily laparoscopic) in correctly identifying the “Critical view of safety” (section 2.6.1). To best achieve this one would preferably want to identify the cystic duct vs. the cystic artery. However, the cystic duct is incredibly small and fragile (section 2.3.2.1). It would be a huge challenge to both identify it correctly, dissect nearby tissue and to measure its exact position during a surgery. For this reason the choice of measurement location instead fell on that which most closely resemble the cystic duct but to not have disadvantages with the size and positioning, namely the common bile duct. Likewise the cystic artery was also dangerously small and fragile, and was therefore voted down vs. an adjoining and larger artery, the proper hepatic artery. The choice of measurement location for the artery also made up a similar parallel structure relationship corresponding to the relationship between cystic duct and artery. The choice of locations was meant so that both the electrode and electrode setup could be tested properly.

5.3.3.1 Reference locations

The choice of reference locations was largely based upon easy accessibility, i.e. what would have the most robust measurement data, and also what would make the most sense for the measurements in general.

The location at the liver was a natural choice for a general reference point. This location was very easy to access on every surgery without any kind of extra assistance. It is also fairly homogeneous in the blade electrode sensitivity field, and has a distinct different characteristic than the main locations (CBD and PHA).

The body of the gallbladder was also a natural choice for reference. It was rarely difficult to access without any extra assistance, and it was a large and well recognizable

structure, even for the inexperienced. The gallbladder is also usually full of bile, which to some extent match up with the characteristic impedance of the CBD measurements.

The lymph node was chosen as a reference point since it is a structure that is usually in close proximity with the CBD and PHA. The point of this location was to see if there was any distinct difference between the very nearby tissue, especially in case the CBD and PHA measurement data were unreliable.

The remaining two reference points are the splenic artery and the spleen. These were added during the 4th operation as the CBD vs. PHA measurement results thus far were of varying quality. They were meant as a more solid reference to the characteristics of an artery vs. some solid nearby tissue. The splenic artery is physically large relative to the blade electrode. It was usually easier to gain access to than Calot's triangle, and there was little to no problems with extracellular fluid distorting the data. All of these qualities made it a more secure, reliable and useful reference point.

5.3.4 Discussion of data

Statistics alone is not always enough to land a conclusion on a set of data. The circumstances surrounding each experiment matters a lot in terms of both precision and accuracy of the measurement data. Please refer to Appendix D for the main data commented on in this section.

5.3.4.1 Impact of electrical noise

During operation 1 and 3 a significant amount of noise can be seen between around 500 kHz and 1 MHz. It can therefore be a bit surprising that the best result from the trials was overall placed in this frequency range for the phase data. The noise however seem to affect all measurements in the same manner. The noise can therefore be regarded as a common external source of EMI. These kinds of sources will still make the ratio between the phase measurements the same, and as such should not necessarily have a very negative impact on the end hypothesis.

5.3.4.2 Impact of anatomy and size

As mentioned in section 5.3.1.2, the size of the PHA and CBD matters a lot for the measurement results. In general, the smaller the pig is, the smaller the size of the PHA and CBD. Operation 4 is a good example of this problem. This was by far the smallest pig out of all the operations (24.5 kg), and the resulting impedance graphs for the CBD and PHA is very hard to distinguish between visually. Neither the unpaired t-test nor the Mann-Whitney U test finds any significant difference between the two data sets regardless of frequency. The opposite of this is operations 7, where there is a clear difference between the PHA and CBD both visually and statistically. This was the largest pig out of all the surgeries with a weight of 30 kg. An observation that was made here is that the difference in reliability of the data based on size is likely because of the human factor. It was very hard to both locate and measure the PHA due to the small size of it. However the largest pig was very easy to both locate anatomically and measure.

5.3.4.3 False positives and operation 9

Out of all the experiments, operation 9 was the only one to return a statistically significant false positive on the measurement results based on the arithmetic means hypothesis. This was based on significance from the Mann-Whitney U test.

Operation 9 was the very last experiment of all, and there were some special circumstances around this operation. First of all, operation 9 was done simultaneously as operation 8, i.e. there were two pigs in the operation theater at the same time. Due to time restrictions towards the end of the operation, the experiment had to be cut short. There was only time to record 3 CBD and 3 PHA measurements. From this reason alone the data from this test is less reliable than the other operations. Two of the measurement showed significant higher impedance overall for the PHA vs. the CBD. The third measurement was vastly lower, though still overall larger than the impedance of the CBD. In addition there were taken no reference measurements on the lymph node, splenic artery or spleen.

Because of all the uncertainties around this operation it is my recommendation that the result should not be taken a statistically significant false positive.

5.3.4.4 Number of data points and normality

A big part of the reliability of all the data gathered during the pig surgeries are the few total amount of data points for each location. With fewer data points on each frequency there is naturally less reliability. There is too few data points to conclude whether or not each frequency is normally distributed, so the unpaired t-test can in general not be trusted. However the Mann-Whitney U test do not depend on normally distributed data as long as the data has the same distribution. This is safer to assume, and as such the Mann-Whitney U test should be more trustworthy than the t-test.

Generally speaking only the Mann-Whitney U and the arithmetic means test should be used as a fair conclusion for the hypothesis of this thesis. There are not enough data points to assume normality and the normal distribution testing across all frequencies do not show any reliable signs of a proper bell curve (see section 4.3.2 and Appendix E).

5.3.5 Future improvements

From the beginning of the pig experiments the plan was to stick to the measurement protocol. However, due to the time restriction problems described in section 5.3.2 the protocol times were often not fully adhered to. In order to remove as many variables as possible from the experiment there should be a very strict time schedule that is to be fully adhered to at all times. For example one could use a strict order with "$artery \rightarrow bile\ duct \rightarrow reference(s)$".

Secondly, scanning the whole frequency spectrum takes a lot of time. Due to the human factor discussed extensively in section 0, one should try to minimize the time required for measuring on any one location. A single or multiple frequencies simultaneously is highly recommended, as this might give a much clearer picture of the impedance or phase at any one moment.

6 Conclusion

Using a regular electrosurgery monopolar electrode setup, there is a statistical significant difference in the phase data of the CBD and PHA in 6 out of 9 (66%) of the pigs experimented on as a part of this thesis. 3 out of 9 (33%) of the results were thus not statistically significant. Using the arithmetic mean test, 5 out of 9 (55%) of the pigs supported our hypothesis that the phase of the PHA are higher than the phase of the CBD at 630 kHz. 1 out of 9 (11%) was a false positive.

6.1.1 Continuation

This thesis is meant as a building block for developing more bioimpedance measurement tools within the field of electrosurgery. The very end goal would be an electrosurgery unit that can read and analyze the characteristic impedance for the current tissue being cut, as its cutting or coagulating the tissue. Further testing of mainly laparoscopic electrodes, for example bipolar setups, would be a very important next step within this field. Further analysis of specific frequencies that looks promising would also be a good continuation of this subject.

7 Literature

Bowen, R. (2001). Secretion of Bile and the Role of Bile Acids In Digestion. Retrieved 2013-11-10, from http://www.vivo.colostate.edu/hbooks/pathphys/digestion/liver/bile.html

Britannica, T. E. o. E. (2013a). dielectric *Encyclopædia Britannica*.

Britannica, T. E. o. E. (2013b). Joule's law *Encyclopædia Britannica*.

Britannica, T. E. o. E. (2013c). resistance (electronic) *Encyclopædia Britannica*.

Bronzino, J. D. (2000). The biomedical engineering handbook (2nd ed. ed.). Boca Raton: CRC Press.

Csikesz, N., Ricciardi, R., Tseng, J. F., & Shah, S. A. (2008). Current status of surgical management of acute cholecystitis in the United States. *World J Surg, 32*(10), 2230-2236. doi: 10.1007/s00268-008-9679-5

Danny A Sherwinter, M., Stalin Ramakrishnan Subramanian, M., Lee S Cummings, M., Michele F Malit, D., Sunny Leah Fink, M., Jerzy M Macura, M., & Harry L Adler, M. (2013). Laparoscopic Cholecystectomy. Retrieved 2013-05-03, from http://emedicine.medscape.com/article/1582292-overview#a15

DataSurg.net. (2013). ANATOMY OF THE EXTRA-HEPATIC BILIARY TREE. Retrieved 2013-12-12, from http://www.datasurg.net/2013/05/04/images-in-operative-ultrasound/14_n1_small/

Duch, B. U., Andersen, H., & Gregersen, H. (2004). Mechanical properties of the porcine bile duct wall. *Biomed Eng Online, 3*(1), 23. doi: 10.1186/1475-925X-3-23

Esteller, A. (2008). Physiology of bile secretion. *World J Gastroenterol*.

Full Report (All Nutrients): 11205, Cucumber, with peel, raw. (2014). from Agricultural Research Service, United States Department of Agriculture http://ndb.nal.usda.gov/ndb/foods/show/3006?qlookup=11205&format=Full&max=25&man=&lfacet=&new=1

Giger, U. F., Michel, J. M., Opitz, I., Th Inderbitzin, D., Kocher, T., Krahenbuhl, L., . . . Thoracoscopic Surgery Study, G. (2006). Risk factors for perioperative complications in patients undergoing laparoscopic cholecystectomy: analysis of 22,953 consecutive cases from the Swiss Association of Laparoscopic and Thoracoscopic Surgery database. *J Am Coll Surg, 203*(5), 723-728. doi: 10.1016/j.jamcollsurg.2006.07.018

Grimnes, S., & Martinsen, T. (2010). *Kirurgisk Diatermi*. Oslo: Rikshospitalet, Oslo Universitetssykehys.

Grimnes, S., & Martinsen, Ø. G. (2008). *Bioimpedance and bioelectricity basics* (2nd ed. ed.). London: Academic.
Hobbs, M. S., Mai, Q., Knuiman, M. W., Fletcher, D. R., & Ridout, S. C. (2006). Surgeon experience and trends in intraoperative complications in laparoscopic cholecystectomy. *Br J Surg, 93*(7), 844-853. doi: 10.1002/bjs.5333
Jon Ivar Einarsson, M., PhD, MPH, & Jon Gould, M. (2013). Overview of electrosurgery. Retrieved 2013-04-05, from http://www.uptodate.com/contents/overview-of-electrosurgery
Kalvøy, H. (2010). *Needle Guidance in Clinical Applications based on Electrical Impedance.* University of Oslo.
Kovacs, J. S. (2001). Coulomb's Law. http://www.physnet.org/modules/pdf_modules/m114.pdf
Liver, Biliary, and Pancreatic Disorders. (2014). Retrieved 2014-02-10, from http://medicalcenter.osu.edu/patientcare/healthcare_services/liver_biliary_pancreatic_disease/Pages/index.aspx
Lygia Stewart, M., Lawrence W. Way, M., & Cynthia O. Dominguez, P. (2007). *BILE DUCT INJURIES DURING LAPAROSCOPICCHOLECYSTECTOMY: A SENSEMAKING ANALYSIS OFOPERATIVE REPORTS.* Paper presented at the The Eighth International NDM Conference, Pacific Grove, CA.
Nezam H Afdhal, M., FRCPI, & Charles M Vollmer, J., MD. (2014). Complications of laparoscopic cholecystectomy. Retrieved 2014-02-02, from http://www.uptodate.com/contents/complications-of-laparoscopic-cholecystectomy
Ooi, R. C., Luo, X. Y., Chin, S. B., Johnson, A. G., & Bird, N. C. (2004). The flow of bile in the human cystic duct. *J Biomech, 37*(12), 1913-1922. doi: 10.1016/j.jbiomech.2004.02.029
Palanivelu, C. (2008). Laparoscopic Bile Duct Injury and Management *Laparoscopic surgery atlas* (Vol. 2, pp. 666-667). New Delhi: Jaypee Brothers Medical Publishers.
Pigs. (2002). Retrieved 2014-02-05, from http://ori.hhs.gov/education/products/ncstate/pig.htm
Samira Y Khera, M., MS, David A Kostyal, P., & Narayan Deshmukh, M. (1999). A comparison of chlorhexidine and povidone-iodine skin preparation for surgical operations. *Curr Surg, 56*(6), 3.
Steiner, C. A., Bass, E. B., Talamini, M. A., Pitt, H. A., & Steinberg, E. P. (1994). Surgical rates and operative mortality for open and laparoscopic cholecystectomy in Maryland. *N Engl J Med, 330*(6), 403-408. doi: 10.1056/NEJM199402103300607
Steven M Strasberg, M., FACS, & L Michael Brunt, M., FACS. (2010). Rationale and Use of the Critical View of Safety in Laparoscopic Cholecystectomy. *J Am Coll Surg, 211*(1), 7.
Stocksley, M. (2001). *Abdominal ultrasound*. London: GMM.
Strasberg, S. M. (2005). Biliary injury in laparoscopic surgery: part 2. Changing the culture of cholecystectomy. *J Am Coll Surg, 201*(4), 604-611. doi: 10.1016/j.jamcollsurg.2005.04.032
Thurley, P. D., & Dhingsa, R. (2008). Laparoscopic cholecystectomy: postoperative imaging. *AJR Am J Roentgenol, 191*(3), 794-801. doi: 10.2214/AJR.07.3485
Tortora, G. J., & Derrickson, B. (2011). *Principles of anatomy & physiology* (International student , 13th ed. ed.). Hobolen, N.J.: Wiley.
William Sircus, M. D. (2013). human digestive system *Encyclopædia Britannica*. Online.
Wu, M. P., Ou, C. S., Chen, S. L., Yen, E. Y., & Rowbotham, R. (2000). Complications and recommended practices for electrosurgery in laparoscopy. *Am J Surg, 179*(1), 67-73.
Zumdahl, S. S., & DeCoste, D. J. (2011). *Introduction to basic chemistry* (7th ed.). Belmont, Calif.: Brooks/Cole, Cengage Learning.

Appendix A – Application for animal models

Søker og medarbeidere

Institusjon	027 UiO - Rikshospitalet, Senter for komparativ medisin
Adresse	Sognsvannsveien 20
	0027 OSLO
Telefon	23073150
E-post	- - -
Ansvarshavende	Gro Furset Flatekval
Ansvarlig søker	Håvard Kalvøy - Forsker (Ansvarlig søker/Prosjektansvarlig) (Kurs i forsøksdyrlære)
Medarbeider 1	Danckert Krohn - Forsker (Ansvarlig søker/Prosjektansvarlig) (Kurs i forsøksdyrlære)
Medarbeider 2	Yngvar Gundersen - Forsker (Ansvarlig søker/Prosjektansvarlig) (Kurs i forsøksdyrlære)
Medarbeider 3	Ansgar Aasen - Professor (Kurs i forsøksdyrlære)
Søknadsdato	25.02.2013

Generelle opplysninger

Id	5143
Søkerens ref.nr.	- - -
Forsøkets arbeidstittel	Bioimpedans som veiledning under kirurgiske inngrep
Dyreart	Pattedyr - svinedyr (Susidae) - Gris (Sus scrofa domesticus)
Institusjon	027 UiO - Rikshospitalet, Senter for komparativ medisin
Type søknad	Nytt forsøk
Akutt forsøk	Ja
Tidligere erfaring med tilsvarende forsøk	Ja
Forskningen er finansiert av	Annen finansieringskilde
Planlagt start	21.02.2013
Planlagt slutt	01.07.2013

Beskrivelse
Vi ønsker å kartlegge elektrisk impedans i vev (Bioimpedans) for utvikling av nye veiledningsmetoder for bruk under kirurgiske inngrep.

Offentlighet

Inneholder søknaden opplysninger som ønskes unntatt fra offentlighet?	Nei
Hvis ja, angi relevante lover og paragrafer (f. eks. Offentlighetsloven, § 13, 1. avsnitt og Forvaltningsloven, § 13, 1. avsnitt, 2. punkt).	Arbeidstakeroppfinnelesloven § 6

Hvis ja, beskriv hvilke opplysninger som ønskes unntatt fra offentlighet.
Det er ønskelig å patentere deler av metoden. En offentlig publisering av metodebeskrivelsen vi kunne forringe mulighetene for en slik prosess. Vi har derfor formulert teksten slik at grunnideen bak oppfinnelsen ikke vil avsløres om en offentliggjøring av informasjon kun inneholder det som beskrives i den følgende søknadsteksten.

Beregning av antall dyr

Gi en begrunnelse for antall forsøksdyr. Ved usikkerhet om populasjonsstørrelse skal det gjennomføres pilotforsøk, jf. forskriftens § 13. Søk hjelp hos statistiker dersom du er i tvil.
I dette prosjektet måles det impedansens avhengighet til målestrømmens frekvens. Målingene analyseres ved mønstergjenkjennelse i et større frekvensområde. I tidligere studier og pilotstudier har det vist seg at vi må ha 10-12 målinger for å kunne utføre en analyse som er robust nok til å trekke en gyldig konklusjon. For en typisk måleserie viser tidligere studier at vi må regne et standardavvik på omtrent samme størrelse som forskjellen i snittet for to vevstyper i et målepunkt.

Gi en oversikt over samtlige forsøksgrupper og gruppestørrelser. Legg gjerne ved en tabell som vedlegg til søknaden.
Vi ønsker her å benytte 10 dyr for å kunne konkludere i studien. Vi ønsker å kartlegge vevsdata i flere typer vev i en gruppe griser med normale variasjoner innen for rasen. Som forklart lengre ned er antallet redusert til et absolutt minimum ved at hvert dyr vil fungere som sin egen kontroll.

Hvilken metode er brukt for beregning av antall dyr. Power analyse

Hvis "Power analyse"/"Ressursligning": Hvilke input er lagt inn?
Hvis "Annen metode": Gi en detaljert beskrivelse av den metoden som er benyttet.
Hvis "Ikke aktuelt": Beskriv hvorfor statistiske metoder ikke kan benyttes.
Konklusjon er basert på tidligere studier som beskrevet over. Støttet av en Power analyse.
Input i Power-analysen var: Type 1 feil: 0,2 Power =0,95 Stdav=50 og forskjell i snitt 50

Bakgrunn og hensikt

Gi en kort presentasjon av bakgrunn og hensikt med forsøket (maksimalt 500 ord), i en allment tilgjengelig språkform. Angi eventuell hypotese som skal testes. Angi særskilt hvis spesielle lovbestemmelser/krav fra offentlige myndigheter krever at forsøket skal utføres.
Hypotese: Elektrisk impedansmåling i biologisk vev (Bioimpedans) kan benyttes til å identifisere vevstype og tilstand i vevet.
Ved forskjellige kirurgiske inngrep er man avhengig av presis bestemmelse av vevstype og tilstanden til vevet det jobbes med. Hvis man ved hjelp av en enkel metode kan bistå kirurgen med å bestemme vevstype og forskjellige tilstander i vevet under operasjon, vil dette være et nyttig hjelpemiddel under mange operasjoner. Feiltolkning av vevstype og tilstand i forskjellige vev, er vanlige årsaker til komplikasjoner under og etter operasjon. Det kan da være snakk om alt fra mindre komplikasjoner til meget alvorlige komplikasjoner. Tidligere studier har vist at bioimpedans har potensiale til å skille mellom forskjellige typer vev og tilstander. En typisk applikasjon kan uføres i et relativt lite og rimelig utstyr, eller legges inn i samspill med allerede eksisterende utstyr. Målet med denne forsøksserien å benytte både kommersielt tilgjengelige elektroder og spesialkonstruerte elektroder, for å samle inn vevsdata (type og tilstand). Vår forskningsgruppe har jobbet med utvikling av slike metoder flere år. For å komme videre i utviklingen av tre konkrete applikasjoner for veiledning under kirurgi, vil vi nå fokusere kartleggingen på bestemte vevstyper og tilstander i disse.

Alternativer/3R

Erstatning ("replacement"): Hvorfor kan man ikke oppnå forsøkets hensikt uten å benytte levende dyr? Hvilke alternativer er vurdert og hvorfor er de forkastet?
Vevets elektriske egenskaper forandres meget raskt når livsfunksjonene opphører. Kartlegging av vitalt vev i forskjellige tilstander kan kun gjennomføres på levende vev. De vevstypene som kartlegges i dyrene er veldig like de vi finner i menneske. Gris ansees derfor som en meget god modell. Det finnes ingen gode alternative modeller eller simuleringer for levende vev ønskede tilstand. Gnagere er for små til at vi kan oppnå sammenlignbare målinger. Det finnes ingen referanser på alternativer til bruk av levende modeller med for måling av bioimpedans i vev i forskjellige tilstander.

Hvilke databaser ble det søkt i og hvilke søkeord ble benyttet for å finne alternativer?
Vi har forsket på impedansemåling i forskjellige typer vev i flere år og har ikke klart å fremskaffe noen tidligere publikasjoner som tar for seg sammenhengen mellom bioimpedans og vev i de ønskede tilstander.

Reduksjon ("reduction"): Når bruk av dyr er uunngåelig: Hvilke tiltak, steg og forholdsregler har du brukt for å minimalisere antall dyr og fremdeles oppnå valide vitenskapelige resultater?
En rekke simuleringer, målinger og test av utstyret er utført for å komme frem til et robust måleoppsett og en god modell for de tilstander vi ønsker i vevet. For å redusere bruk av antallet dyr har vi under forsøk 4481 benyttet ledig tid til pilotmålinger. Hele det tekniske oppsettet er også testet og tilpasset i flere serier med laboratorietester (in-vitro). Det er mulig å måle forskjellige tilstander og vevstyper i samme dyr. Hvert individ kan derfor benyttes som sin egen kontroll. Dette gjør at vi kan redusere antallet dyr kraftig ved å unngå en kontrollgruppe. På denne måten har vi optimalisert utstyret, modellen og prosedyrene for å kvalitetssikre resultatene og maksimere utbyttet fra hvert enkelt dyr.

Raffinering ("refinement"): Når bruk av dyr er uunngåelig: Hvilke forbedringer av stell og prosedyrer er gjort for å minimalisere smerte, lidelse, ubehag og varig skade og for å øke dyrevelferden i forhold til tidlige lignende forsøk? (Stikkord: anestesi, analgesi, endepunkter, miljøberikelse, operasjonsteknikk, prøvetakningsteknikk osv).
Forsøkene gjøres i full narkose som startes i dyrestallen. Overvåkning og vedlikehold av fullstendig narkosen vedvarer frem til dyrene er avlivet i avslutningen av forsøkene.

Metodebeskrivelse

Forberedelsen av dyrene før inngrep:
For feltforsøk: Beskriv evt. sporing, innfanging, fikseringsmetode, transport osv.
For labforsøk: Beskriv evt. innkjøp, transport, karantene/akklimering, oppstalling, miljøberikelse, fôringsregime, merking, veiing osv.
Vanlig håndtering av dyrene i dyrestallen på Rikshospitalet. Dyrene tas inn fra godkjent oppdretter dagen før eller noen dager før forsøket for akklimatisering.

Hvilke inngrep (kirurgi, administrasjon av teststoff, merking av viltlevende dyr, fysiske behandlinger m.m.) skal gjøres på dyret under selve forsøket? Legg evt. ved tegninger, protokoller, tidslinjer (aktivitetskart) eller lignende som vedlegg til søknaden.
Forsøkene krever at buken på grisene åpnes på vanlig måte for gastro-kirurgi. Det vil da være tilgang til de noen av de ønskede organene uten videre kirurgi. De resterende målingene vil foregå i området rundt leveren. Det vil da måtte dissekeres noe i tillegg for å få tilgang til disse organene. Impedansmålingene gjennomføres med standard impedansmåleutrustning (Solartron 1260/1294) og elektroder som plasseres i direkte kontakt med overflaten på de forskjellige vevstypene. Målingene gjentas gjentatte ganger for å kartlegge impedansegenskapene til de forskjellige vevstypene. For noen av måleseriene vil det fokuseres på vevets utvikling over tid. Målingene vil derfor gjentas med faste tidsintervaller over de 6 timene forsøket varer.

Hvilke registreringer skal gjøres og hvilke prøver skal tas i løpet av forsøket?
I tillegg til vanlige monitorering for å ivareta grisen som puls, O2-metning, blodgass, arterietrykk og ventilasjonsparametre, vil det kun måles elektriske impedansverdier som funksjon av tid, vevstype og blodgjennomstrømning.

Angi oppfølging og overvåkning av dyrene under hele forsøket (før, under og etter aktuelle inngrep). Legg gjerne ved relevant scoringsskjema:
Overvåkningen følger av parametrene som måles. Dette er de vanlige sirkulasjonsparametrene som puls, Blodtrykk, EKG og Swan-Ganz parametre som PCWP, PAP og ventilasjonsparametre.
Det vil bli tatt regelmessig blodgass-målinger.

Angi avlivingsmetode og hvorfor denne metoden er valgt. Ved bruk av preparater oppgi generisk navn, preparatnavn og dosering:
Penthobarbital ca 100 mg/kg til alle parametere har flatet ut i narkosen.

Angi kriterier for humane endepunkter (dvs. kriterier for å avbryte forsøket for det enkelte dyr/grupper av dyr fordi belastningen for dyret er større enn det som er nødvendig for å oppnå formålet med forsøket).
Målet er å innhente data fra vev i dyr under full narkose som blir avlivet i narkose uten lidelser.
Kriteriene for død er at alle overvåknings-kurver flater ut og fravær av egenrespirasjon og egenbevegelser.
Dersom man under forsøket opplever avvik fra forventet forløp vil dyret om nødvendig bli avlivet før forsøket er avsluttet.

Hvilke tiltak vil bli aktuelt å iverksette hvis dyrene når humant endepunkt (f. eks. behandling av symptomer, redusere eksponering, avliving)?
Avlivning.

Forsøksdyr (art, medikamentbruk og smertevurdering)

Dyreart	Pattedyr - svinedyr (Susidae) - Gris (Sus scrofa domesticus)
Linje/Stamme	- - -
Kjønn	Begge
Antall	10
Vekt ved oppstart	20-30kg
Vekt ved avslutning	uforandret
Alder	ca 3mnd
Antall dyr ved gjenbruk (jf. § 15)	Gjenbruk er ikke relevant
Erfaring med denne dyreart	Ja
Beskriv fordeling av antall dyr i forhold til kjønn, vekt og alder	- - -
Varighet av hele forsøket for det enkelte dyr (d, t, min).	0, 6, 0

Dyr med en avvikende fenotype (se prinsipputtalelse).

Har dyrene arvelig sykdom/lidelse som kan påvirke deres veldferd (eksempler: diabetes, autoimmun sykdom, økt forekomst av tumor, lidelser i bevegelsesapparatet, tanndefekter m.m.)?

- - -

Slike lidelser er ikke kjent/beskrevet i litteraturen ☑

Hvilke tiltak/behandling skal iverksettes for å sikre velferden for dyr med arvelig/medfødt sykdom/lidelse nevnt over, og når regner du med at det blir nødvendig?

- - -

Slike tiltak vil ikke bli nødvendig ☑

Sedasjon, analgesi og anestesi

Periode	Type	Preparat	Induksjonsdose (mg/kg)	Vedlikeholdsdose (mg/kg)	Administrasjonsmåte
Før	Sedasjon	Stressnill			im
Under	Anestesi	Isoflurane			inhalasjon
Under	Anestesi	fentanyl	0,004	0,004	iv

Annen medikamentering (alle andre medikamenter/testsubstanser som anvendes)

Atropin

Neuromuskulære blokkere vil bli benyttet ☐

Begrunnelse for bruk av neuromuskulær blokker:

- - -

Smerte og ubehag

Forsøket innebærer smerte, men analgesi må utelates ☐

Begrunnelse for at analgesi unnlates

Dyret avlives før smerte inntrer

Forsøket anses å innebære betydelig/ vedvarende smerte eller ubehag. ☐

Begrunnelse for vurderinger

- - -

Styrke av smerte/ubehag	Ubetydelig
Varighet av smerte/ubehag	Sekunder

Begrunnelse for valg av dyremodell

Gi en begrunnelse for valg av dyremodell, jf. forskriftens § 8 - dyreart, linje, kjønn, alder, spesielle egenskaper, genmodifikasjoner

Gris har mange likehetstrekk med menneske når det gjelder vevsegenskaper og størrelse.

Appendix B – Response from "Forsøksdyrutvalget"

FORSØKSDYRUTVALGET

Deres ref: Vår ref: Dato: 27.02.2013

hkalvoy@ous-hf.no

VEDTAK OM BRUK AV FORSØKSDYR - FOTS ID 5143

Behandlet av lokalt ansvarshavende, 27.02.2013.
Dokumenter i saken:

Behandling:
Vedtak:
Søknaden er godkjent.

Begrunnelse:
Forsøket er av en art og natur slik at det kan godkjennes av ansvarshavende, jvf Forskrift om forsøk med dyr, nr 23, 15/1, 1996, § 11.

-Forsøket godkjennes i hht. søknaden jmf. forskriftens §§ 7 og 8. Forsøket vurderes å være av vitenskapelig og samfunnsmessig relevans og interesse og oppfyller dermed forsøksdyrforskriftens generelle vilkår for dyreforsøk, gitt i § 8, første ledd. Det foreligger ikke anvendelige alternativer til bruk av levende dyr i hht. kravet beskrevet i forskriftens § 8, tredje ledd.

-Det forutsettes at alle som deltar i forsøket er angitt i søknaden, jvf forskriftens § 12, tredje ledd og § 13 første ledd.

-Eventuelle avvik og endringer fra den godkjente søknad må meddeles skriftlig til ansvarshavende og evt. som søknad om endring av forsøket.

-Søker er ansvarlig for hvert år innen 1. mars å levere årsrapport til FDU over antallet dyr som er brukt i forutgående kalenderår, jvf. forskriftens § 24. Etter forsøkets avslutning leveres sluttrapport til FDU.

-Søker må opplyse om HMS-tiltak som kreves i forbindelse med bruk av spesielle legemidler/ kjemikalier etc. i gjeldende prosjekt.

Vedtak kan påklages til Mattilsynet, jfr. lov 10 feb 1967 om behandlingsmåten i forvaltningssaker (forvaltningsloven) § 28. Klagefristen er 3 uker fra mottak av dette brev, jfr. forvaltningsloven § 29. Klagen stiles til Mattilsynet, Hovedkontoret, men sendes via Forsøksdyrutvalget.

Med hilsen for Forsøksdyrutvalget

sign
Gro Furset Flatekval
Ansvarshavende 027 UiO - Rikshospitalet, Senter for komparativ medisin

Kopi: ansvarshavende/koordinator
postmottak@mattilsynet.no

Adresse: Forsøksdyrutvalget
c/o Mattilsynet, Felles postmottak
Postboks 383
N- 2381 Brumunddal

Telefaks: **23 21 68 01**
e-post: postmottak@mattilsynet.no
Hjemmeside: www.fdu.no

Sekretariat: Gunvor Knudsen **23216663**
Johanne Holmen **23216692**

Appendix C – Protocol for bioimpedance measurements on pigs – Spring 2013

This is a copy of the pig surgery protocol used as a reference for all 9 surgeries involved in this thesis. It also documents the other experiments going on simultaneously. The copy held by the Institute for Surgical Research at Oslo University Hospital is written in Norwegian; this is a translated version.

1 Experiment overview

1.1 Discrimination of ischemic small intenstine

The impedance measurements is performed by Runar Strand-Amundsen.

1.1.1 Measurement details

1.1.1.1 Measurement series A1-6

Solartron setup: 100mV, 1MHz-1k, logarithmic, interval = 10, mean through 10 periods.
All measurements are performed with a custom electrode setup.
Choice of 2 or 3 electrode setup during measurement series A. The chosen electrode setup is thereafter used in all following experiments.
Measurements are performed on various areas around the jejunum, carefully watch the impedance variations and improve the electrode setup accordingly.

1.1.1.2 Measurement series B1-20

Solartron setup: 100mV, 1MHz-1k, logarithmic, interval = 10, mean through 10 periods.
All measurements are performed with a custom electrode setup.
Measurements of the ischemic model and the healthy reference jejunum.

1.2 Discrimination of tissue

The impedance measurements C1 – E5 is performed by Lars Andreas Pedersen and F1-8 by Håvard Kalvøy.

1.2.1 Measurement details

1.2.1.1 Measurement series C1-4

Solartron setup: 100mV, 1MHz-1k, logarithmic, interval = 10, mean through 10 periods.
All measurements are performed using a stainless steel electrosurgery electrode and a neutral dispersive plate in a 2-electrode setup.
Measurements on the gallbladder and liver as reference.

1.2.1.2 Measurement series D1-4

Solartron setup: 100mV, 1MHz-1k, logarithmic, interval = 10, mean through 10 periods.
All measurements are performed using a stainless steel electrosurgery electrode and a neutral dispersive plate in a 2-electrode setup.
Measurements are performed on the bile ducts in order to document any electrical properties.

1.2.1.3 Measurement series E1-5

Solartron setup: 100mV, 1MHz-1k, logarithmic, interval = 10, mean through 10 periods.
All measurements are performed using a stainless steel electrosurgery electrode and a neutral dispersive plate in a 2-electrode setup.
Measurements on the artery and vein of the gallbladder in order to document any electrical properties.

1.2.1.4 Measurement series F1-8

Solartron setup: 30mV, 1MHz-1k, logarithmic, interval = 10, mean through 10 periods.
Measurements are performed using Braun Stimuplex A needles and standard ECG-electrodes in a 3-electrode setup. The needle is inserted in proximity of the popliteal sciatic nerve using ultrasound guidance. The position in the nerve can also be confirmed using a nerve stimulator (Braun HNS12).

t	m	#	Protokoll
	-30		The pig is sedated and placed on location in the operating theater 0700
	-25		
	-20		
	-15		
	-10		
	-5		
-1	0		The surgeon creates open access to the abdominal cavity 0800
	-55		
	-50		
	-45		Surgeon makes access to the proximity of the gallbladder.
	-40		Referance measurements of Solartron1260/1294.
	-35		
	-30	*A1*	"Baseline" -measurements on healthy jejunum. 0845
	-25	*A2*	”Baseline” - measurements on healthy jejunum.
	-20	*A3*	”Baseline” - measurements on healthy jejunum.
	-15	*A4*	”Baseline” - measurements on healthy jejunum.
	-10	*A5*	”Baseline” - measurements on healthy jejunum.
	-5	*A6*	”Baseline” - measurements on healthy jejunum.
0	0		Surgeon initiates ischemic model
	5		
	10		
	15	*B1*	1 measurement on ischemic model and reference.
	20		
	25	*C1*	1 Reference measurement of the gallbladder and liver.
	30	*B2*	1 measurement on ischemic model and reference.
	35		
	40	*C2*	1 Reference measurement of the gallbladder and liver.
	45	*B3*	1 measurement on ischemic model and reference.
	50		
	55	*C3*	1 Reference measurement of the gallbladder and liver.

1	0	*B4*	1 measurement on ischemic model and reference.
	5		
	10	*C4*	1 Reference measurement of the gallbladder and liver.
	15	*B5*	1 measurement on ischemic model and reference.
	20		
	25	*D1*	2 measurements on the bile duct.
	30	*B6*	1 measurement on ischemic model and reference.
	35		
	40	*D2*	2 measurements on the bile duct.
	45	*B7*	1 measurement on ischemic model and reference.
	50		
	55	*D3*	2 measurements on the bile duct.
2	0	*B8*	1 measurement on ischemic model and reference.
	5		
	10	*D4*	2 measurements on the bile duct.
	15	*B9*	1 measurement on ischemic model and reference.
	20		
	25	*E1*	1 measurement on the artery, vein and the gallbladder.
	30	*B10*	1 measurement on ischemic model and reference.
	35		
	40	*E2*	1 measurement on the artery, vein and the gallbladder.
	45	*B11*	1 measurement on ischemic model and reference.
	50		
	55	*E3*	1 measurement on the artery, vein and the gallbladder.
3	0	*B12*	1 measurement on ischemic model and reference.
	5		
	10	*F1*	Measurements on muscle tissue with 2 needle positions.
	15	*B13*	1 measurement on ischemic model and reference.
	20		
	25	*F2*	Measurements on muscle tissue with 2 needle positions.
	30	*B14*	1 measurement on ischemic model and reference.
	35		
	40	*F3*	Measurements on muscle tissue with 2 needle positions.
	45	*B15*	1 measurement on ischemic model and reference.
	50		
	55	*F4*	Measurements on connective tissue/other, 2 pos.
4	0	*B16*	1 measurement on ischemic model and reference.
	5		
	10	*F5*	Measurements on the epineurium, 2 positions.
	15	*B17*	1 measurement on ischemic model and reference.
	20		
	25	*F6*	Measurements on the epineurium, 2 positions.
	30	*B18*	1 measurement on ischemic model and reference.
	35		
	40	*F7*	Measurements on the perineurium, 2 positions.
	45	*B19*	1 measurement on ischemic model and reference.
	50		
	55	*F8*	Measurements on the perineurium, 2 positions.

5	0	*B20*	1 measurement on ischemic model and reference.
	5		The pig is euthanized.
	10		
	15		
	20		
	25		
	30		
	35		
	40		
	45		
	50		

Appendix D – Graphs for impedance vs. frequency and phase vs. frequency for pig experiments

This appendix contains impedance vs. frequency and phase vs. frequency plots for all 9 surgeries performed as a part of this thesis. The graphs shows the impedance and phase for the common bile duct (CBD) and proper hepatic artery (PHA), including the arithmetic mean for all n-measurement series of each type. The number of measurement series n is written above each graph for both the CBD and the PHA.

Operation 1

$CBD\ n = 9$
$PHA\ n = 7$

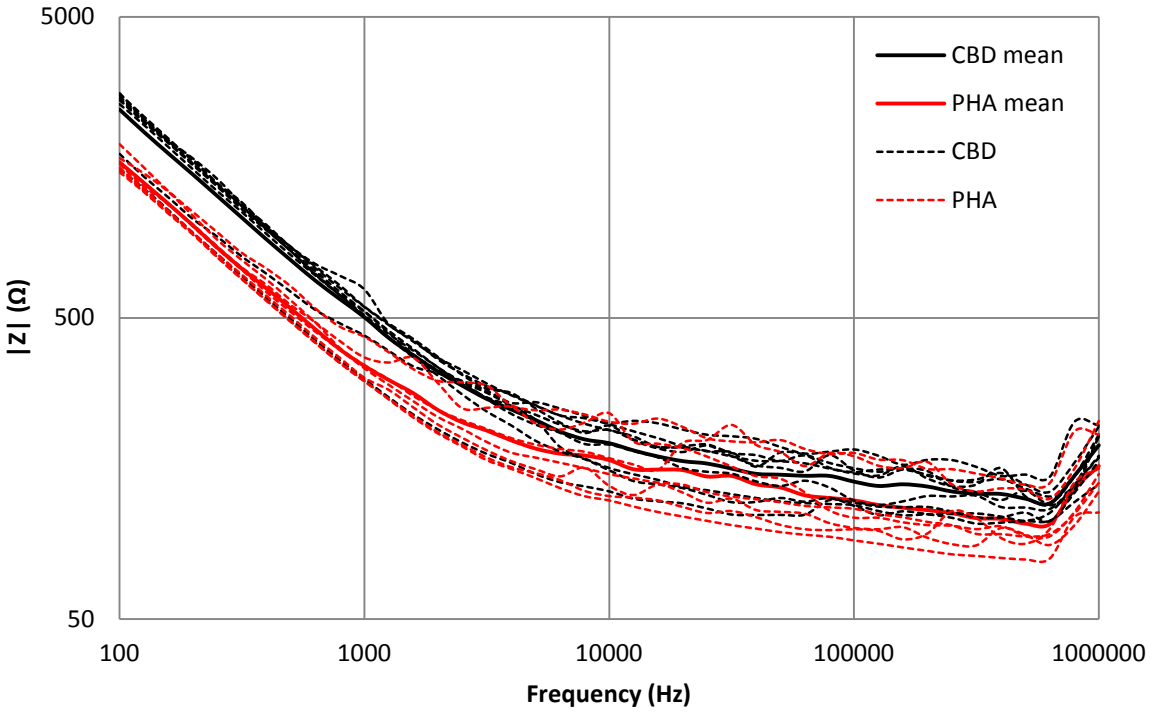

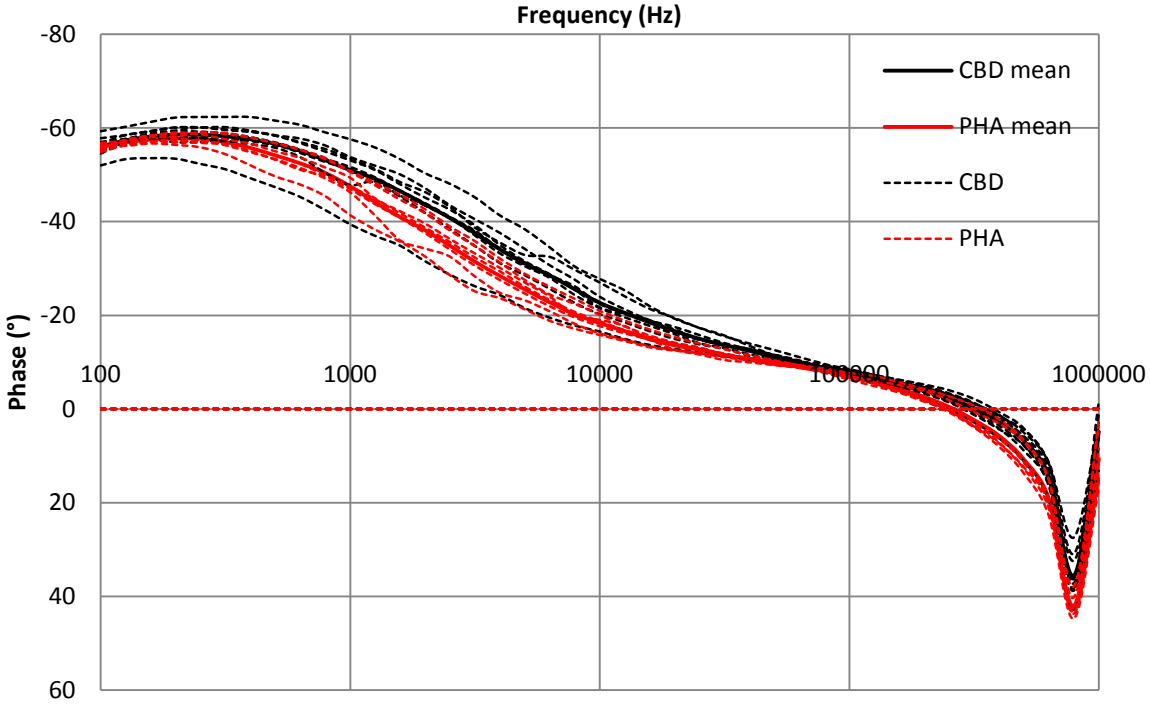

Operation 2

$CBD\ n = 6$
$PHA\ n = 6$

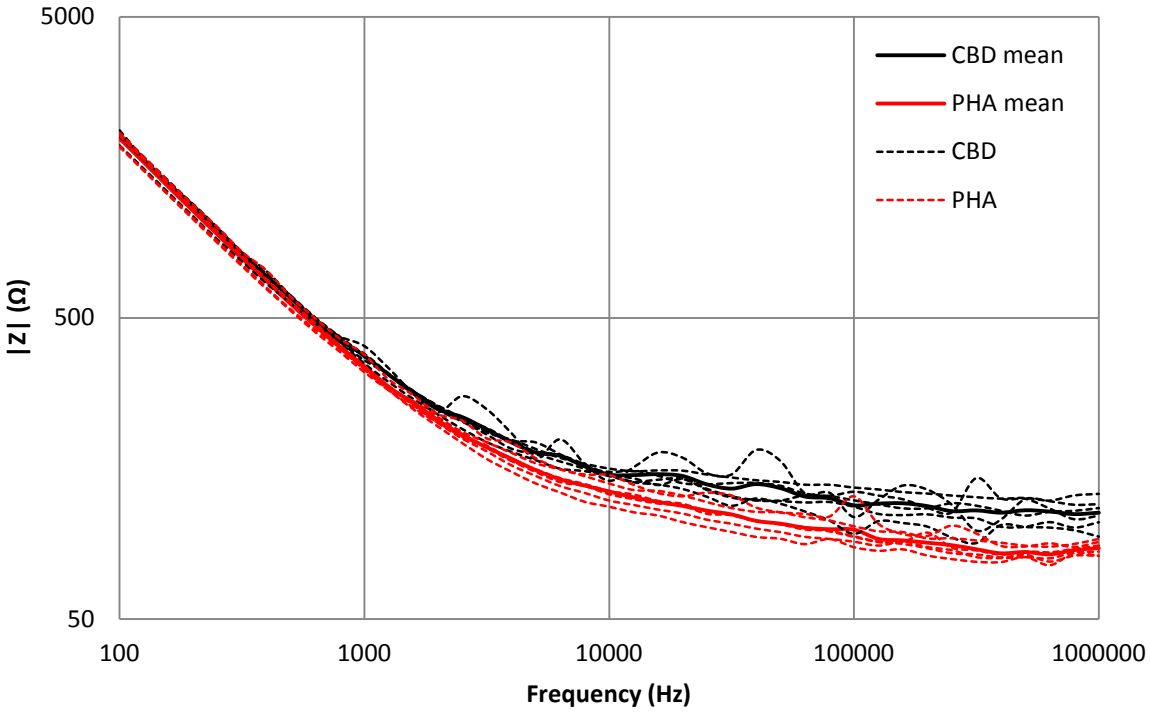

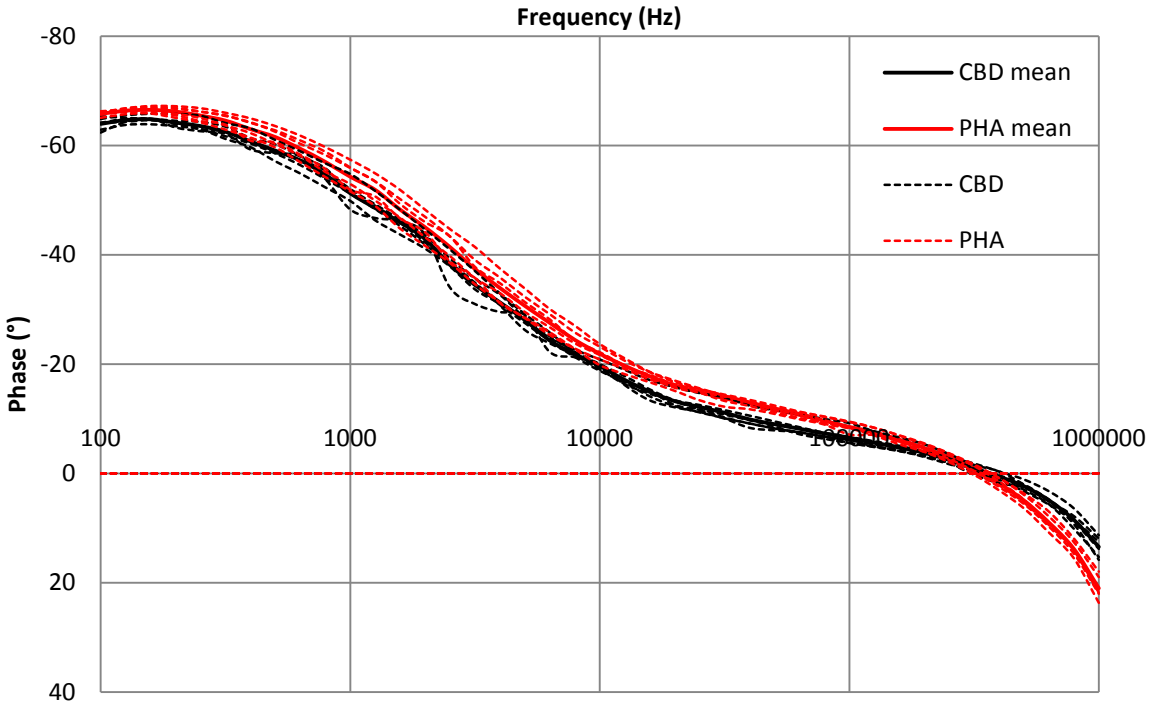

Operation 3

$CBD\ n = 6$
$PHA\ n = 11$

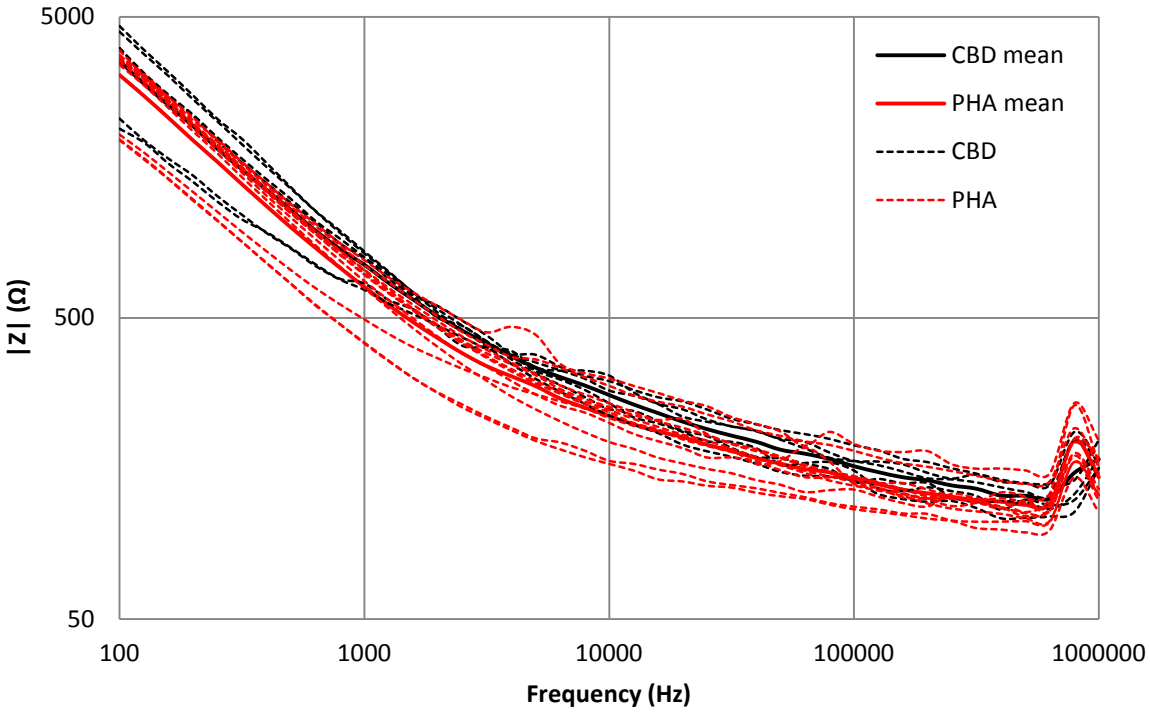

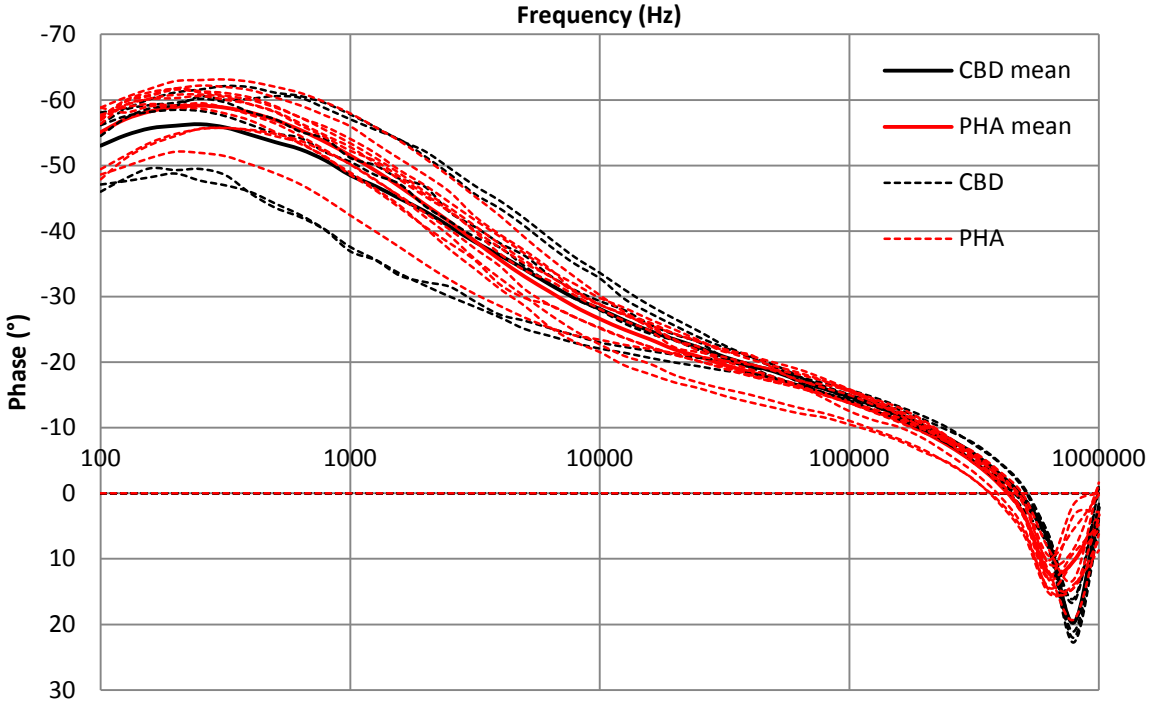

Operation 4

$CBD\ n = 4$
$PHA\ n = 8$

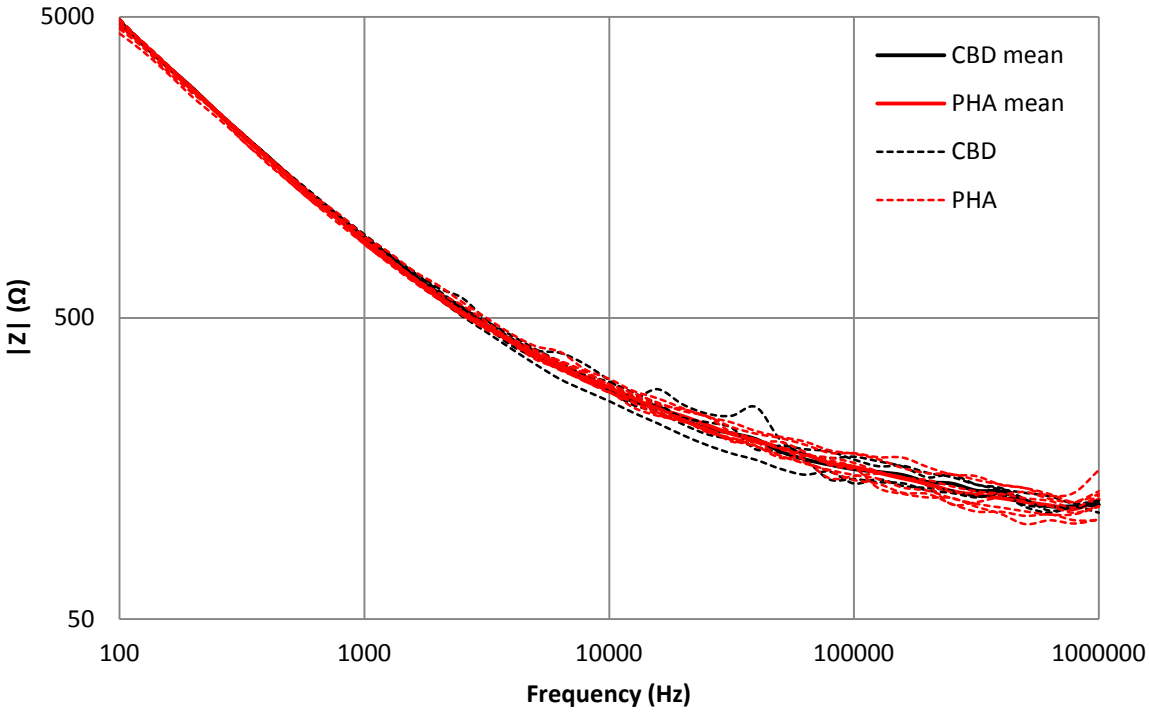

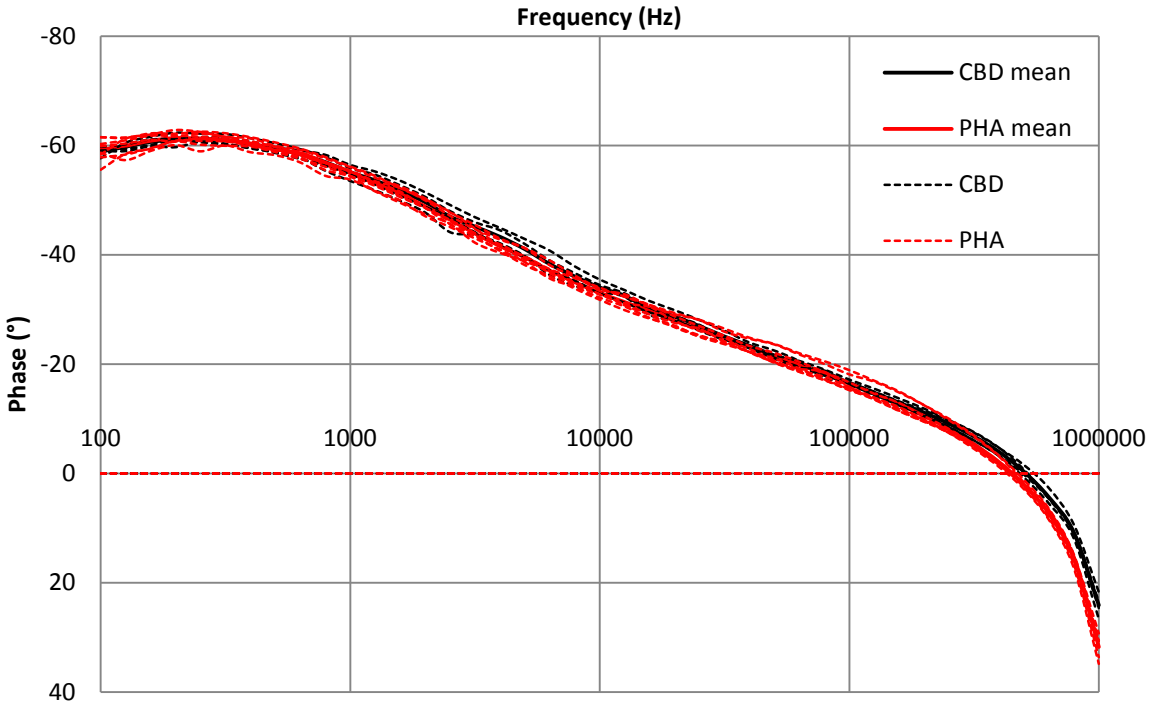

Operation 5

$CBD\ n = 5$
$PHA\ n = 5$

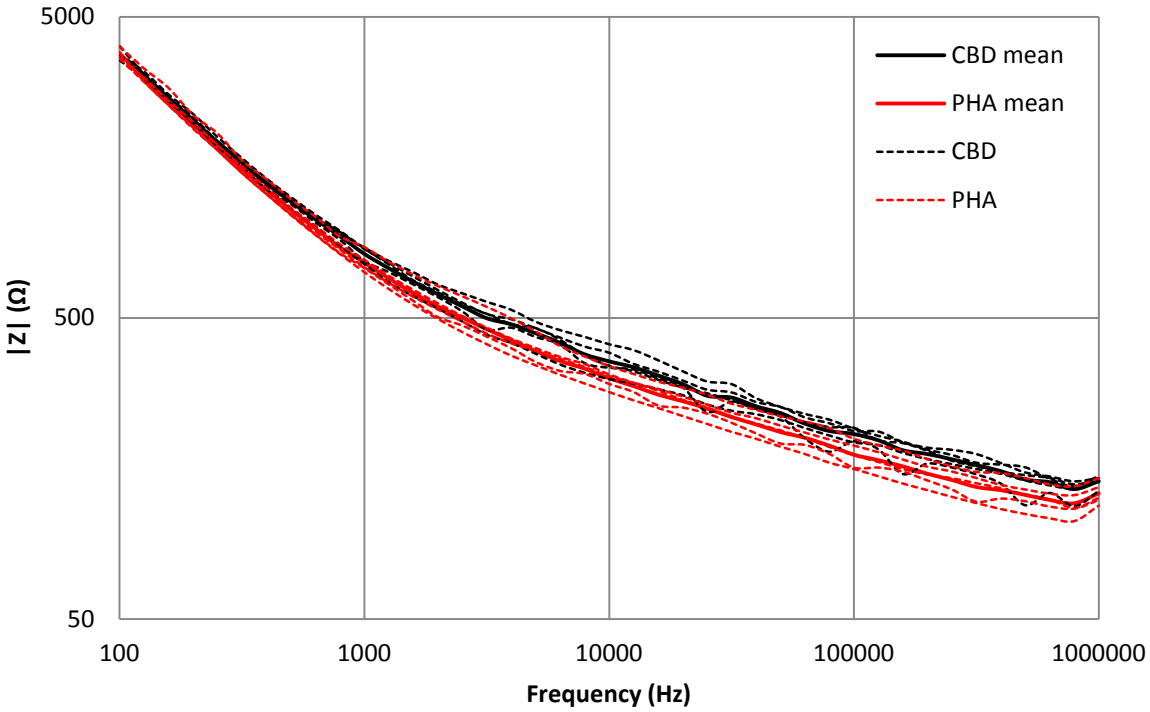

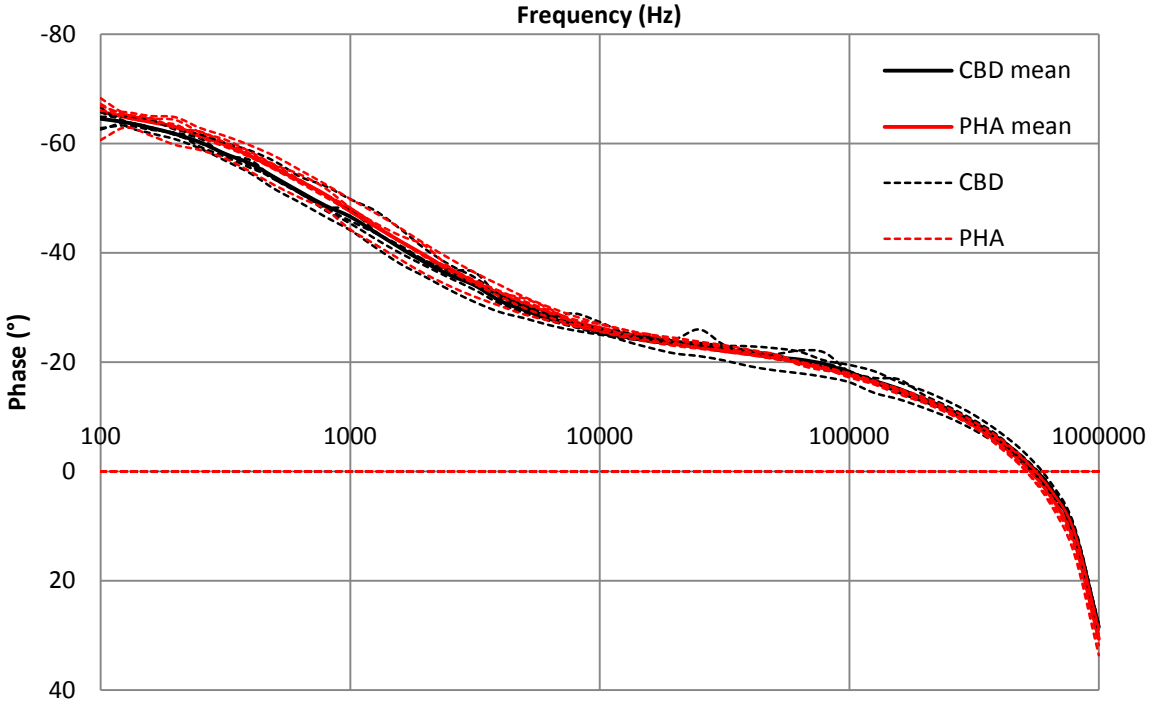

Operation 6

$CBD\ n = 5$
$PHA\ n = 5$

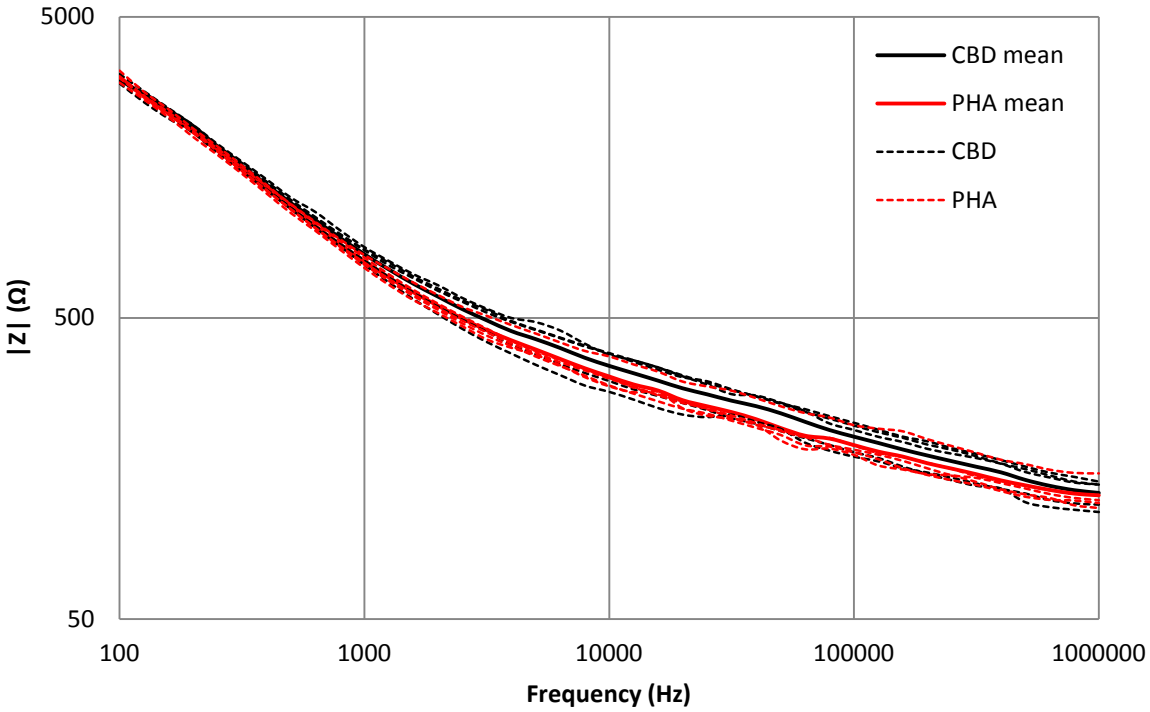

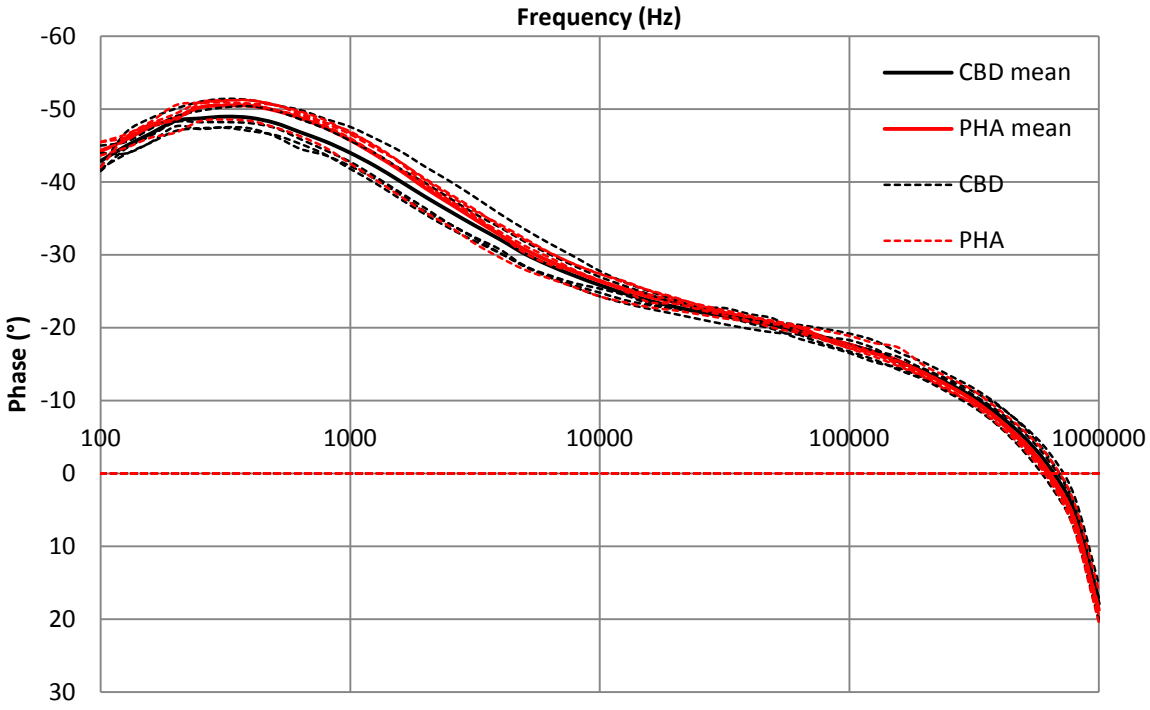

Operation 7

$CBD\ n = 5$
$PHA\ n = 5$

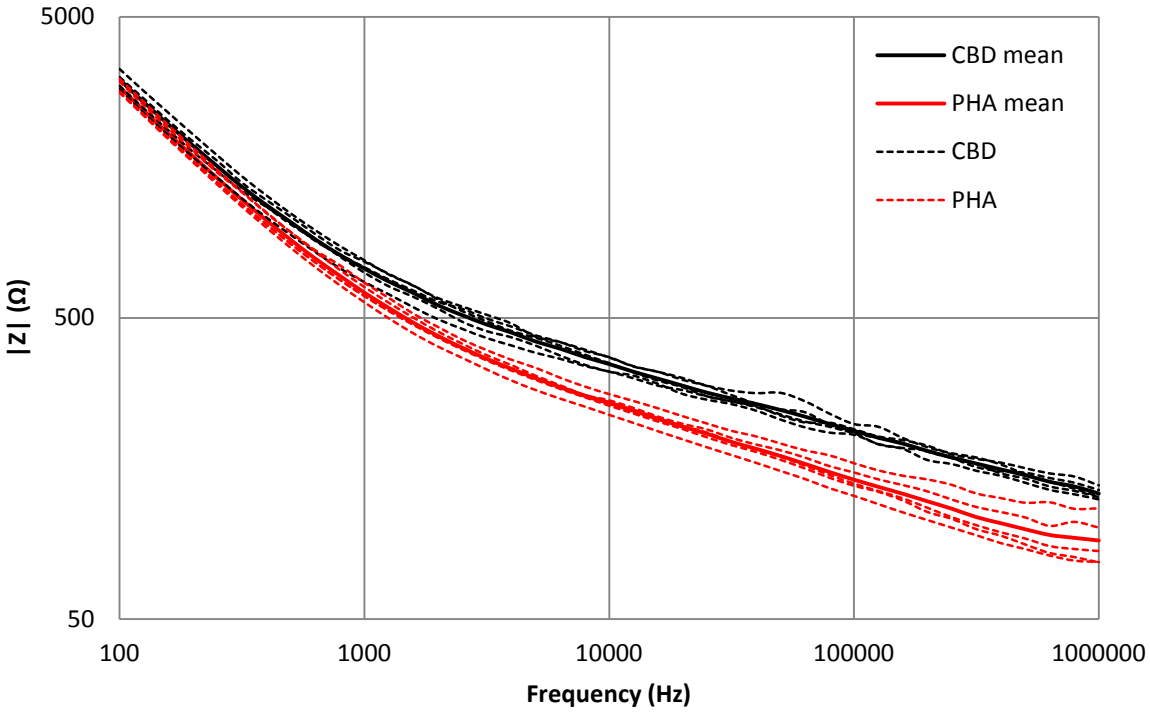

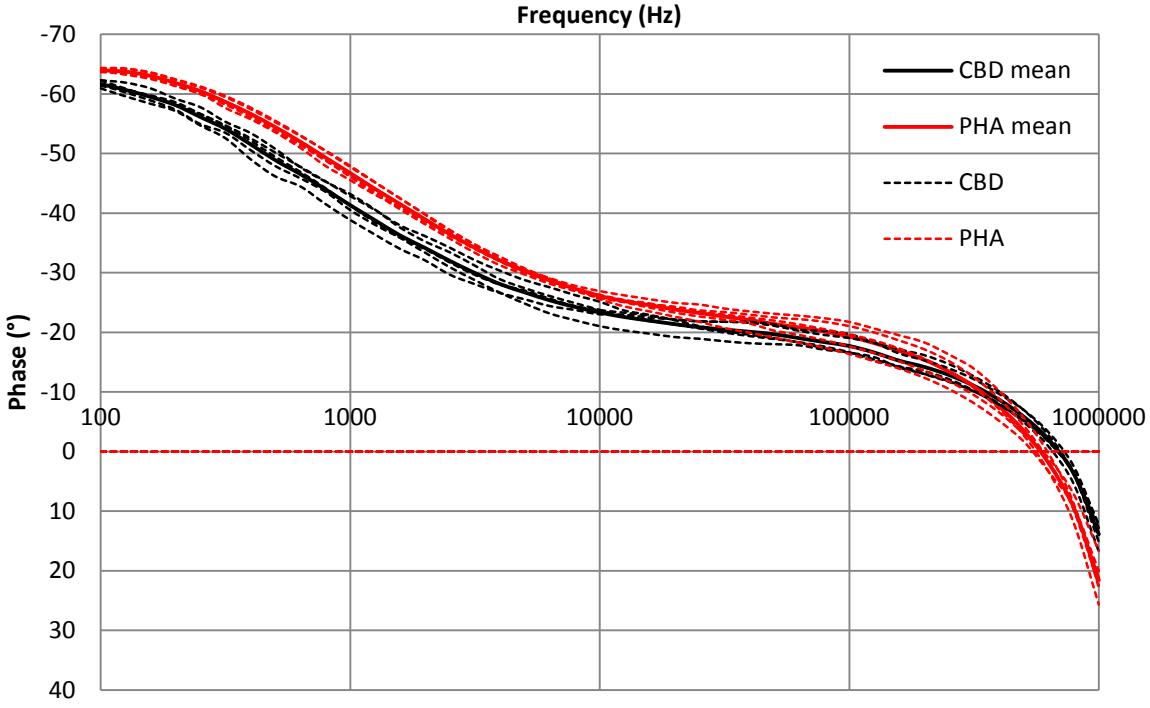

Operation 8

$CBD\ n = 5$
$PHA\ n = 5$

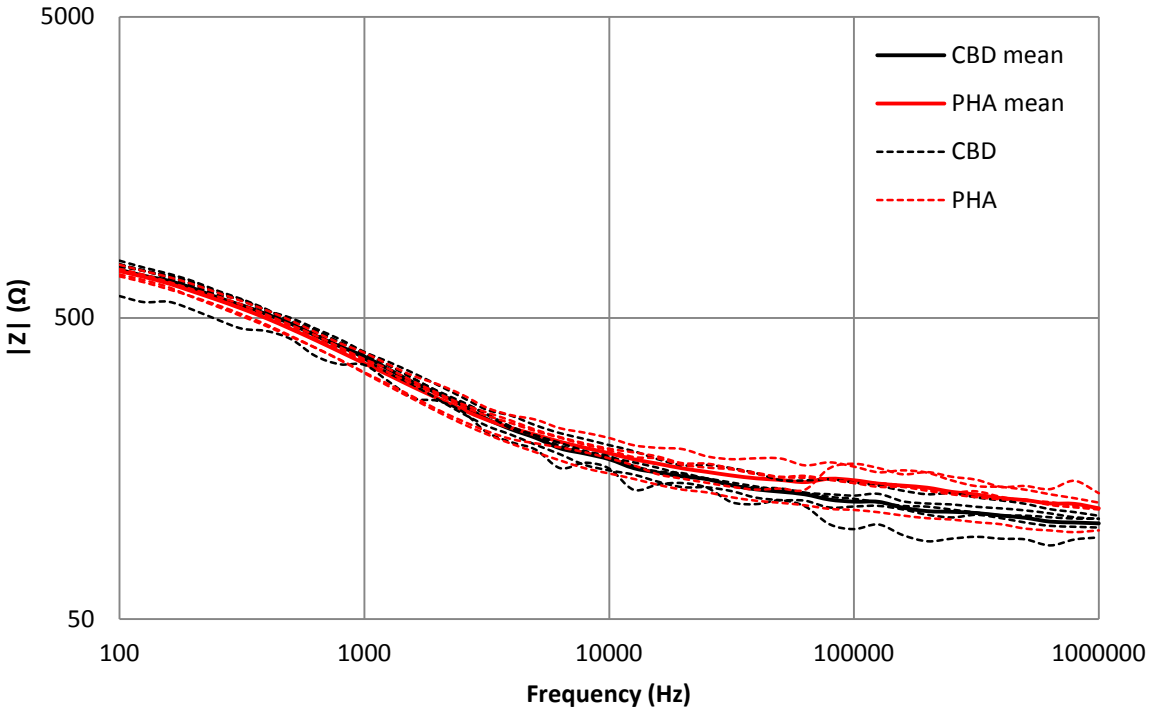

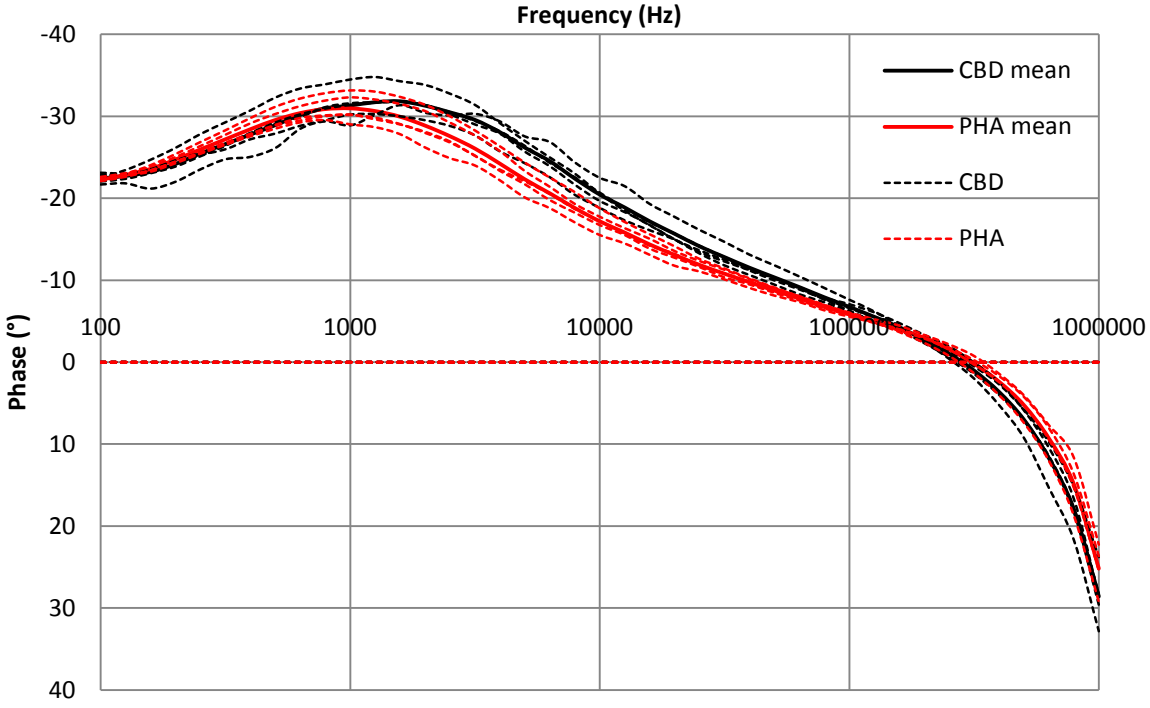

Operation 9

$CBD\ n = 3$
$PHA\ n = 3$

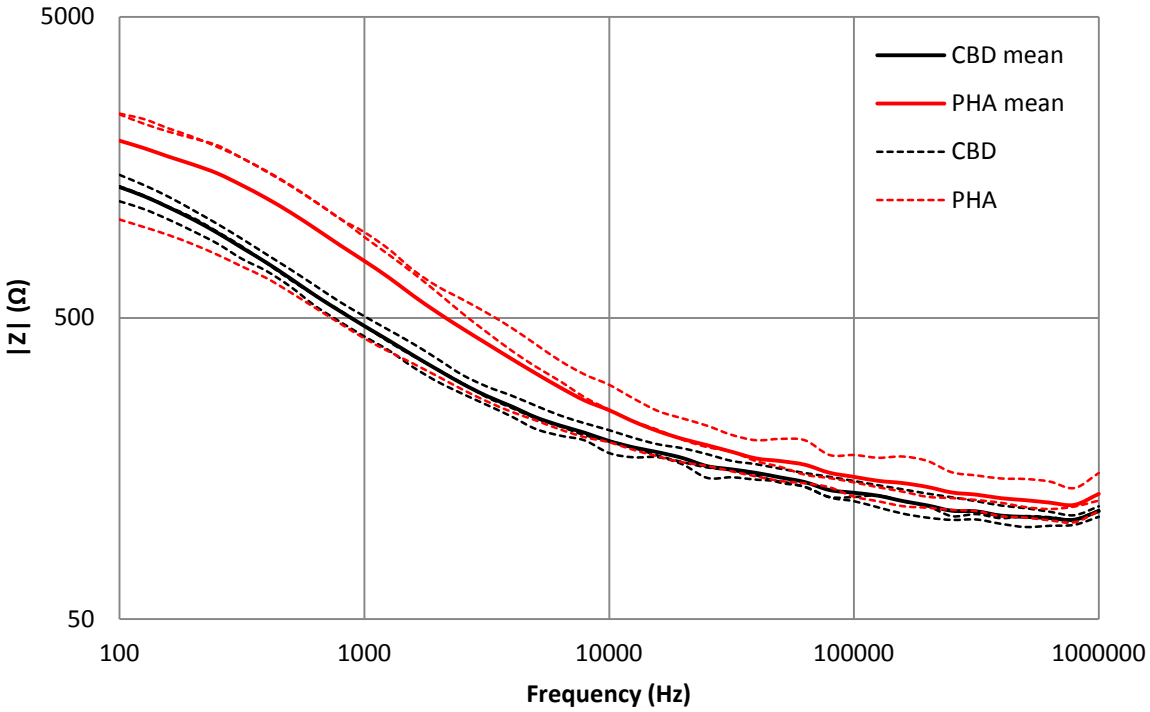

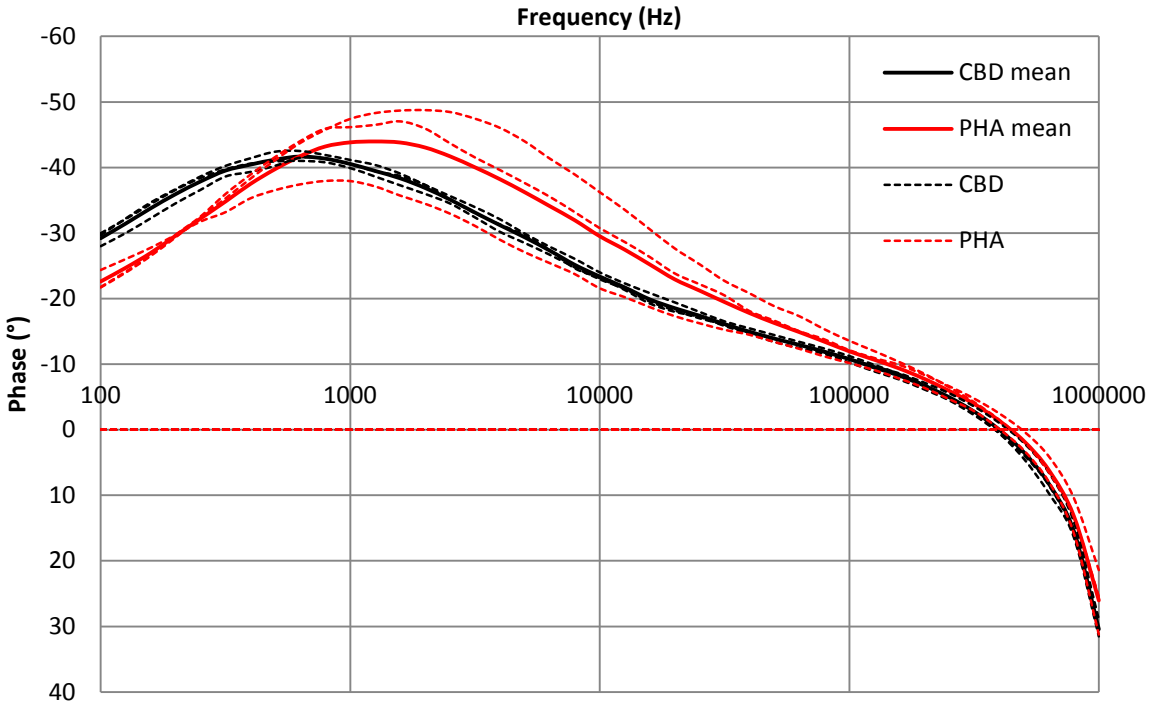

Appendix E – Distribution graph for common bile duct and proper hepatic artery measurements

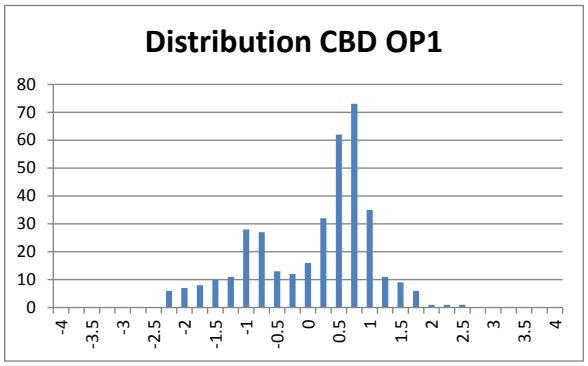

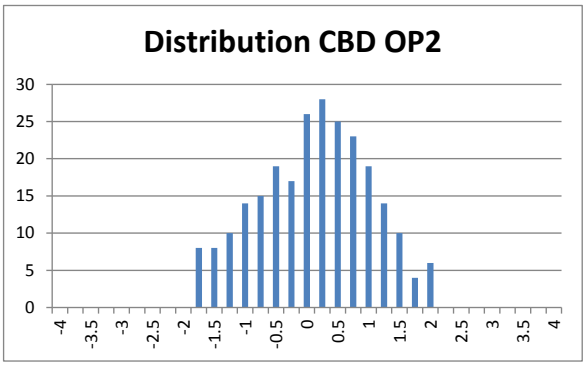

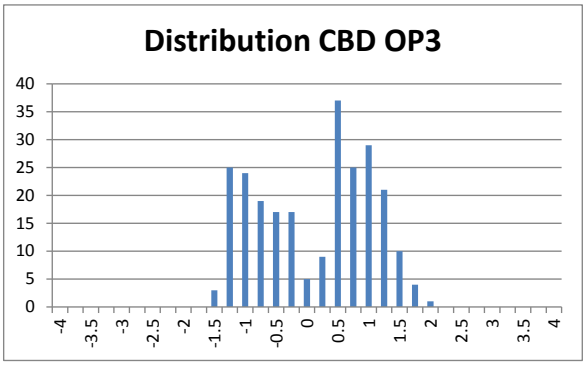

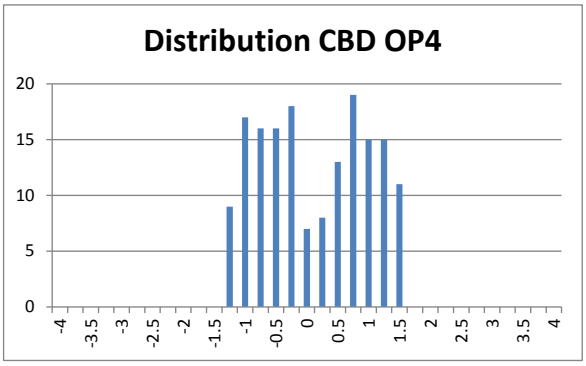

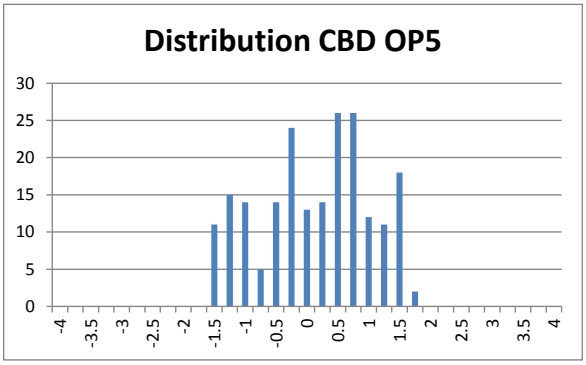

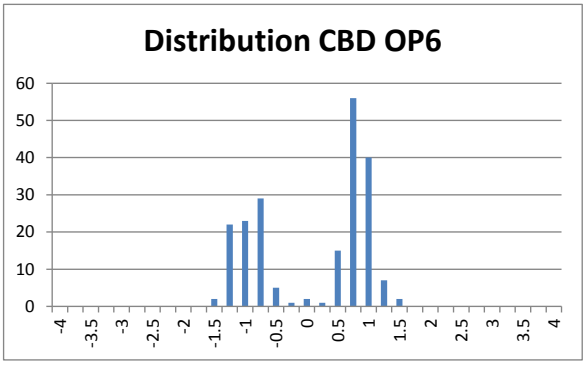

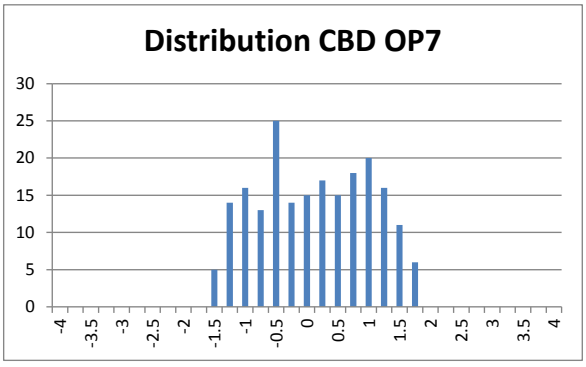

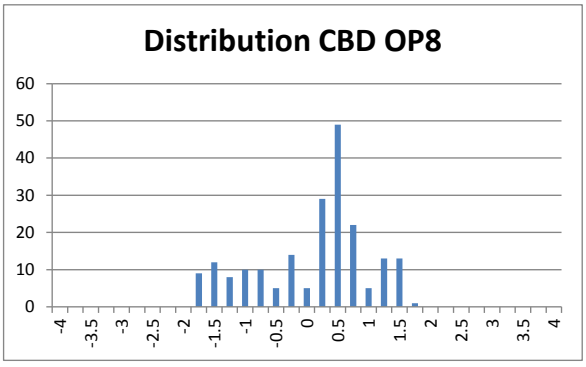

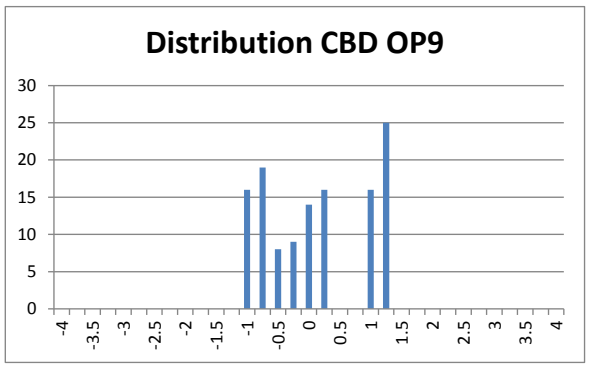
Distribution CBD OP9

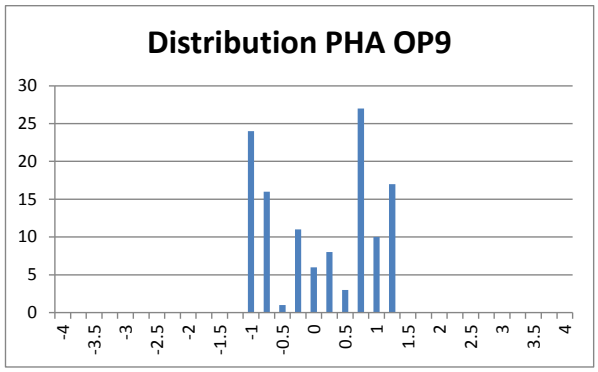
Distribution PHA OP9

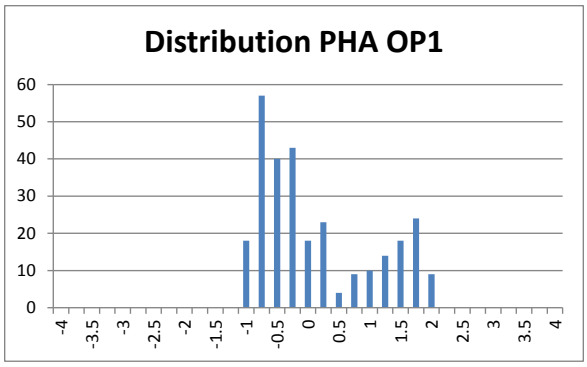
Distribution PHA OP1

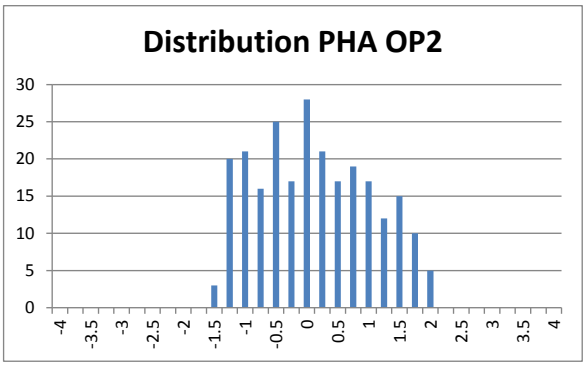
Distribution PHA OP2

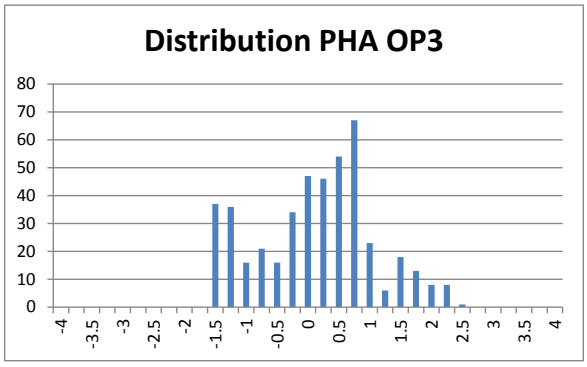
Distribution PHA OP3

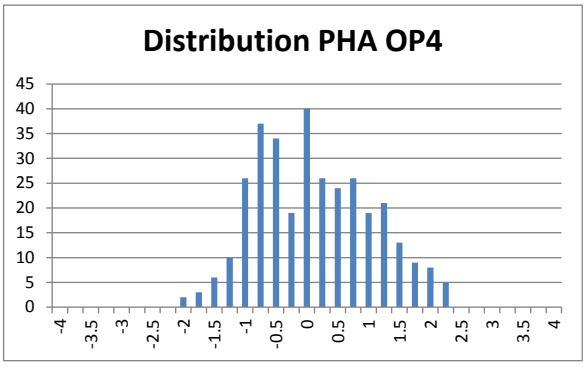
Distribution PHA OP4

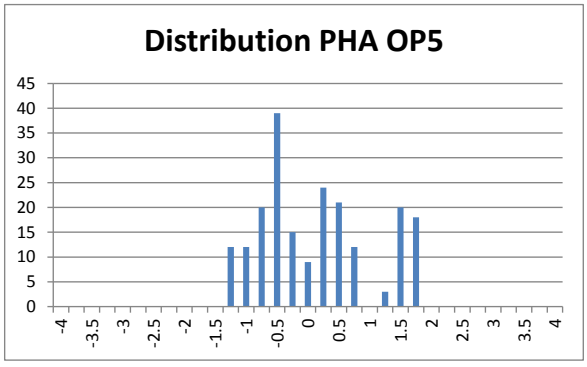
Distribution PHA OP5

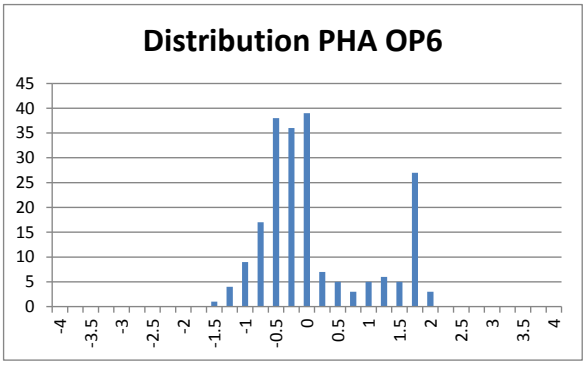
Distribution PHA OP6

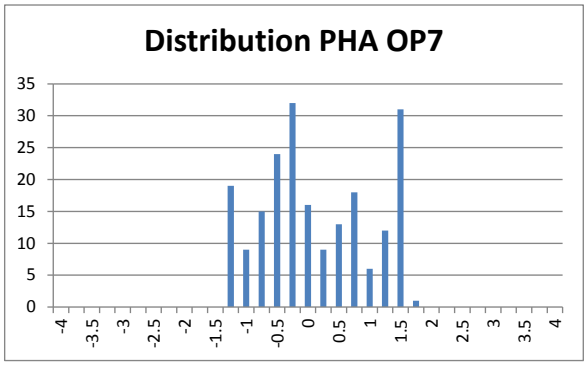
Distribution PHA OP7

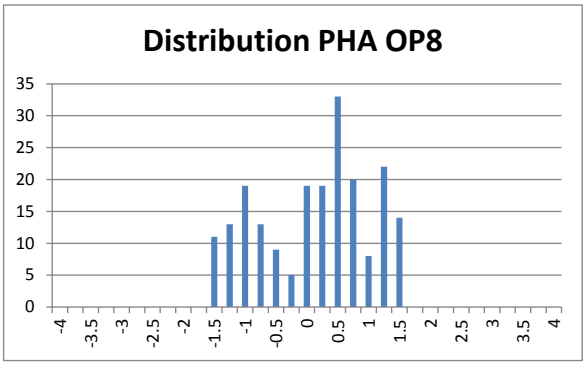
Distribution PHA OP8

Appendix F – True/False table for the Wilcoxon signed-rank test on CBD vs. PHA data

CBD vs. PHA impedance, $\alpha = 0.05$, assuming normal distribution.

Frequency	OP1	OP2	OP3	OP4	OP5	OP6	OP7	OP8	OP9
1.00E+06	FALSE	TRUE	FALSE	FALSE	FALSE	FALSE	TRUE	FALSE	FALSE
7.94E+05	FALSE	TRUE	TRUE	FALSE	TRUE	FALSE	TRUE	FALSE	FALSE
6.31E+05	FALSE	TRUE	FALSE	FALSE	TRUE	FALSE	TRUE	FALSE	FALSE
5.01E+05	FALSE	TRUE	FALSE	FALSE	FALSE	FALSE	TRUE	FALSE	FALSE
3.98E+05	FALSE	TRUE	FALSE	FALSE	TRUE	FALSE	TRUE	FALSE	FALSE
3.16E+05	FALSE	TRUE	FALSE	FALSE	TRUE	FALSE	TRUE	FALSE	FALSE
2.51E+05	FALSE	TRUE	FALSE	FALSE	TRUE	FALSE	TRUE	FALSE	FALSE
2.00E+05	FALSE	TRUE	FALSE	FALSE	TRUE	FALSE	TRUE	FALSE	FALSE
1.58E+05	FALSE	TRUE	FALSE	FALSE	FALSE	FALSE	TRUE	FALSE	FALSE
1.26E+05	FALSE	TRUE	FALSE	FALSE	TRUE	FALSE	TRUE	FALSE	FALSE
1.00E+05	FALSE	FALSE	FALSE	FALSE	TRUE	FALSE	TRUE	FALSE	FALSE
7.94E+04	FALSE	TRUE	FALSE	FALSE	TRUE	FALSE	TRUE	FALSE	FALSE
6.31E+04	FALSE	TRUE	FALSE	FALSE	FALSE	FALSE	TRUE	FALSE	FALSE
5.01E+04	FALSE	TRUE	FALSE	FALSE	TRUE	TRUE	TRUE	FALSE	FALSE
3.98E+04	FALSE	TRUE	FALSE	FALSE	TRUE	TRUE	TRUE	FALSE	FALSE
3.16E+04	FALSE	FALSE	FALSE	FALSE	TRUE	TRUE	TRUE	FALSE	FALSE
2.51E+04	FALSE	TRUE	FALSE	FALSE	TRUE	FALSE	TRUE	FALSE	FALSE
2.00E+04	FALSE	TRUE	FALSE	FALSE	TRUE	FALSE	TRUE	FALSE	FALSE
1.58E+04	FALSE	TRUE	FALSE	FALSE	TRUE	FALSE	TRUE	FALSE	FALSE
1.26E+04	FALSE	TRUE	FALSE	FALSE	FALSE	FALSE	TRUE	FALSE	FALSE
1.00E+04	FALSE	FALSE	FALSE	FALSE	FALSE	FALSE	TRUE	FALSE	FALSE
7.94E+03	FALSE	TRUE	FALSE	FALSE	FALSE	FALSE	TRUE	FALSE	FALSE
6.31E+03	FALSE	TRUE	FALSE	FALSE	FALSE	FALSE	TRUE	FALSE	FALSE
5.01E+03	FALSE	FALSE	FALSE	FALSE	FALSE	FALSE	TRUE	FALSE	FALSE
3.98E+03	FALSE	FALSE	FALSE	FALSE	FALSE	FALSE	TRUE	FALSE	FALSE
3.16E+03	FALSE	FALSE	FALSE	FALSE	FALSE	FALSE	TRUE	FALSE	FALSE
2.51E+03	TRUE	FALSE	FALSE	FALSE	FALSE	FALSE	TRUE	FALSE	FALSE
2.00E+03	TRUE	FALSE	FALSE	FALSE	FALSE	FALSE	TRUE	FALSE	FALSE
1.58E+03	TRUE	FALSE	FALSE	FALSE	FALSE	FALSE	TRUE	FALSE	FALSE
1.26E+03	TRUE	FALSE	FALSE	FALSE	FALSE	FALSE	TRUE	FALSE	FALSE
1.00E+03	TRUE	FALSE	FALSE	FALSE	FALSE	FALSE	TRUE	FALSE	FALSE
7.94E+02	TRUE	FALSE	FALSE	FALSE	FALSE	FALSE	TRUE	FALSE	FALSE
6.31E+02	TRUE	FALSE	FALSE	FALSE	TRUE	FALSE	TRUE	FALSE	FALSE
5.01E+02	TRUE	FALSE	FALSE	FALSE	FALSE	FALSE	TRUE	FALSE	FALSE
3.98E+02	TRUE	FALSE	FALSE	FALSE	TRUE	FALSE	TRUE	FALSE	FALSE
3.16E+02	TRUE	FALSE	FALSE	FALSE	TRUE	FALSE	TRUE	FALSE	FALSE
2.51E+02	TRUE	FALSE	FALSE	FALSE	FALSE	FALSE	TRUE	FALSE	FALSE
2.00E+02	TRUE	FALSE	FALSE	FALSE	FALSE	FALSE	TRUE	FALSE	FALSE
1.58E+02	TRUE	FALSE	FALSE	FALSE	FALSE	FALSE	TRUE	FALSE	FALSE
1.26E+02	TRUE	FALSE	FALSE	FALSE	FALSE	FALSE	TRUE	FALSE	FALSE
1.00E+02	TRUE	FALSE	FALSE	FALSE	FALSE	FALSE	TRUE	FALSE	FALSE

CBD vs. PHA phase, $\alpha = 0.05$, assuming normal distribution.

Frequency	OP1	OP2	OP3	OP4	OP5	OP6	OP7	OP8	OP9
1.00E+06	TRUE	TRUE	FALSE	FALSE	TRUE	FALSE	TRUE	FALSE	FALSE
7.94E+05	TRUE	TRUE	TRUE	FALSE	TRUE	FALSE	TRUE	FALSE	FALSE
6.31E+05	TRUE	TRUE	TRUE	FALSE	FALSE	FALSE	TRUE	FALSE	FALSE
5.01E+05	TRUE	TRUE	TRUE	FALSE	FALSE	FALSE	FALSE	FALSE	FALSE
3.98E+05	TRUE	TRUE	FALSE	FALSE	FALSE	FALSE	FALSE	FALSE	FALSE
3.16E+05	TRUE	TRUE	FALSE	FALSE	FALSE	FALSE	FALSE	FALSE	FALSE
2.51E+05	TRUE	FALSE	FALSE	FALSE	FALSE	FALSE	FALSE	FALSE	FALSE
2.00E+05	TRUE	FALSE	FALSE	FALSE	FALSE	FALSE	FALSE	FALSE	FALSE
1.58E+05	TRUE	TRUE	FALSE	FALSE	FALSE	FALSE	FALSE	FALSE	FALSE
1.26E+05	TRUE	TRUE	FALSE	FALSE	FALSE	FALSE	FALSE	TRUE	FALSE
1.00E+05	TRUE	TRUE	FALSE	FALSE	FALSE	FALSE	FALSE	TRUE	FALSE
7.94E+04	TRUE	TRUE	FALSE	FALSE	FALSE	FALSE	TRUE	TRUE	FALSE
6.31E+04	TRUE	TRUE	FALSE	FALSE	FALSE	FALSE	FALSE	TRUE	FALSE
5.01E+04	TRUE	TRUE	FALSE	FALSE	FALSE	FALSE	TRUE	TRUE	FALSE
3.98E+04	TRUE	TRUE	FALSE	FALSE	FALSE	FALSE	TRUE	TRUE	FALSE
3.16E+04	TRUE	TRUE	FALSE	FALSE	FALSE	FALSE	TRUE	TRUE	FALSE
2.51E+04	FALSE	TRUE	FALSE	FALSE	FALSE	FALSE	TRUE	TRUE	FALSE
2.00E+04	FALSE	TRUE	FALSE	FALSE	FALSE	FALSE	TRUE	TRUE	FALSE
1.58E+04	FALSE	TRUE	FALSE	FALSE	FALSE	FALSE	TRUE	TRUE	FALSE
1.26E+04	FALSE	TRUE	FALSE	FALSE	FALSE	FALSE	TRUE	TRUE	FALSE
1.00E+04	FALSE	TRUE	FALSE	FALSE	FALSE	FALSE	TRUE	TRUE	FALSE
7.94E+03	FALSE	TRUE	FALSE	FALSE	FALSE	FALSE	TRUE	TRUE	FALSE
6.31E+03	FALSE	TRUE	FALSE	FALSE	FALSE	FALSE	TRUE	TRUE	FALSE
5.01E+03	FALSE	FALSE	FALSE	FALSE	FALSE	FALSE	TRUE	TRUE	FALSE
3.98E+03	FALSE	FALSE	FALSE	FALSE	FALSE	FALSE	TRUE	TRUE	FALSE
3.16E+03	FALSE	FALSE	FALSE	FALSE	FALSE	FALSE	TRUE	TRUE	FALSE
2.51E+03	FALSE	FALSE	FALSE	FALSE	FALSE	FALSE	TRUE	TRUE	FALSE
2.00E+03	FALSE	FALSE	FALSE	FALSE	FALSE	FALSE	TRUE	FALSE	FALSE
1.58E+03	FALSE	FALSE	FALSE	FALSE	FALSE	FALSE	TRUE	FALSE	FALSE
1.26E+03	FALSE	FALSE	FALSE	FALSE	FALSE	FALSE	TRUE	FALSE	FALSE
1.00E+03	FALSE	FALSE	FALSE	FALSE	FALSE	FALSE	TRUE	FALSE	FALSE
7.94E+02	FALSE	FALSE	FALSE	FALSE	FALSE	FALSE	TRUE	FALSE	FALSE
6.31E+02	FALSE	FALSE	FALSE	FALSE	FALSE	FALSE	TRUE	FALSE	FALSE
5.01E+02	TRUE	FALSE	FALSE	FALSE	FALSE	TRUE	TRUE	FALSE	FALSE
3.98E+02	TRUE	FALSE	FALSE	FALSE	FALSE	FALSE	TRUE	FALSE	FALSE
3.16E+02	FALSE	FALSE	FALSE	FALSE	FALSE	FALSE	TRUE	FALSE	FALSE
2.51E+02	FALSE	FALSE	FALSE	FALSE	FALSE	FALSE	TRUE	FALSE	FALSE
2.00E+02	FALSE	FALSE	FALSE	FALSE	FALSE	FALSE	TRUE	FALSE	FALSE
1.58E+02	FALSE	TRUE	FALSE	FALSE	FALSE	FALSE	TRUE	FALSE	FALSE
1.26E+02	FALSE	TRUE	FALSE	FALSE	FALSE	FALSE	TRUE	FALSE	FALSE
1.00E+02	FALSE	TRUE	FALSE	FALSE	FALSE	FALSE	TRUE	FALSE	FALSE

Please see section 4.3.3.2 of this thesis for a full explanation of what these tables means.

Appendix G – Impedance and phase graphs for spleen and splenic artery measurements

This appendix contains all measurements on the spleen and splenic artery reference locations for the pig trials. These were only recorded at operations 4 through 8. The spleen are always represented as black lines, while the splenic artery is represented by red lines.

Operation 4

$Spleen\ n = 2$
$Artery\ n = 6$

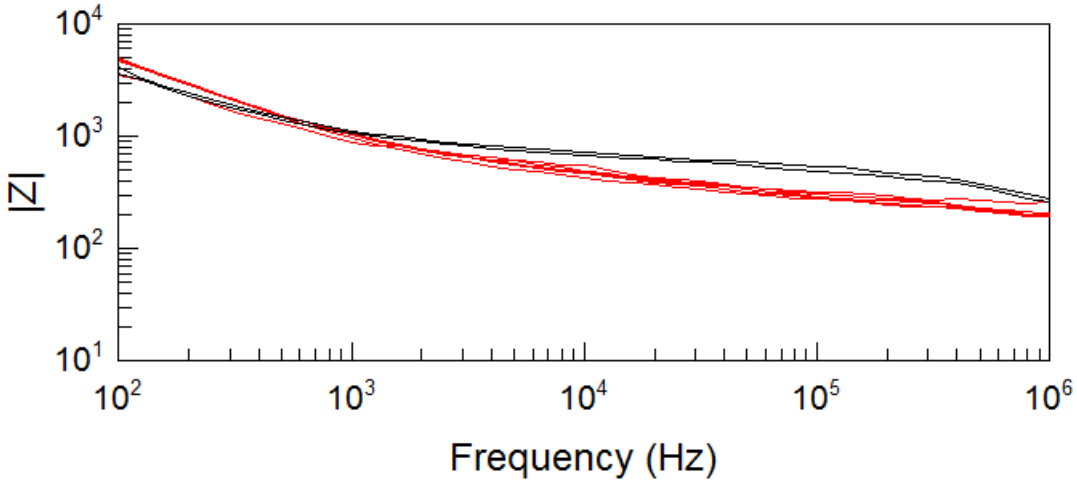

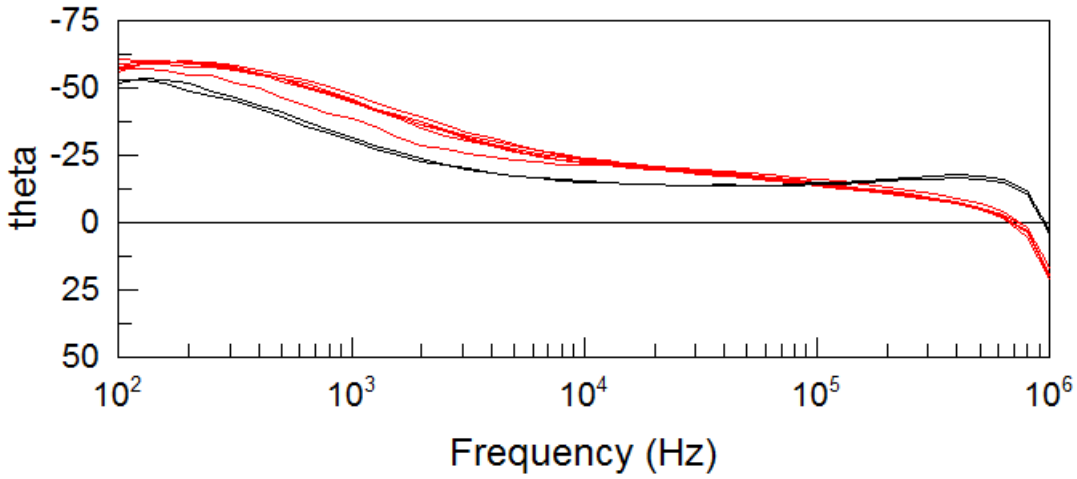

Operation 5

$Spleen\ n = 5$
$Artery\ n = 5$

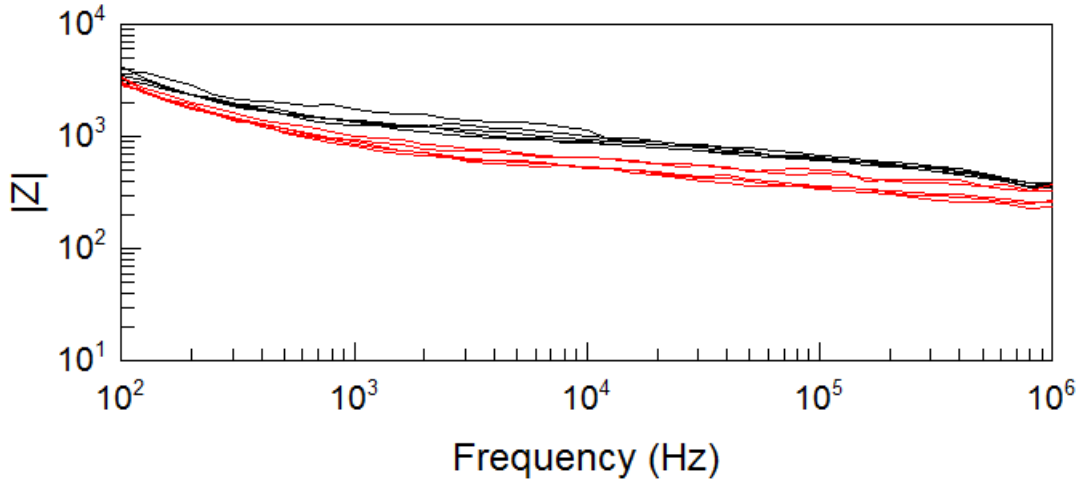

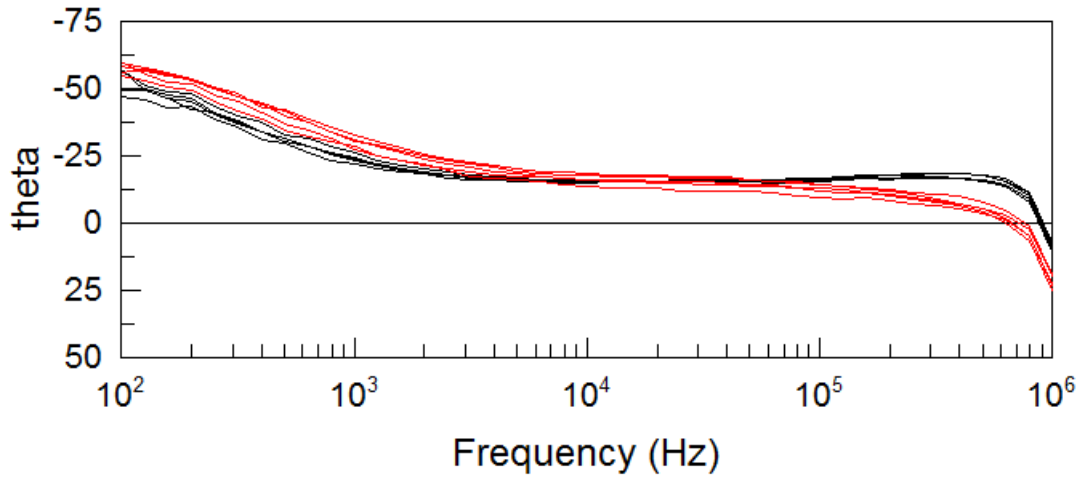

Operation 6

$Spleen\ n = 5$
$Artery\ n = 5$

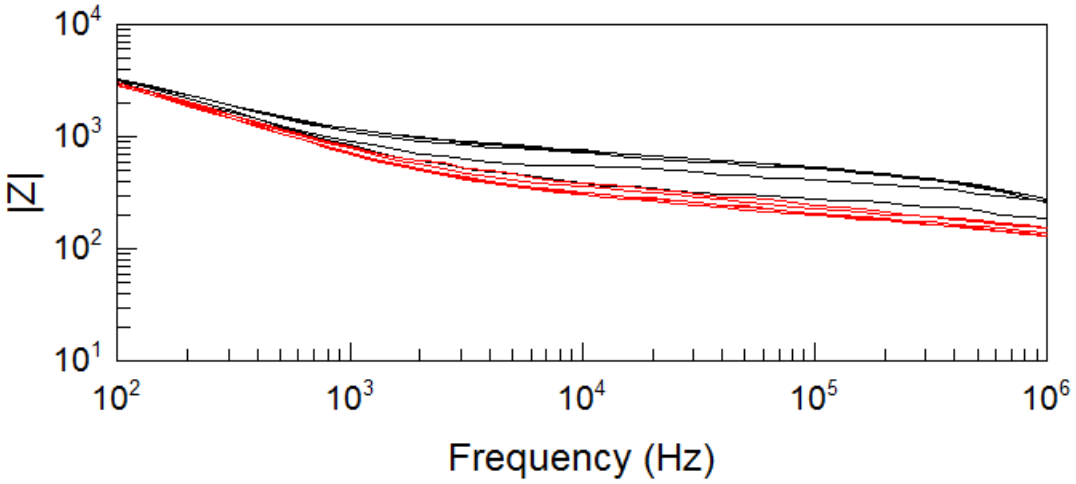

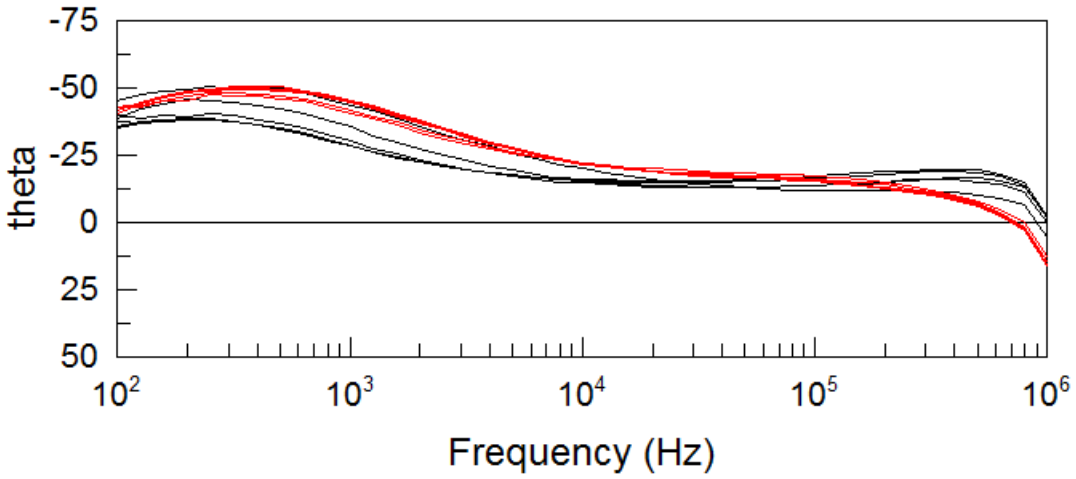

Operation 7

$Spleen\ n = 3$
$Artery\ n = 5$

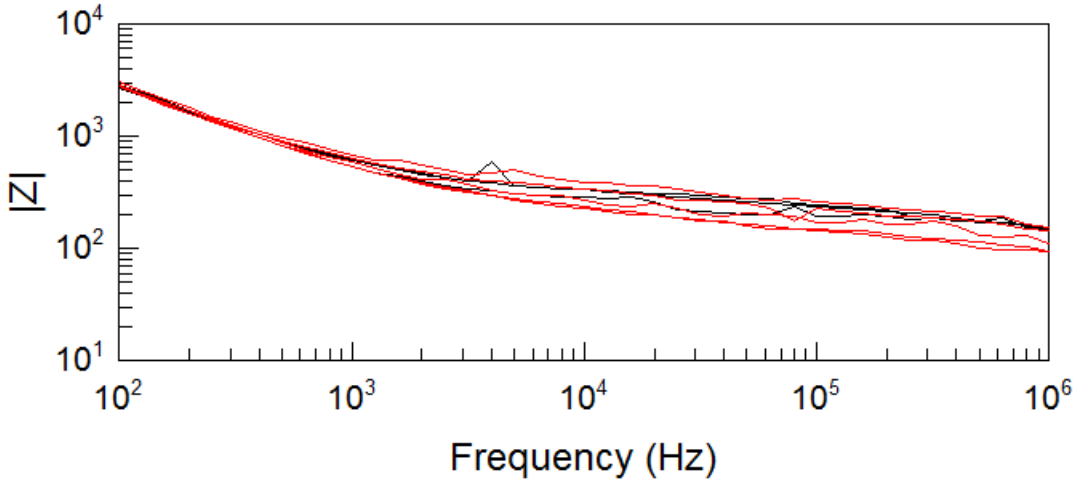

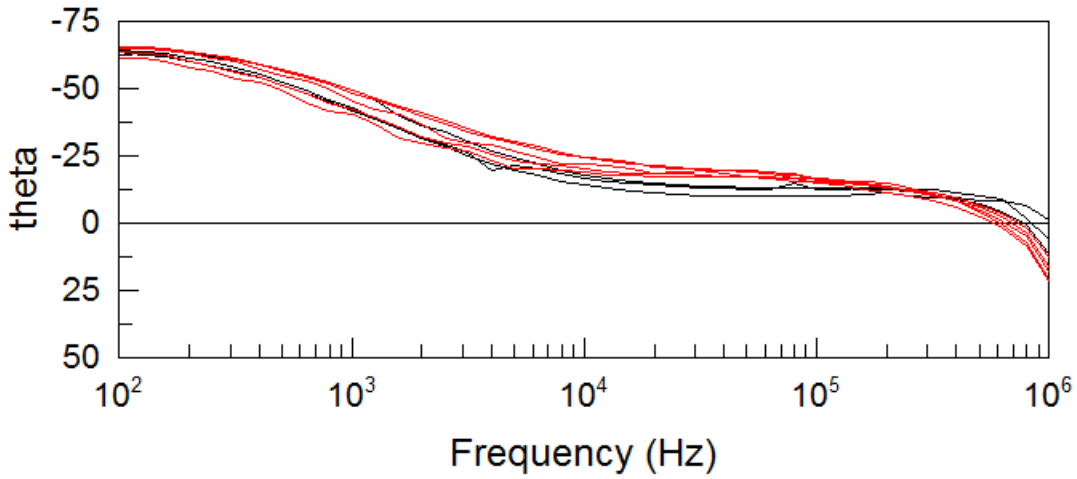

Operation 8

$Spleen\ n = 5$
$Artery\ n = 5$